

Water relations in deciduous forest trees under elevated
CO₂

INAUGURALDISSERTATION

zur Erlangung der Würde eines Doktors der Philosophie

vorgelegt der
PHILOSOPHISCH-NATURWISSENSCHAFTLICHEN FAKULTÄT
der Universität Basel

von

SEBASTIAN LEUZINGER

aus Basel

Basel, 2006

Genehmigt von der Philosophisch-Naturwissenschaftlichen Fakultät auf Antrag von

Prof. Dr. Christian Körner
Prof. Dr. Nina Buchmann

Basel, den 19. September 2006

Prof. Dr. Hans-Jakob Wirz
Dekan

Stomata orchestrate one of plant biology's greatest concerts

Stan Wullschleger

Acknowledgements

First and foremost thanks go to Christian Körner, for the excellent guidance he provided, for his enthusiasm towards my project, for tireless proof-reading of my manuscripts, for his faith in my ability to carry on.

Pascal Niklaus and Reto Stöckli from ETH Zürich provided most valuable advice, excellent collaboration and many hours of stimulating discussions. I wish to thank Roland Vogt for help and advice on thermography and micrometeorology and Barbara Köstner for interesting discussions and advice on sap flow. Thanks also to Nina Buchmann from ETH Zürich for co-examining my thesis. I am greatly indebted to Erwin Amstutz for countless hours of (nightly) crane operations, technical help and deciphering thermal images. Also thanks to Roman Asshoff, Olivier Bignucolo, Patrick Cech, Georges Grun, Dieter Häring, Erika Hiltbrunner, Hans-Christoph Im Hof, Hamlyn Jones, Sonja Keel, Susanna Peláez-Riedl, Eva Spehn and Gerhard Zotz for general help and everybody else from the Botanical Institute for creating a very inspiring working environment.

I am further grateful to the supervisors of my MSc thesis in statistics which I pursued in parallel to the PhD programme, Marie-Agnès Moravie, Sylvain Sardy and Anthony Davison, their input greatly influenced my PhD thesis.

Funding came from the Swiss National Science Foundation (NCCR climate, Project 3.3) and a research grant to C. Körner (3100-059769.99). The crane was sponsored by the Swiss Federal Office for the Environment (FOEN).

I would like to thank you Alana for all the support you provided during these three years, for being patient when I came home late, for listening and encouraging me when things did not go so well. Thank you Matteo for giving me that smile before I leave home in the morning. Finally, I thank my parents, they first awoke my interest in biology and supported me in all I have ever done since.

The title page shows a thermal image of the crane, taken from the gondola. Temperatures range from ca. 16° C (black) to ca. 30 ° C (red). The false-colour image contains the information of 320 x 240 = 76'800 temperature measurements, printed in numbers rounded to one degree Celsius on the back of the title page (not for the farsighted among us).

Contents

1	General Introduction	9
2	Water savings in mature deciduous forest trees under elevated CO ₂ - a multifactorial approach	15
3	Responses of deciduous forest trees to severe summer drought in Central Europe	27
4	Stomatal conductance in mature deciduous forest trees exposed to elevated CO ₂	39
5	Tree species diversity affects canopy leaf temperatures in a mature temperate forest	49
6	A sensitivity analysis of leaf temperature to changes in transpiration	59
7	A model predicting sap flow from environmental data	67
8	The analysis of relative data - A novel approach with the example of sap flow data	77
9	Summary	85

Chapter 1

General Introduction

General Introduction

Global change, climate change, CO₂ and plants

Depending on whether one adopts a more anthropogenic or a more ecological perspective, poverty and global change will be the two most pressing problems humanity will have to face in the 21st century (The Millennium Development Goals Report 2005, Millennium Ecosystem Assessment 2005). In many ways however, the global social and ecological problems of the 21st century will interact, and any attempt to find a solution must involve the consideration of both. The term ‘global change’ summarises all large-scale alterations to the planet’s atmosphere, hydrosphere, pedosphere and biosphere brought along by human activity (Körner, 2003). If biodiversity is taken as a proxy for the planet’s wellbeing, land-use change has been estimated to have the largest impact, followed by global warming, N-deposition, biotic exchange (introduction of foreign species to an ecosystem) and the increase of atmospheric CO₂-concentration (Sala *et al.* 2000). Large-scale exploitation of most terrestrial ecosystems, intensive agriculture and the burning of fossil fuel are the results of an overexponential growth of the human population during the last three centuries. Human activities have already resulted in such drastic transformations of the earth’s global properties (climate, vegetation cover, biodiversity) that the onset of a new geological era (the ‘anthropocene’) was suggested by Crutzen (2002).

Climatic change as one facette of global change is mainly caused by the burning of fossil fuels and the resulting enrichment of CO₂ in the atmosphere. Changes in land-use (deforestation, agriculture, urbanisation) further contribute to climate change through the creation of new carbon sinks, the burning of soil carbon, other greenhouse gas emissions and a change of the surface albedo. The human-induced increase in atmospheric CO₂ concentration from the ‘pre-industrial’ 270 ppm (ca. 1850) to the current 380 ppm (Figure 1) and its effect on global warming have been recognised by the scientific community (Rodhe 1990, Crowley 2000). The present level of atmospheric CO₂ and the rate of increase as experienced over the past 250 years is unprecedented during

the last 640’000 years (Petit *et al.* 1999, Siegenthaler *et al.* 2005). The projected 500 to 900 ppm of atmospheric CO₂ are expected to increase the mean surface temperature of the planet by ca. 2 to 6° C from 1990 to 2100, depending on the emission scenario (IPCC Synthesis Report, 2001).

Besides its role as the main greenhouse agent, carbon dioxide constitutes the most important substrate of photosynthetic carbon assimilation by plants. It is therefore likely that any change in atmospheric CO₂ concentration also has plant physiological effects. This is because of the saturation function of the rate of photosynthesis over CO₂ concentration: at the current atmospheric CO₂ level, photosynthesis of C3 plants is not saturated and can be stimulated with higher levels of CO₂. Thus, plants are subjected to both CO₂-induced climatic change and CO₂-induced direct influences on their metabolism. The metabolic (photosynthetic) effects may sound beneficial for plants at first sight, the cascade of secondary processes induced beyond a sheer shift to the right in the photosynthesis-CO₂-concentration curve, result in a multitude, not necessarily beneficial consequences. For instance stoichiometric constraints may limit any growth response (Loladze 2002, Körner 2003). Nutrients will control long-term plant growth stimulation under elevated CO₂ (Oren *et al.* 2001, Johnson *et al.* 2006). Secondly, biodiversity is likely to be affected through differential responses of plant functional groups (Körner, 2000). For example, lianas as shade-adapted plants tend to benefit from a shift in the light-compensation point of photosynthesis to lower light intensities. A vigorous growth of lianas however may greatly influence forest succession and eventually revert initial growth effects of elevated CO₂ (Körner, 1998). More important than the issue of accelerated plant growth is the question whether this results in increased carbon sequestration. Because even if under elevated CO₂ plants grew faster, this may simply speed up plant succession, and not necessarily tie up more carbon in the plant biomass (Körner 2004, Figure 4). This problem, although of great interest for policy makers, is not entirely solved, but major shifts in the amount of sequestered carbon are unlikely for various reasons summarised by Körner (2000).

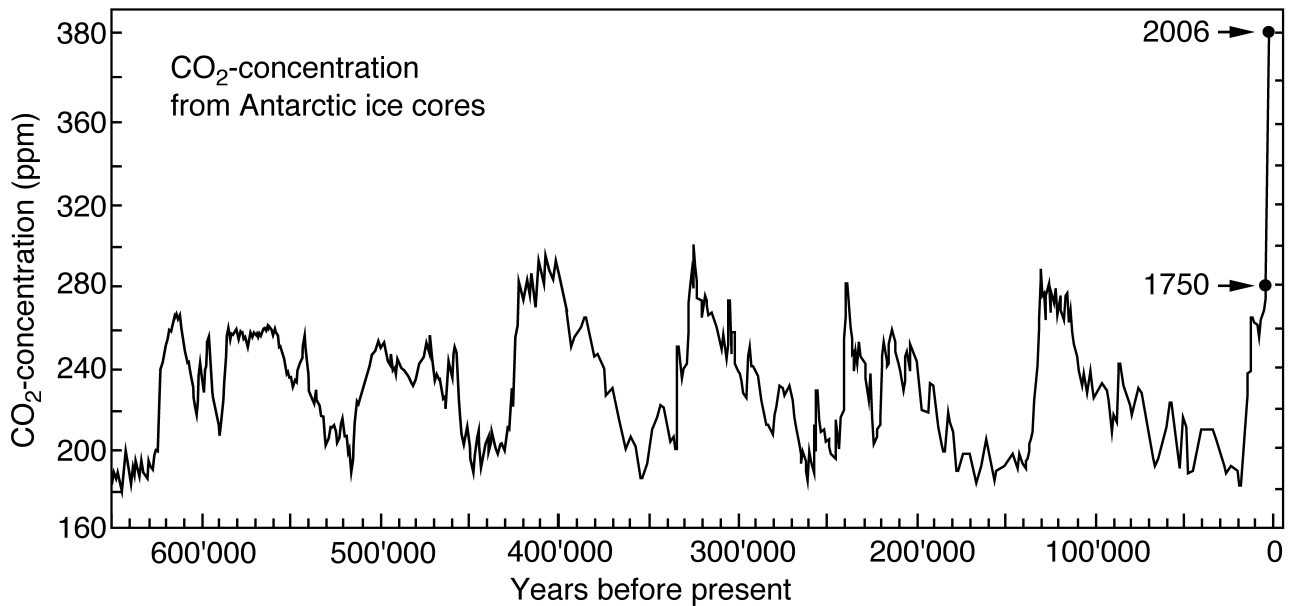


Figure 1: Atmospheric CO₂-concentration over the past 640'000 years, reconstructed from ice cores of the antarctic ice shield. The latest data are from CO₂-measurements at the Mauna-Loa observatory, Hawaii (Petit *et al.* 1999, Siegenthaler *et al.* 2005)

CO₂, plants and water

The leaf pores (stomata) controlling the gas exchange between the leaf and the surrounding air, constitute the centrepiece of the plant's dilemma between 'hunger' (stomata closed, no CO₂-uptake but water is conserved) and 'thirst' (stomata open, CO₂-uptake but water is lost). This trade-off is, in a first approximation, shifted towards less water loss at constant (or even increased) CO₂-uptake as a consequence of partial stomatal closure in response to elevated CO₂-concentration. This mechanism was first documented in 1898 (Darwin, 1898 as cited in Raschke 1986). Since 70 % of all water entering the atmosphere over land passes through stomata, their reaction to rising CO₂ is certainly of key interest to the global water cycle. It is comparatively straight-forward to quantify reduced stomatal conductance (a measure for stomatal opening) in response to different levels of CO₂ under controlled (greenhouse) conditions (for a review see Curtis & Wang 1998, Medlyn *et al.* 2001). To predict total net water savings of a future ecosystem however needs scaling up from the leaf to the whole canopy and finally the whole region (Jarvis & McNaughton, 1986). Further, it involves soil processes (Morgan, 2002) and the consideration of a combination of environmental drivers likely to coincide in global change scenarios (warming, altered precipitation patterns, Shaw *et al.* 2002). Finally, water savings will be compromised or enhanced by atmospheric feedback effects, which can only be uncovered by modelling land-surface processes (see below). An example to schematically illustrate this added com-

plexity of natural, open systems, are biodiversity effects. If, in a greenhouse experiment, species A shows 20 % less stomatal conductance and A remains unaffected by elevated CO₂, a field experiment could show that species B profits from A's savings and starts transpiring even more.

Vegetation-atmosphere interactions

The initial CO₂-response of a plant in terms of reduced stomatal closure entails a reduced humidification of the atmosphere. From here, several imaginable argumentations for feedback effects are possible: if the atmosphere is drier, this could cause plants to transpire even less because of stomatal downregulation. Alternatively, the plants' initial reaction of less transpiration could be mitigated because leaf temperature increases and hence an increase of the leaf to air vapour pressure gradient (Idso *et al.*, 1993). Yet another argumentation is that through a less humid atmosphere, there is less cloud formation, hence more photosynthetic active radiation and therefore more transpiration (R. Stöckli, unpublished data). Given there is less transpiration in plants under higher levels of CO₂, the planetary boundary layer (PBL) may simply grow higher during the diurnal cycle, leaving atmospheric moisture content entirely unchanged. Similar feedback effects may occur in the even less accessible and studied soil system (Morgan, 2002). Herein lies a fundamental and intrinsic drawback of all studies exposing vegetation to elevated CO₂, be they conducted in as natural a surrounding as pos-

sible: due to logistic constraints, the comparatively small CO₂-enriched area will always be surrounded by vegetation growing under ambient conditions, preventing all large-scale feedback. Land-surface models on the other hand, can account for feedback effects, but often suffer from a countless number of parameters, whose quantification critically influences the model's outcome. Most regional coupled soil-vegetation-atmosphere models do not yet account for elevated atmospheric CO₂ (Vidale & Stockli, 2005). Jacobs & Debruin (1992) for the first time modelled possible feedback mechanisms, but their vegetation response was based on a rather unrealistic photosynthesis model. A more realistic approach would be to determine a series of transpiration response curves under elevated CO₂, in particular the response of transpiration to atmospheric vapour pressure deficit. Thus, a realistic plant response to a given atmospheric moisture can be fed back to the model.

Water relations of forest trees

Whereas all terrestrial and aquatic biomes are affected by global change and in particular by climate change, forests deserve prime attention because they cover about 30 % of the earth's land surface and contain about 80 % of all carbon bound in plant biomass (Olson *et al.* 1983, Roy J. 2001). Although the carbon cycle and especially carbon sequestration in forests are ecologically and politically very topical issues, I here concentrate on forest water relations. Forests, particularly tropical rainforests, have a major climate-regulatory function, where deforestation has large effects on the whole ecosystem (cloud formation, precipitation, soil moisture Shukla *et al.* 1990). Even a decline in evapotranspiration rates and subsequent surface warming could potentially cause a collapse of the Amazon forests (Cox *et al.*, 2000). In order to be trusted however, such model results rely on (mostly unavailable) field data for parametrisation and model testing. Moorcroft (2006) points out the potential errors that may arise in climate forecasts if species-specific plant physiological responses are not accounted for. On the other hand, field research involving forest trees and their canopies usually requires heavy logistics, and in situ collection of leaf-level water status parameters was extremely cumbersome for a long time. Since the early 1990s, canopy cranes facilitate tree crown access and allow large-scale studies of gas exchange at the leaf- and whole tree level (Basset *et al.*, 2003).

The water status of a tree can be assessed using a number of methods that can generally be divided into leaf-level and whole-canopy approaches. Leaf-level measurements (gas exchange, porometry, water potential, stable isotope analysis) have the advantage of yielding absolute signals per leaf area, but

they are often compromised by large within-crown variation. Every leaf experiences its very own microclimatic conditions and history, depending on the exact position and exposure within the canopy, which introduces a lot of variability. Whole-canopy approaches (sap flow, thermal imagery, soil water potential/moisture) in contrast integrate signals over the whole canopy, with the drawback of only yielding relative signals. Particular attention has to be paid to changes in leaf area index (LAI), which can confound signals measured both at leaf and canopy level.

The number of water relation studies, conducted on mature forest trees under elevated CO₂ is still limited due to logistic constraints. Currently, there are approximately 20 free air CO₂-enrichment (FACE) experiments, but only three out of these are testing trees taller than five meters (Ellsworth *et al.* 1995, Wullschleger & Norby 2001, Schäfer *et al.* 2002, Cech *et al.* 2003). The Swiss Canopy Crane (SCC) site hosts the only FACE device testing the influence of elevated CO₂ on tall broad-leaved forest trees, an important vegetation type in large parts of the temperate zone.

In summary, reported responses of forest trees to elevated CO₂ in terms of reduced water consumption vary widely from no response (Ellsworth 1999, for *Pinus taeda*) to 25 % in *Liquidambar styraciflua* (Wullschleger & Norby 2001, Schäfer *et al.* 2002). Most studies report sap flow or stomatal conductance data. While this is a needed first step, it is important to note that neither sap flow density (confounded with stem repletion) nor stomatal conductance (in series with other conductances, i.e. canopy conductance) are linearly related to tree transpiration. Summarising results from different studies is also delicate, because the exact weather conditions greatly influence net CO₂ effects. Long-term studies help to average responses across many different environmental conditions. Of particular interest are studies that combine environmental drivers likely to coincide in the future, above all warming, elevated CO₂ and precipitation frequency/abundance. However, in field experiments with tall trees, such combinations of environmental drivers cannot be planned (because weather conditions are not foreseeable). The species-specific response of tree water consumption on the interaction of these drivers will be the key to future predictions of forest water use.

In the studies cited above, one single method (sap flow or stomatal conductance) is applied to estimate reduced water consumption of forest trees (mostly one or two species) under elevated CO₂. Comparing several species and especially the parallel use of various methods can substantiate such predictions. Soil

moisture as a relatively simple measure of net water use (integrating effects of stomatal conductance, LAI, canopy resistance) is rarely reported in sufficient temporal and spatial resolution to discern CO₂-effects (Ellsworth 1999, Gunderson *et al.* 2002, Schäfer *et al.* 2002). Latest advances in high-resolution infrared thermography not only allow an accurate way of assessing plant transpiration Leinonen *et al.* (2006), they also permit to describe temperature frequency distributions of plant leaves in an unprecedented resolution. The methodology has not yet been applied to detect leaf warming under elevated CO₂ due to reduced latent heat flow in forest trees.

This doctoral thesis attempts to assess water relations of tall deciduous forest trees subjected to elevated CO₂ under normal weather conditions and in combination with drought. A series of partly novel techniques (e.g. thermography) were used to this end. After the general introduction, chapter 2 estimates total water savings using sap flow, soil moisture and thermography data (*Global Change Biology*, in revision). Chapter 3 reports responses of forest trees to the centennial drought over Central Europe in the summer of 2003, partly combined with the effect of CO₂ (published 2005 in *Tree Physiology*). Chapter 4 (co-authored) compiles stomatal conductance data over the first 4 years of CO₂-enrichment at the SCC site (*Trees*, in revision). Chapter 5 analyses spatial and temporal temperature distributions of deciduous forest trees, irrespective of the CO₂ treatment (submitted to *Agricultural and Forest Meteorology*). Chapters 6 to 8 are short unpublished analyses: chapter 6 is a sensitivity analysis to assess the plausibility of detecting reduced transpiration by leaf warming, with the given variation at the site. Chapter 7 suggests a predictive model for sap flow with environmental variables as predictors. Chapter 8 is a short note on the problematic of analysing relative data in general, with sap flow data as an example. Chapter 9, the general summary, concludes the thesis.

References

- Basset Y, Horlyck V, J WS (2003) *Studying Forest Canopies from Above: The International Canopy Crane Network*. Smithsonian Tropical Research Institute, Panama.
- Cech PG, Pepin S, Körner C (2003) Elevated CO₂ reduces sap flux in mature deciduous forest trees. *Oecologia*, **137**, 258–268.
- Cox PM, Betts RA, Jones CD, Spall SA, Totterdell IJ (2000) Acceleration of global warming due to carbon-cycle feedbacks in a coupled climate model (vol 408, pg 184, 2000). *Nature*, **408**, 750–750.
- Crowley TJ (2000) Causes of climate change over the past 1000 years. *Science*, **289**, 270–277.
- Crutzen PJ (2002) Geology of mankind. *Nature*, **415**, 23–23.
- Curtis PS, Wang XZ (1998) A meta-analysis of elevated CO₂ effects on woody plant mass, form, and physiology. *Oecologia*, **113**, 299–313.
- Ellsworth DS (1999) CO₂ enrichment in a maturing pine forest: are CO₂ exchange and water status in the canopy affected? *Plant Cell and Environment*, **22**, 461–472.
- Ellsworth DS, Oren R, Huang C, Phillips N, Hendrey GR (1995) Leaf and Canopy Responses to Elevated CO₂ in a Pine Forest under Free-Air CO₂ Enrichment. *Oecologia*, **104**, 139–146.
- Gunderson CA, Sholtis JD, Wullschleger SD, Tissue DT, Hanson PJ, Norby RJ (2002) Environmental and stomatal control of photosynthetic enhancement in the canopy of a sweetgum (*Liquidambar styraciflua* L.) plantation during 3 years of CO₂ enrichment. *Plant Cell and Environment*, **25**, 379–393.
- Idso SB, Kimball BA, Akin DE, Kridler J (1993) A general relationship between CO₂-induced reductions in stomatal conductance and concomitant increases in foliage temperature. *Environmental and Experimental Botany*, **33**, 443–446.
- IPCC Synthesis Report (2001) *Climate Change 2001*. IPCC, Geneva, Switzerland.
- Jacobs CMJ, Debruin HAR (1992) The Sensitivity of Regional Transpiration to Land-Surface Characteristics - Significance of Feedback. *Journal of Climate*, **5**, 683–698.
- Jarvis PG, McNaughton SJ (1986) Stomatal control of transpiration: scaling up from leaf to region. *Advances in Ecological Research*, **15**, 1–49.
- Johnson MG, Rygielwicz PT, Tingey DT, Phillips DL (2006) Elevated CO₂ and elevated temperature have no effect on Douglas-fir fine-root dynamics in nitrogen-poor soil. *New Phytologist*, **170**, 345–356.
- Körner C (1998) Tropical forests in a CO₂-rich world. *Climate Change*, **39**, 297–315.
- Körner C (2000) Biosphere responses to CO₂ enrichment. *Ecol. Appl.*, **10**, 1590–1619.
- Körner C (2003) Ecological impacts of atmospheric CO₂ enrichment on terrestrial ecosystems. *Philosophical Transactions of the Royal Society of London Series A - Mathematical Physical and Engineering Sciences*, **361**, 2023–2041.

- Körner C (2004) Die Biosphäre als Energiequelle und Kohlenstoffsенке. *Nova Acta Leopoldina*, **NF 91**, **Nr. 339**, 287–303.
- Leinonen I, Grant OM, Tagliavia CPP, Chaves MM, Jones HG (2006) Estimating stomatal conductance with thermal imagery. *Plant Cell and Environment*, **29**, 1508–1518.
- Loladze I (2002) Rising atmospheric CO₂ and human nutrition: toward globally imbalanced plant stoichiometry? *Trends in ecology & evolution*, **17**, 457–461.
- Medlyn BE, Barton CVM, Broadmeadow MSJ, *et al.* (2001) Stomatal conductance of forest species after long-term exposure to elevated CO₂ concentration: a synthesis. *New Phytologist*, **149**, 247–264.
- Millennium Ecosystem Assessment (2005) *Ecosystems and Human Well-being: Synthesis*. Island Press, Washington DC.
- Moorcroft P (2006) How close are we to a predictive science of the biosphere? *Trends in Ecology and Evolution*, **21 (7)**, 400–407.
- Morgan JA (2002) Looking beneath the surface. *SCIENCE*, **298**, 1903–1904.
- Olson JS, Watts J, LJ A (1983) Carbon in live vegetation of major world ecosystems. *Report ORNL-5862, Oak Ridge National laboratory, Oak Ridge, TN*.
- Oren R, Ellsworth DS, Johnsen KH, *et al.* (2001) Soil fertility limits carbon sequestration by forest ecosystems in a CO₂-enriched atmosphere. *Nature*, **411**, 469–472.
- Petit JR, Jouzel J, Raynaud D, *et al.* (1999) Climate and atmospheric history of the past 420,000 years from the Vostok ice core, Antarctica. *Nature*, **399**, 429–436.
- Raschke K (1986) *Carbon dioxide enrichment of greenhouse crops. Volume 2. Physiology, yield and economics*, chapter The influence of the CO₂ content of the ambient air on stomatal conductance and the CO₂ concentration in leaves., pp. 87–102. CRC Press, Boca Raton, Florida, USA.
- Rodhe H (1990) A comparison of the contribution of various gases to the greenhouse-effect. *Science*, **248**, 1217–1219.
- Roy J MH Saugier B (2001) *Global terrestrial productivity*. Academic Press, San Diego, pp. 1-6 pp.
- Schäfer KVR, Oren R, Lai CT, Katul GG (2002) Hydrologic balance in an intact temperate forest ecosystem under ambient and elevated atmospheric CO₂ concentration. *Global Change Biology*, **8**, 895–911.
- Shaw MR, Zavaleta ES, Chiariello NR, Cleland EE, Mooney HA, Field CB (2002) Grassland responses to global environmental changes suppressed by elevated CO₂. *Science*, **298**, 1987–1990.
- Shukla J, Nobre C, Sellers P (1990) Amazon deforestation and climate change. *Science*, **247**, 1322–1325.
- Siegenthaler U, Stocker TF, Monnin E, *et al.* (2005) Stable carbon cycle-climate relationship during the late Pleistocene. *Science*, **310**, 1313–1317.
- The Millenium Development Goals Report (2005) United Nations Department of Public Information.
- Vidale PL, Stockli R (2005) Prognostic canopy air space solutions for land surface exchanges. *Theoretical and Applied Climatology*, **80**, 245–257.
- Wullschlegel SD, Norby RJ (2001) Sap velocity and canopy transpiration in a sweetgum stand exposed to free-air CO₂ enrichment (FACE). *New Phytologist*, **150**, 489–498.

Chapter 2

Water savings in mature deciduous forest trees under elevated CO₂ - a multifactorial approach

Water savings in mature deciduous forest trees under elevated CO₂ - a multifactorial approach

Global Change Biology, in revision

Sebastian Leuzinger and Christian Körner

Abstract Stomatal conductance of plants exposed to elevated CO₂ is often reduced. Whether this leads to water savings in tall forest-trees under future CO₂ concentrations is largely unknown but could have significant implications for climate and hydrology. Forest-trees of ca. 35 m height and 100 years of age exposed to elevated CO₂ concentration (540 ppm during daylight hours) using free air CO₂ enrichment (FACE) and the Swiss Canopy Crane (SCC) in NW-Switzerland indicate reduced water consumption by year 4 and 5, but signals are highly variable between species (*Quercus petraea*, *Fagus sylvatica* and *Carpinus betulus*). Across species and a wide range of weather conditions, sap flow was reduced by 14 % in trees subjected to elevated CO₂, but this signal is likely to diminish as atmospheric feedback comes into play at landscape scale. Because sapwood cannot reliably be assessed in these experimental trees and because the position of individual crowns in the upper canopy varies, we standardised the sap flow of each individual tree with its own maximum during the period in consideration. This analysis arrived at water savings of ca. 16 to 20 %. The CO₂-effect is greatest at low vapour pressure deficit (vpd). The effect was largely produced by *Carpinus* and *Fagus*, with *Quercus* contributing little. In line with these findings, soil moisture at 10 cm depth decreased at a slower rate under high-CO₂ trees than under control trees during rainless periods, with a reversal of this trend during prolonged drought when CO₂-treated trees take advantage from initial water savings. High resolution thermal images taken at different heights above the forest-canopy did only detect reduced water loss through altered energy balance at close distance (0.44 K leaf warming of CO₂-treated *Fagus* trees). Short discontinuations of CO₂ supply had no measurable canopy temperature effects, most likely because the stomatal effects were small compared to the aerodynamic constraints in these dense, broad-leaved canopies.

Introduction

Partial stomatal closure under elevated CO₂ can lead to substantial water savings (Morison & Gifford 1984, Medlyn *et al.* 2001) and therefore has the potential to significantly influence our climate (Field *et al.* 1995, Morgan *et al.* 2004). However, a lot of the information available to date comes from small plants, in the case of trees from seedlings, young saplings or branches and much less is known for entire tall forest trees exposed to elevated CO₂. On average, stomatal conductance (g_s) of trees is reduced by 9 %, (non-significant, leaf based data from 10 studies in adult broad-leaved and coniferous trees, Medlyn *et al.* 2001). Out of the currently ca. 15 free air CO₂ enrichment (FACE) experiments, only five are testing trees, out of these, three use trees higher than 5 m (Ellsworth *et al.* 1995, Ellsworth 1999, Wullschlegel and Norby 2001, Schäfer *et al.* 2002, Cech *et al.* 2003). These studies report water savings under elevated CO₂ ranging from no response at all (Ellsworth 1999, for *Pinus taeda*) over an average of 13 to 25 % in *Liquidambar styraciflua* (Wullschlegel & Norby 2001, Schäfer *et al.* 2002), to a maximum of (marginally significant) 22 % at low vpd for six different deciduous forest-tree species during the initial experimental month at the Swiss Canopy Crane (SCC) site (Cech *et al.*, 2003).

Depending on the aerodynamic coupling, net water savings of forests under elevated CO₂ - the actual quantity of interest - are lower than expected from stomatal response alone. Stomata appear to respond in such a way that the total transfer resistance (including the aerodynamic component) meets the plant's needs (Meinzer *et al.*, 2001). Therefore, it is not possible to accurately infer actual transpiration from stomatal conductance data often collected in CO₂ experiments. As an example, well coupled conifers, less coupled deciduous trees and poorly coupled grassland supposedly arrive at similar water savings at strongly diverging stomatal conductance (Körner *et al.*, 2006): there is no measurable change in g_s in tall conifers (Ellsworth 1999, Körner 2003), 50 % reduction of g_s in dense grassland (Niklaus &

Körner 2004, Morgan *et al.* 2004) with adult deciduous trees holding an intermediate position (e.g. Keel *et al.* 2006, in review). Even if actual transpiration responses to elevated CO₂ are known, it still remains unclear to what extent atmospheric feedback (less humidified air and slight increases in foliage temperature) will mitigate plot scale CO₂-effects on water consumption (Field *et al.* 1995, Jacobs & de Bruin 1997, Amthor 1999, Morgan *et al.* 2004). Assessing whole tree transpiration and in particular its vpd-response to CO₂ enrichment in tall trees is a much needed first step. Even if feedback processes mitigate or even enhance the initially found water savings effects, species specific vpd-response curves are the basis for all modelling attempts aimed at uncovering the final net water savings occurring in a forest ecosystem.

There are three ways to study tree-forest water vapour loss: (1) stem flow measurements, (2) soil moisture responses and (3) measurements in or above the canopy using leaf gas exchange techniques or micrometeorological methods. We adopted all three approaches, but emphasis was on sap flow with the advantage that the signal averages across leaf, branch or crown-level variation and permits continuous readings without interfering with the leaves' environment.

Sap flow can be assessed in various ways (Köstner *et al.*, 1998), for the present long-term study in tall trees, we found the least invasive method by Granier (1985) most appropriate.

Soil moisture offers an indirect measure of reduced water consumption, is easy to measure but is rarely reported in the CO₂ literature. Only three studies from the other FACE experiments with trees show data for soil moisture or soil water potential differences. Two find a non-significant trend for higher soil moisture or soil water potential under elevated CO₂ (Ellsworth 1999, Gunderson *et al.* 2002). Schäfer *et al.* (2002) find no differences in the calculated soil water storage between CO₂-treatments. In the other cases, differences became greater with drying soil. Interpreting soil moisture signals in terms of absolute water uptake would require data for the full rooted profile, which is impossible to obtain in our case, because of the rocky underground and unknown maximum rooting depth. However, top soil signals provide a qualitative estimate of water use by trees.

For assessing actual canopy water loss, the conventional eddy flux covariance method cannot reliably be applied at the small scales needed, but the leaf energy balance can be assessed using the canopy crane. We employed an energy balance approach using a latest technology, high-resolution thermal camera, which yields canopy surface temperature (a proxy for latent heat flux through altered leaf temperature; Jones 1999). All factors being constant, a reduction in canopy transpiration should entail an increase in

canopy temperature as has been demonstrated in the laboratory and for agricultural crops (Fuchs, 1990). This technique has never been applied to tall tree foliage. Although the leaf energy balance of leaves is difficult to quantify in a rough natural forest canopy, a relative relative comparison is still possible (Jones, 1999).

This study builds upon earlier results from the same site by Cech *et al.* (2003) who, in the first three months of CO₂-enrichment, only found a slight tendency of reduced water consumption of treated trees, based on sap flow data only. Here, we apply two additional, completely independent approaches, namely soil moisture and thermal imaging, to assess potential water savings of deciduous forest trees under future CO₂ concentration. Most importantly, however, we provide species specific vpd-response curves of transpiration at ambient and elevated CO₂. These responses permit modelling of the water balance of forests under future climatic conditions.

Materials and Methods

Site description and studied species

The experiment was conducted in a diverse mixed forest stand located 15 km south of Basel, Switzerland (47° 28' N, 7° 30' E; elevation: 550 m a.s.l.). The forest is approximately 100 years old with canopy tree heights between 30 and 38 m. The stand has a stem density of 415 trees ha⁻¹ (diameter ≥ 10 cm), a total basal area of 46 m² ha⁻¹ and a leaf area index of ca. 5 in the experimental area. It is dominated by *Fagus sylvatica* L. and *Quercus petraea* (Matt.) Liebl., with *Carpinus betulus* L., *Tilia platyphyllos* Scop., *Acer campestre* L. and *Prunus avium* L. present as companion species. In addition, the site has a strong natural presence of conifers outside of the CO₂-enriched zone (*Abies alba* Mill., *Picea abies* L., *Pinus sylvestris* L.). For the present investigation, we selected the most abundant *Quercus petraea*, *Fagus sylvatica* and *Carpinus betulus*, henceforth referred to by their genus only. We used six trees each (three treated, three controls) for all analyses, i.e. 18 trees in total.

The soil is a silty-loamy rendzina that developed on calcareous bedrock. Deep soil water was assessed independently of the CO₂-treatment to roughly estimate the vertical soil moisture distribution using four 90 cm PRB-F time domain reflectometry probes (Environmental Sensor, Victoria, BC, Canada). Soil water was nearly uniformly distributed between 0 and 90 cm throughout the 2004 and 2005 growing season. However, with increasing rock density at depth, fine substrate becomes very scarce and the actual moisture per total bulk volume becomes very small. The climate is a typical humid temperate zone climate,

characterised by mild winters and moderately warm summers. During the two study years (2004 and 2005), the growing season of deciduous trees lasted from the end of April to the end of October (ca. 180 days, Asshoff *et al.* 2006, Körner *et al.* 2005 and unpublished data). Mean January and July temperatures are 2.1 and 19.1° C. Total annual precipitation at the study site was 950 mm in 2004 and 910 mm in 2005, which is in close correspondence to the expected long-term average at that site (990 mm). Normally, two-thirds fall during the growing season. The growing season 2004 can be considered much drier than the one in 2005, as only 41 % of the precipitation occurred during May to September (64 % in 2005), while 36 % occurred in January and October combined.

At the start of the two 22-day test periods (see below) studied in 2004 and 2005, initial soil moisture was similar, but total cumulative rainfall in the 2004 period amounted to 16 mm only, while 60 mm of rain fell during the 2005 test period.

Free air CO₂ enrichment system (FACE)

A 45-m freestanding tower crane equipped with a 30-m jib and a working gondola provided access to 64 dominant trees in an area of ca. 3000 m². A group of 14 adult broad-leaved trees (3 *Fagus*, 4 *Quercus*, 4 *Carpinus*, 1 *Tilia*, 1 *Acer* and 1 *Prunus*), covering a canopy area of ca. 550 m² were selected for CO₂ enrichment. For this study, only nine CO₂-treated trees (three each from *Quercus*, *Fagus*, and *Carpinus*) were used. Nine non-treated trees (three per species) located in the remaining crane area at sufficient distance from the CO₂ release zone were used as controls. A series of pre-treatment measurements assured that there was no hidden background effect between the two groups (Cech *et al.* 2003, Asshoff *et al.* 2006). CO₂-enrichment of the forest canopy was achieved by a free-air, pure CO₂ release system that consisted of a web of 4 mm plastic tubes (ca. 0.5 km per tree) with 0.5 mm laser punched holes (spaced at 30-cm intervals) emitting pure CO₂ into the tree canopy (FACE). For a more detailed description, see Pepin & Körner (2002).

Climatic data

Wind speed, photon flux density, rainfall, air temperature and relative humidity were measured above the tree canopy using a weather station located at the top of the crane (anemometer AN1, quantum sensor QS and a tipping bucket rain gauge RG1, all from Delta-T, Cambridge, UK). Measurements were performed every 30 s and data were recorded as 10-min means using a data logger (DL3000, Delta-T, Cambridge, UK). Vapour pressure deficit (henceforth referred to as vpd) was calculated from wet and dry bulb, self-made aspiration psychrometer (10-min

averages) located at canopy height.

Soil moisture data

We assessed potential treatment effects on soil moisture by three different probe types: firstly, we used a handheld TDR device (Trime-FM, Imko, Ettlingen, Germany, here referred to as the 'handheld TDR probe') for manual sampling of soil moisture in the top 10 cm on May 17 and August 12 2004. The device allowed us to take readings from ca. 80 spots within two hours. For better temporal resolution, we also used probes working with the capacitance principle (ECH2O, Decagon, Pullman, Washington; henceforth referred to as 'echo probes'). Thirty of these probes (half of which in the treated area) were placed at 10 cm depth and read out daily during dry periods. Thirdly, eight (5 ambient, 3 elevated) time domain reflectometry probes (ML2x probes, Delta-T, Cambridge, UK; henceforth referred to as 'TDR probes') logged hourly in order to provide high time resolution.

Sap flow measurements

Sap flow sensors consisted of two 20-mm long and 2-mm diameter probes (each equipped with a copper-constantan thermocouple and coated with heating wire) inserted radially into the sapwood after phloem removal at breast height with a vertical spacing of 15 cm using 2 mm aluminium tubes (UP, Kolkwitz, Germany). Two pairs of sensors per tree (installed on opposite sides of the stem) were used and the average of both readings per tree was taken for further analysis. Sensors were protected against rain and external thermal influences with aluminium covers filled with polyester wool. Readings were taken at 30 s intervals and recorded as 10-min means using multi-channel data loggers (DL2e, Delta-T, Cambridge, UK). Sensors were removed during the winter and re-installed in new positions in spring 2005, as recommended by Köstner *et al.* (1998). The upper of the two probes received a constant power of 200 mW while the lower reference probe remained unheated. During conditions of minimal sapflow such as at night or during prolonged rain events the temperature difference, ΔT , between the two probes reached a maximum (ca. 9-15 K, depending on thermal conductivity of the surrounding wood, exact sensor position etc.). Sap flow during the day thus causes a decrease in ΔT . Sap flow measurements were performed during most of the growing season in 2004 and 2005, but due to periodic sensor and logger failure, we had to select periods with reliable and continuous data for the analyses (two times 22 days, June 16 to July 6, 2004 and July 20 to August 10, 2005). Due to a time-stamp problem with one data logger in 2004, we can only show the cumulative data (Figure 1) for this year. Millivolt data were converted to sap flow

density according to Granier (1985), except that we divided by the absolute maximum (extreme outliers removed) of the whole 22-day period instead of pre-nightly maxima. This had marginal ($< 5\%$) effects on sap flow density because our readings were stable and our comparisons restricted to 22 days. This procedure also avoided daily step changes of signals (monotonic signals required for our alternative data analysis, see below). Another advantage is the possibility of analysing night-time sap flow. For the right panel in Figure 1, we divided the sap flow series by the maximum (mean of 10 highest values per tree) of the according species (again per 22 day period), in order to prevent the pooled results from being overridden by a species effect. Given the unknown stem characteristics, it was impossible to arrive at an absolute sap flow density (J_s , $\text{m}^3 \text{H}_2\text{O m}^{-2}$ per sapwood area s^{-1}). Any such calculations using existing equations would be highly pretentious. We therefore do not specify units and refer to our data as ‘relative’ sap flow. For Figure 1, we calculated cumulative sap flow (sum over all 10 minute time steps of each 22-day period. We have no pretreatment sap flow data (from years before 2001), but a number of other tree variables (Cech et al., 2003) suggest that there were no a priori differences between the two groups of trees. Most importantly, the pre-treatment rate of growth of trees (as assessed by tree rings) did not differ (Asshoff et al., 2006).

The variation in sap flow between trees was high despite using the mean of two sensors per tree. We attribute this to the natural growth conditions of these trees and their variation in stem diameter and canopy position. We divided each tree’s sap flow readings by its own maximum, i.e. we standardised the 2005 22-day time series to a range from 0 to 1 (here referred to as ‘standardised’ sap flow data). We calculated the ratio of the mean flux under elevated CO_2 (E) to that under ambient air (A) (all species pooled). The resultant E/A ratio curve of 22 diurnal courses was then compacted by randomly resampling (with replacement) 99 times every time of day (from 0:00 to 23:50, 10 min intervals) out of the 22-day series, in order to yield one average daily E/A curve. As will be discussed later, standardisation by noon maxima inevitably removes any signal from midday, but retains differences at the two diurnal tails at contrasting vpd (morning, evening), for which water savings under elevated CO_2 can be estimated.

Thermal imaging

Leaf temperatures were measured using a state-of-the-art thermal camera (VarioCam, Infratec, Dresden, Germany) with a resolution of 240×320 pixels, providing 76’800 temperature readings with a 0.1 K resolution. We measured at three different scales: from the crane gondola (ca. 5 m above the

canopy), from the counter jib of the crane (ca. 12 m above the canopy) and from a helicopter (ca. 200 m above the canopy). At the smallest scale, we monitored adjacent, similarly exposed, treated and non-treated trees on two sunny days in 2004 taking IR-pictures at 0.2 Hz from the crane gondola of *Quercus* and *Fagus* during a period of 50 minutes. Picture matrices were accumulated (averaged), then the mean of the control and the treated area was calculated. Due to the given distance between treated and non-treated *Carpinus* trees, there are no data for this species (within-picture analysis was impossible). For the on/off experiments (discontinuation of CO_2 supply during one hour), the camera was attached to a pole reaching out from the counter jib of the crane in order to centre the camera over the CO_2 -treated area. We took IR-pictures at a frequency of 1 Hz on two cloud-free days with little wind. On June 24, we scanned from 7:30 to 10 hours (true local time) and switched off the CO_2 supply from 8 to 9 hours. On August 17, we monitored temperature of a different part of the canopy from 7:20 11:50 hours, interrupting the CO_2 supply from 7:50 to 8:50 and again from 9:50 to 10:50 hours. All thermal images were cleaned from what was clearly identified as background and non-leaf temperatures (e.g. branches, forest soil). In 2004, thermal pictures of the SCC FACE site (including a large control area) were taken from a helicopter at ca. 200 m above ground around noon on a cloud-free day. Hence we have covered a spatial range from 100 m to a few cm and temporal ranges from simple images to a frequency of 1 Hz during nearly one hour.

Data processing and statistical analysis

A non-parametric Wilcoxon rank sum test was used where replication was low and/or error distribution was not normal. Readings of the ‘TDR probes’ were compared by ranks, in order to avoid a violation of the assumption of normally distributed data. For analyses of thermal images, Irbis professional (Infratec, Dresden, Germany) was used. The free software package ‘R’, version 2.1.0 (R Development Core Team, 2004) was used for all data processing, statistical analyses and graphics.

Results

Sap flow

Mean relative sap flow (sum over all 10-min readings) was ca. 14 % lower in CO_2 -treated trees than in control trees during two periods of 22 days in summer 2004 and 2005 (all species and both years pooled, two sample Wilcoxon test, p-value = 0.028, Figure 1 right panel). In line with earlier findings obtained during the first three months of CO_2 -enrichment

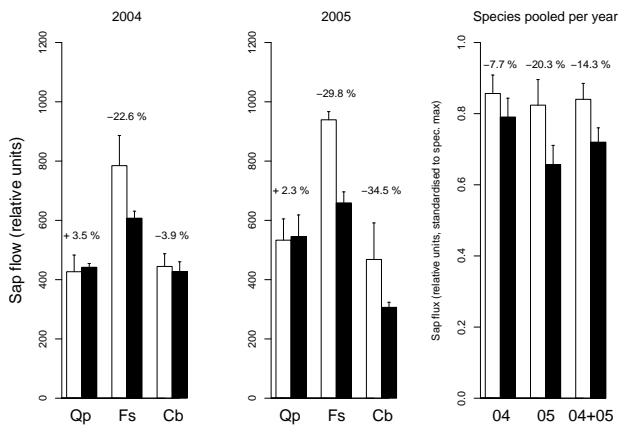


Figure 1: Total cumulative sap flow (relative units) of *Quercus* (Qp), *Fagus* (Fs) and *Carpinus* (Cb) from June 16 to July 6 2004 (22 days, left panel) and from July 20 to August 10 2005 (centre panel) with percent change from ambient (white columns) to elevated (filled columns) trees indicated. Error bars represent one standard error. Right panel: species pooled for same periods, but with data standardised to highest value per species and year to exclude absolute differences between species. Only pooled species were tested using a two sample Wilcoxon test, p-value = 0.26 for 2004, 0.16 for 2005 and 0.028 for both years pooled, n=9 trees per treatment.

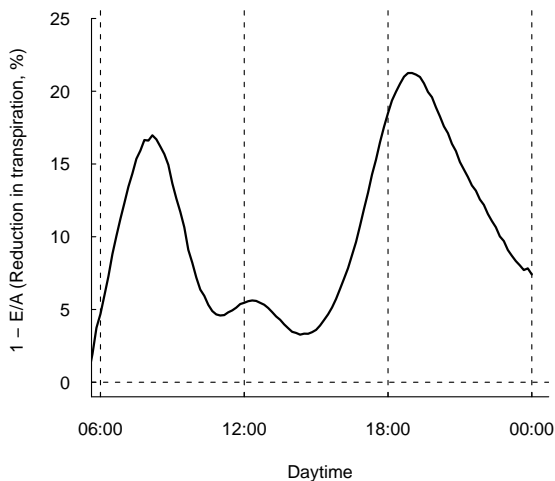


Figure 2: The ratio of 1 minus the CO_2 -treated to ambient (1-E/A) series of standardised sap flow data (bootstrapped data of the 2005 22-day period (July 20 to August 10) and all species pooled, each tree standardised to its own mean maximum within the period, n=9 trees per treatment). Time is plotted against one minus this ratio which corresponds to % reduced transpiration of treated trees compared to control trees. Note the two humps in the morning and late afternoon indicate reduced transpiration in CO_2 -treated trees, whereas the midday depression originates from the fact that all trees have been standardised to their own maximum in sap flow. This procedure removes any tree or taxon specificity of sap flow, at the price of losing midday signals.

(Cech *et al.*, 2003), this response was largely due to *Carpinus* and *Fagus*, but statistical power was too low for testing effects at the species level. *Quercus* did not show any reduction in transpiration under elevated CO_2 in both years. The CO_2 -effect across trees was less pronounced during the drier 2004 period. Apart from the CO_2 effect, tree size, canopy architecture and sapwood thickness influence the direct sap flow readings. Standardised data instead permit a qualitative comparison of the sap flow responses, irrespective of the actual readings of the probes. The mean bootstrapped 1-elevated/ambient (1-E/A) ratio curve for an average day out of the 2005 22-day period (Figure 2) shows 16 and 20 % water savings in the morning and in the afternoon respectively. This is in close agreement with the whole-day water savings of the non-standardised data for this year presented in Figure 1. The curve is obviously forced to near zero around midday and thus contains no signal for this period (peak flow was set to 1.0 irrespective of treatment and tree).

The fact that the 1-E/A flow ratio curve stays above zero at night indicates that some water savings may occur even during the night, i.e. there is less flow to replenish daytime deficits in trees exposed to elevated CO_2 during the day. Flow maxima averaged in tree-specific relative signals were reached ca. 30 min earlier in CO_2 -treated trees (Wilcoxon test, p = 0.028), a time shift which may explain the small hump around noon in the 1-E/A ratio series (Figure 2).

To determine the dependency of transpiration on evaporative demand in a CO_2 -enriched atmosphere, we plotted relative sap flow data against vpd (Figure 3). At any given vpd, sap flow of CO_2 treated trees (all species pooled) was lower than sap flow of control trees, but there was a ca. 20 % diminishing of the water saving effect as vpd rose from close to 0 to 17 hPa (translating into a 20 % increase in the E/A percentile ratio over this vpd range, Figure 3, bottom panel). Differences between species were pronounced: *Quercus* showed no change in the vpd response curve under enriched CO_2 , both ambient and elevated trees reached the turning point (where saturation of sap flow starts) at around 4.5 hPa (Figure 3, top panel). However, in *Fagus* and *Carpinus*, the sap flow saturation point was shifted markedly to the right (higher vpd) under high CO_2 . For all species pooled, the ratio of the elevated to the ambient slope (linear regression with the first four 95th percentiles, see Figure 3) is 0.68, representing the difference in vpd-response that is attributable to tree properties alone (stomata, crown specific

aerodynamics).

Soil moisture

With two out of the three methods applied to monitor soil moisture under treated and non-treated trees, the mean was higher under trees exposed to elevated CO₂ than under control trees, except during and immediately after significant rainfall (Figure 4, bottom panel) or after long periods of drought such as in the year 2003 (Leuzinger et al. 2005). The spatially highly replicated measurements with the handheld TDR probe yielded a ca. 2 % higher soil moisture in the top 10 cm of the treated area (mean values of May 25 and August 12 2004, $\bar{x} = 28.6 \% \pm 0.62$ s.e., $n=56$ in the control area and $\bar{x} = 30.7 \% \pm 0.64$ s.e., $n = 61$ in the treated area, t-test, $p < 0.05$). Because of less spatial replication, the signal was not detectable between the 2 x 15 echo probes (because of the high spatial variation) neither in absolute terms nor when each sensor was standardised to its own maximum, i.e. its field capacity after rain (Wilcoxon test, p-value = 0.70). Finally, the treated versus control readings of the TDR probes were entirely apart by their ranks both in their mean values and, more importantly, in their slopes (rate of drying) during both 22-day periods ($n=5$ in the control area and $n=3$ in the treated area, Figure 4). The relatively slower drying of soils during rainless periods in the CO₂-treated area provides stronger evidence for reduced transpiration under elevated CO₂ than the mere means of absolute difference in soil moisture at one point in time, which are strongly influenced by the local topography and varying soil bulk density due to vole activity. During the nearly completely rainless period in 2004 (Figure 4, upper panel), we could observe the deviation of the two drying rates to stop (ca. day of year 175) and even a slight reverse effect later (ca. day of year 182).

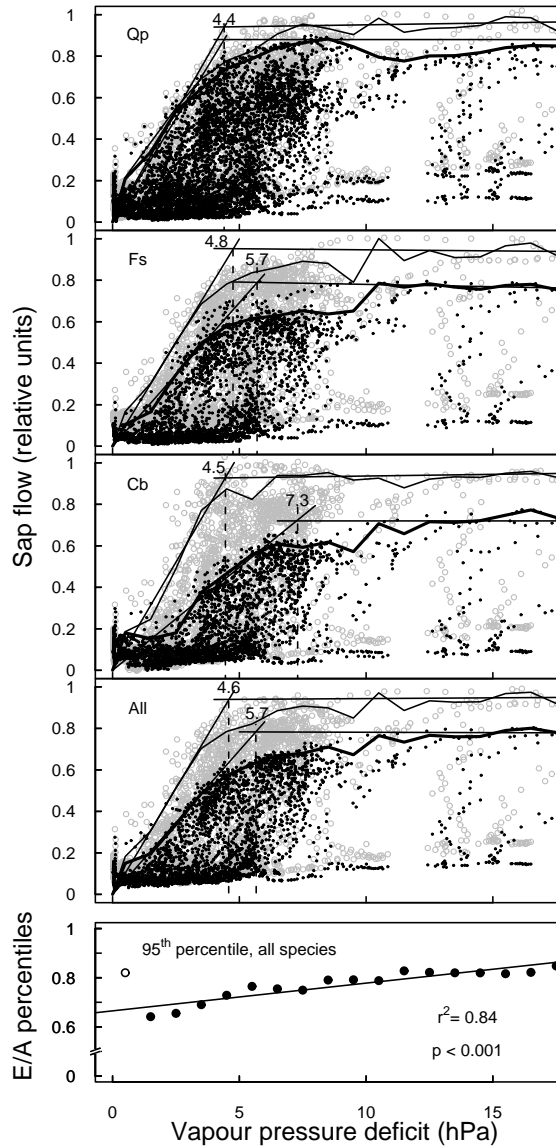


Figure 3: Response of sap flow to vapour pressure deficit between July 20 and August 10 2005 for *Quercus*, *Fagus*, *Carpinus* and all species pooled, $n=9$ trees per treatment. Open grey circles are control trees (A), filled circles CO₂-treated trees (E). Thin lines show 95th percentiles for vpd (class width 1 hPa) of control trees, bold lines represent the equivalent for CO₂-treated trees. The marked turning points at which saturation starts, are inferred from the intersection of two linear regressions (first four and last seven percentile classes). The bottom panel shows the E/A ratio of the 95th percentiles of all species. Note the decrease of the effect as vpd increases (translating into a rise of the E/A percentile ratio).

Canopy surface temperature

At only one out of the three scales at which canopy temperature was monitored, we were able to discern foliage temperature differences due to altered leaf transpiration. At the smallest scale, comparing treated and non-treated parts of the canopy within the same image, the temperature distributions of CO₂ treated and non-treated *Fagus* foliage differed clearly ($\bar{x}_{control} = 25.89^\circ$ C, $\bar{x}_{treated} = 26.33^\circ$ C; $T_{air} = 24.7^\circ$ C), suggesting less latent heat loss of the CO₂-treated canopy. Corresponding with results from sap flow data, this difference did not appear in *Quercus* ($\bar{x}_{control} = 24.04^\circ$ C, $\bar{x}_{treated} = 23.97^\circ$ C; $T_{air} = 23.8^\circ$ C, Figure 5; no data for *Carpinus* because CO₂-treated trees and control trees were too

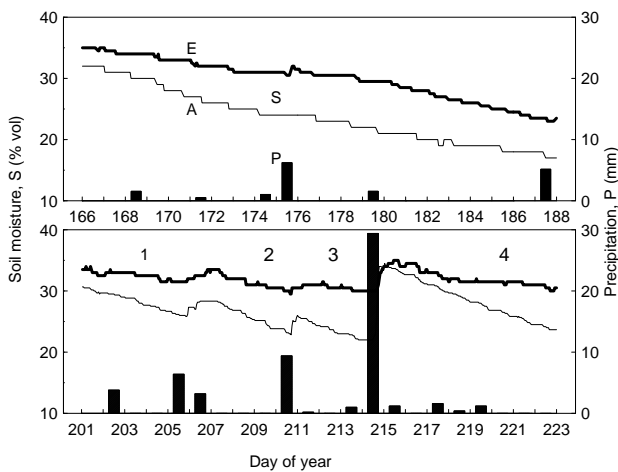


Figure 4: Soil moisture (TDR-probes, S_A , S_E at 10 cm depth, $n=3$ elevated area and $n=5$ control area) and rainfall (P) during the two 22-day periods in 2004 (June 16 to July 6) and 2005 (July 20 until August 10). Thick lines represent data from the CO_2 enriched area. Note the reverse effect in the nearly completely rainless 2004 period. The four dry periods in the bottom panel marked 1-4 are used to calculate the average ratio of slopes between elevated to ambient soil moisture decrease ($=0.62$, see text).

far apart to be captured in one image). At the intermediate scale (ca. 12 m above the canopy), we performed on/off experiments (switching off the CO_2 supply for one hour), taking sequel images (1Hz) from the counter jib of the crane on two cloud free mornings. Counter expectations neither increased sap flow significantly, nor did it cause canopy surface temperature to drop within the resolution of the available equipment (Figure 6). Lastly, single thermal images were taken from a helicopter at ca. 200 m above ground around noon. They included the complete CO_2 -treated area plus a large control area with similar species composition. The mean temperature of the treated area (ca. 2000 measurement points averaged) was 21.91°C and did not differ from the mean of the averages of 12 equally sized areas located in adequate distance around the CO_2 area ($21.88 \pm 0.15^\circ\text{C}$ s.e., t-test $p=0.5$; $T_{air}=24.2^\circ\text{C}$, Figure 7).

Discussion

Two completely independent approaches (sap flow and soil moisture) revealed water savings under elevated CO_2 in these adult deciduous forest trees. The third approach, high-resolution thermal imaging, yielded the weakest signal, only detectable at

Water savings - a multifactorial approach

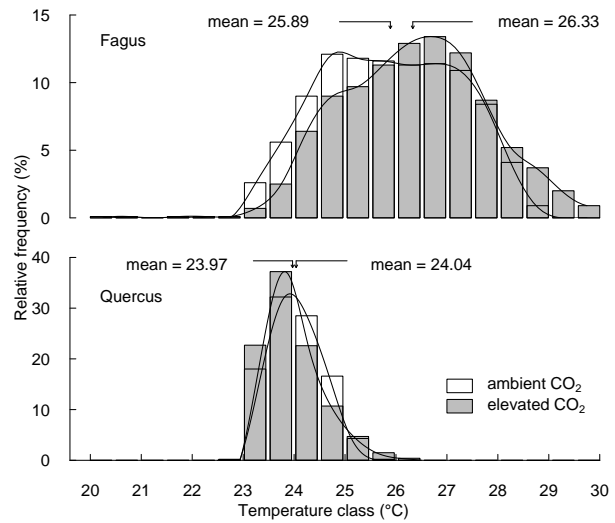


Figure 5: Temperature distributions in the CO_2 -treated canopy (class width = 0.5 K, black columns) and control canopy (white columns) of *Fagus* (top panel) and *Quercus* (lower panel). Pictures were taken at 0.2 Hz on cloud free, nearly calm days during noon (windspeed $< 1 \text{ ms}^{-1}$. Temperature matrices were overlain and averaged over 50 minutes.

the smallest scale (pairs of parts of elevated/ambient tree crowns). Though not significant, the trends in differences among species in relative sap flow were pronounced and confirmed initial data soon after the onset of CO_2 -enrichment (Cech *et al.*, 2003) and monitoring with porometry in the canopy over four years (Keel *et al.*, in review) with *Carpinus* always showing the strongest response to CO_2 (Figure 1).

Sap flow measurements have often been interpreted in absolute terms per unit sapwood area or to calculate the total amount of water transpired by a tree (Granier, 1985). This may work in individual trees with known sap wood properties or in homogenous, monospecific plantations with equally sized individuals. To obtain such quality of data, we would have to damage our trees or use more intrusive techniques, which is not an option in this long-term experiment. We had enough trees and sensors however to obtain a reliable relative sap flow signal that points at a significant reduction in tree water consumption of ca. 14% across all years and species (Figure 1). The variance was large however. This is due to the nature of our experiment that represents natural conditions where individuals differ beyond their taxonomic identity in size, exposure, sap wood thickness and canopy architecture. When standardised to their own maximum, transpiration data across species become more homogenous at the expense of losing the absolute signal at maximum sap flow (i.e. during late noon). However, as the flow rates decrease to either side of the midday peak, the standardisation bias decreases to close to zero early in the morning and late in the afternoon, yielding significant shape differences be-

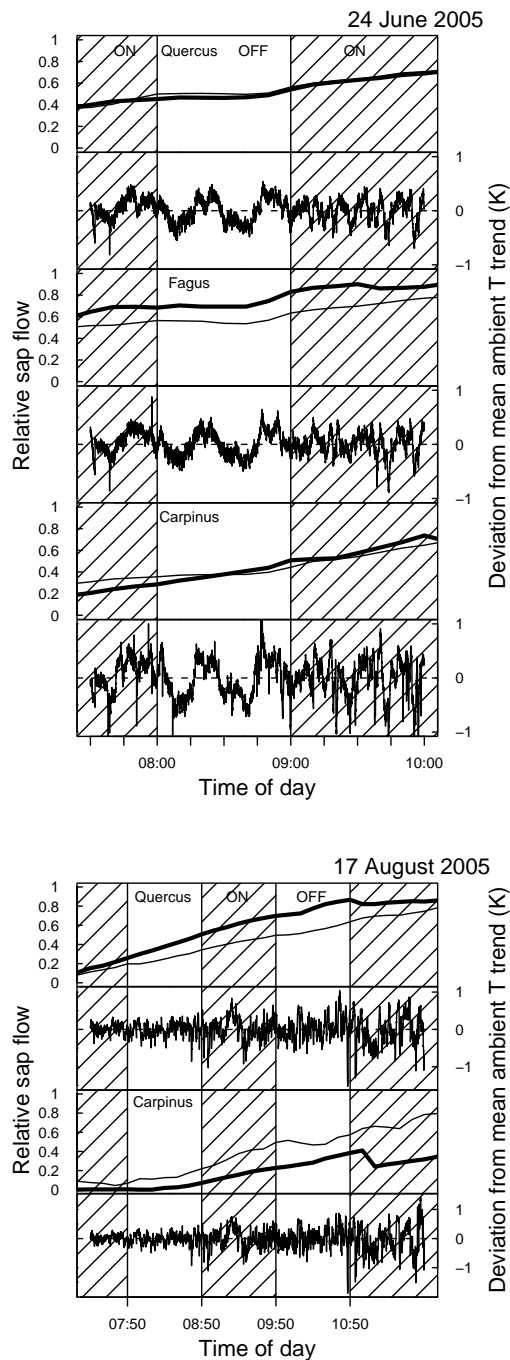


Figure 6: Relative flow and deviation from the mean canopy temperature trend during on/off experiments on June 24 (upper panel) and August 17 (lower panel). Non-hatched areas show times when CO₂ supply was interrupted. Three species were monitored on June 24 (*Quercus* n=3, *Fagus* n=1 and *Carpinus* n=2) and on August 17 (*Quercus* n=3, *Carpinus* n=2). During ‘off’ periods, sap flow would be expected to increase and temperature to decrease in CO₂-enriched trees, but no such pattern was observed in any of the shown examples.

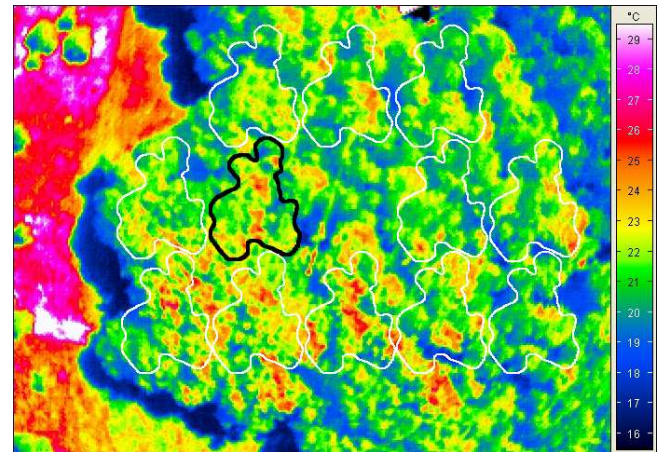


Figure 7: Airborne infrared photograph of the CO₂-treated area (black line) and 12 equally sized adjacent control areas on a clear day in July 2004. The mean surface temperature of the CO₂-plot is 21.91° and does not differ from the mean of the 12 control areas (21.88 ± 0.15 °C s.e.) at an air temperature of 24.2° C at the top of the crane.

tween the two mean, bootstrapped diurnal courses (symmetric for morning and evening, Figure 2). If the high and low CO₂-curves of the two groups of trees had the same shape, but only differed systematically in absolute values because of stem properties (sap wood thickness), the standardisation to noon maxima should remove elevated vs. ambient differential signals at all times, which is clearly not the case. The combination of the analysis of both (noisy) raw data and standardised relative data from three species provides strong evidence for overall water savings of CO₂-treated trees of around 16%. Cech et al. assumed ca. 10% reduction for the same trees during the first three months of CO₂-enrichment. We now have consolidated signals for water savings after a series of years of growth under elevated CO₂. The magnitude of the response is within the 13 to 25% range of sap flow reduction found for *Liquidambar styraciflua* (L.) (Wullschleger and Norby 2001, Schäfer et al. 2002). Remarkably, the CO₂-effect on sap flow was lower in the overall drier year 2004 (Figure 1 and 4). This may originate from substantial improvements in tree water status in elevated CO₂ during rainless periods, mitigating or even reversing the initial effect over a transition period, before soils become dessicated under elevated CO₂-trees as well (Figure 4, top panel). Prolonged reduction of water consumption under CO₂-enrichment leading to such a reverse effect was found earlier by Schäfer et al. (2002).

Water saving effects in a CO₂-enriched atmosphere need to be compared for defined evaporative conditions. We found that responses were most pronounced when atmospheric humidity was high (low vpd), which confirms the earlier observations by Cech et al. (2003) and Wullschleger et al. (2002). The

species specific differences of sap flow in response to vpd suggest that species composition in a catchment will be of prime importance for forest hydrology in a high-CO₂-atmosphere.

Total water loss by forests compared to precipitation also depends on interception losses by the canopy and evaporation from the forest floor, both most likely unaffected by elevated CO₂. Hence, at ecosystem scale, total CO₂-driven water savings will be reduced by ca. 30 % (Wullschleger *et al.*, 2002). Interception losses at our site were in fact 28 % (20 throughfall collectors) over the growing seasons 2004 and 2005. This alone (evaporation and stem flow neglected) reduces the net seasonal water savings in the CO₂ enriched area from 14 to 10 %. Accounting for stem flow and soil evaporation, the remaining CO₂-signal will become smaller than 10 %. Based on our data, we believe Gedney *et al.* (2006) overestimated the contribution to elevated CO₂ to enhanced run-off, at least for catchments in the temperate zone. It also came as a puzzle that in their analysis the same algorithms for stomatal effects arrive at continent-wide CO₂-driven water savings between 10 and 50 % depending on the continent. Data for temperate grassland water savings suggested a ca. 6 % reduction in evapotranspiration (Stocker *et al.*, 1997), even less of what we found here. Hence, the run-off signal assumed by Gedney *et al.* (2006) is likely to be reflecting other phenomena.

Night-time CO₂-signals of sap flow (when supply was switched off) came at a surprise. Out of the three drivers for night-time sap flow (night time transpiration, stem water repletion and xylem-phloem counter flow due to assimilate transport), stem repletion is the only one likely to be affected by daytime CO₂ enrichment. Daytime water savings of CO₂-enriched trees may indeed entail reduced stem repletion during the night. Further, we have evidence of moderated predawn water potentials in elevated CO₂ (Leuzinger *et al.*, 2005).

Although we cannot say much about species specific responses, there is a discrepancy between reduced sap flow in *Fagus* seen here (up to 30 % savings) and of a weak or absent stomatal response to elevated CO₂ in *Fagus sylvatica* (Dufrene *et al.* 1993, Cech *et al.* 2003, Keel *et al.*, in review, Figure 1). Apart from statistics, part of this divergence maybe related to methodology (branch bag CO₂-enrichment vs. FACE, Dufrene *et al.* 1993), differences due to the duration of CO₂-enrichment (Cech *et al.* 2003 2-3 months; here 4-5 years) or leaf level (Keel *et al.*, in review) vs. whole tree signals. We have evidence from litter traps, that *Fagus* grown in elevated CO₂ had its leaf canopy reduced by year 4 of the treatment in 2004 (Körner *et al.*, 2005) and this was retained 2005 (unpublished data), which would explain much of the sap flow signal we detected. If this trend

persisted into a new steady state, this would enhance canopy throughfall and hence soil moisture, adding an indirect, whole canopy component to the overall CO₂-signal. Such canopy scale feedback on water relations had not yet been reported.

Reduced forest evapotranspiration (ET) of ca. 10 % should result in slower drying of the soil, and it clearly does. More specifically, the ratio of the elevated to the ambient soil moisture depletion during dry weather should equal approximately 0.8-0.9, but this depends on the soil horizon from which roots absorb moisture. In the top horizon (0-10 cm) where 90 % of tree fine roots are located, soil moisture had been depleted more slowly under trees exposed to elevated CO₂ than under trees exposed to ambient conditions (Figure 4) and the ratio of the slopes is on average 0.63, indicating a higher than expected divergence in soil moisture between treatments in this critical soil layer. The only explanation we have is that trees growing at elevated CO₂ consumed an underproportional fraction of moisture from the 0 to 10 cm layer under the test conditions. Any water savings in the top soil would enhance nutrient availability and facilitate microbial processes in this layer. Slower soil water depletion under elevated CO₂ have previously been observed (Ellsworth 1999, Gunderson *et al.* 2002), but quantitative inferences are difficult in open ground systems with unknown soil depth which trees extract water from. Enhanced nitrogen concentration had indeed been found in the soil solution under our CO₂-treated trees (P. Schläppi *etal.*, unpublished data).

Whenever transpiration i.e. latent heat flux is reduced, leaves should warm up and induce enhanced sensible heat flux. Other factors being constant and T_L being above T_{air}, ΔT_{L-A}, the leaf to air temperature difference of CO₂-treated trees should be greater than ΔT_{L-A} of control trees. From ca. 5 m above the canopy, we did find a leaf temperature in *Fagus* (Figure 5). Here, we want to explore how close the observed effect comes to the expected one applying a leaf energy balance model. Expressing ΔT as a function of the isothermal net radiation energy Φ_{ni}, the parallel resistance of air to heat and radiation r_{HR}, and E, the rate of leaf transpiration, we get

$$\Delta T = \frac{(\Phi_{ni} - \lambda E)r_{HR}}{\rho_a c_p}$$

(ρ_a is the density of air, c_p the thermal conductivity of air and λ the latent heat of vapourisation of water, all assumed constant, see Jones 1992). At low values of ΔT (typically < 1 K in our case), leaf warming induced by a 16 % reduction in transpiration (as derived from our sap flow data) should in fact be around 0.3 K. However, when r_{HR} varies a lot, this difference can often be reduced to close to zero (H.G. Jones and I. Leinonen, personal communication) and hence fall well below the detection threshold of 0.2

K of our instrument (power test on the basis of the observed variation). From greater distance (airborne single pictures from ca. 200 m above ground, Figure 7; temperature series images from the crane's counter-jib during on/off experiments, Figure 6), we did not detect the CO₂ effect on transpiration via leaf warming. We therefore conclude for such rough, heterogenous forest canopies, that thermal imaging is only able to detect differences in transpiration due to CO₂-treatment from close distance (<5 m), using serial images of the same foliage area. Scanning from greater distance, the signal may be overridden by microclimatic variation or blurred by background signals due to increasing area per pixel.

The on/off signal was absent in the sap flow curves. At the same site however, Cech *et al.* (2003) observed an abrupt increase in sap flow following discontinuation of CO₂-supply for ca. 3 hours during midday in the first 2-3 months of CO₂ enrichment. Here, we tried to avoid the bell shaped midday phase of the sap flow curve and selected the more linear early day part for these on/off experiments. The absence of the on/off sap flow signal in our case may be associated with the buffering (time lag) of the signal through stem and other plant tissue water storage during this early time of the day when the conducting tissue is not yet under full tension (see Zweifel *et al.* 2001, Zweifel & Häslner 2001).

Conclusions

Our data suggest a ca. 14 % reduction of tree transpiration and a 10 % reduction of evapotranspiration and thus, a proportionally reduced humidification of the atmosphere above forests of this type. The strength of this signal largely comes from *Carpinus* and *Fagus*, not from *Quercus*, the more drought resistant taxon (Leuzinger *et al.* 2005). Conifers also have shown to exhibit little transpiration response to elevated CO₂ (Ellsworth 1995, 1999, Körner 2003). The causes for the canopy scale signals obtained are stomatal in the case of *Carpinus*, but possibly (partly) LAI in the case of *Fagus*, underlining the need for long-term observation periods for such canopy scale structural responses to materialise and stabilise. The vpd-response curves of sap flow obtained for *Fagus* and *Carpinus* (the two responsive taxa) indicate that stomata delay transpiration so that relative (not the absolute) maxima of flow occur late in the morning, when vpd has already reached higher values. These response functions provide input to hydrological models and estimates of atmospheric feedback. Should all forests or all vegetation in a landscape show such responses, evaporative demand would increase and partly compensate (further diminish) the effects seen here. Our data thus represent an upper limit of CO₂ driven water savings in such forests.

Acknowledgements We thank Erwin Amstutz and Olivier Bignucolo for crane operations, Roland Vogt for advice on thermography, the Swiss Federal Office for the Environment (FOEN) and the University of Basel. Financial support came from the Swiss National Science Foundation (NCCR climate P3.3, P3.2 of J. Fuhrer and Grant 3100-059769.99 to C. Körner.)

References

- Amthor JS (1999) Increasing atmospheric CO₂, water use, and water stress: scaling up from the plant to the landscape. In: *Carbon Dioxide and Environmental Stress* (eds Luo Y, Mooney HA), pp. 33–59. Academic Press, San Diego.
- Asshoff R, Zotz G, Körner C (2006) Growth and phenology of mature temperate forest trees in elevated CO₂. *Global Change Biology*, **12**, 848–861.
- Cech PG, Pepin S, Körner C (2003) Elevated CO₂ reduces sap flux in mature deciduous forest trees. *Oecologia*, **137**, 258–268.
- Dufrene E, Pontailier JY, Saugier B (1993) A branch bag technique for simultaneous CO₂ enrichment and assimilation measurements on beech (*Fagus sylvatica* L.). *Plant Cell and Environment*, **16**, 1131–1138.
- Ellsworth DS (1999) CO₂ enrichment in a maturing pine forest: are CO₂ exchange and water status in the canopy affected? *Plant Cell and Environment*, **22**, 461–472.
- Ellsworth DS, Oren R, Huang C, Phillips N, Hendrey GR (1995) Leaf and Canopy Responses to Elevated CO₂ in a Pine Forest under Free-Air CO₂ Enrichment. *Oecologia*, **104**, 139–146.
- Field CB, Jackson RB, Mooney HA (1995) Stomatal responses to increased CO₂: implications from the plant to the global scale. *Plant, Cell and Environment*, **18**, 1214–1225.
- Fuchs M (1990) Infrared measurement of canopy temperature and detection of plant water-stress. *Theoretical and Applied Climatology*, **42**, 253–261.
- Gedney N, Cox PM, Betts RA, Boucher O, Huntingford C, Stott PA (2006) Detection of a direct carbon dioxide effect in continental river runoff records. *Nature*, **439**, 835–838.
- Granier A (1985) A new method of sap flow measurement in tree stems. *Annales des Sciences Forestieres*, **42**, 193–200.
- Gunderson CA, Sholtis JD, Wullschleger SD, Tissue DT, Hanson PJ, Norby RJ (2002) Environmental and stomatal control of photosynthetic enhancement in the canopy of a sweetgum (*Liquidambar styraciflua* L.) plantation during 3 years of CO₂ enrichment. *Plant Cell and Environment*, **25**, 379–393.

- Jacobs CMJ, de Bruin HAR (1997) Predicting regional transpiration at elevated atmospheric CO₂: Influence of the PBL-vegetation interaction. *Journal of Applied Meteorology*, **36**, 1663–1675.
- Jones HG (1992) *Plants and microclimate*. Cambridge University Press.
- Jones HG (1999) Use of thermography for quantitative studies of spatial and temporal variation of stomatal conductance over leaf surfaces. *Plant Cell and Environment*, **22**, 1043–1055.
- Keel SG, Pepin S, Leuzinger S, Körner C (2006) Stomatal conductance in mature deciduous forest trees exposed to elevated CO₂. *Trees, in review*.
- Körner C (2003) Ecological impacts of atmospheric CO₂ enrichment on terrestrial ecosystems. *Philosophical Transactions of the Royal Society of London Series A - Mathematical Physical and Engineering Sciences*, **361**, 2023–2041.
- Körner C, Asshoff R, Bignucolo O, *et al.* (2005) Carbon flux and growth in mature deciduous forest trees exposed to elevated CO₂. *Science*, **309**, 1360–1362.
- Köstner B, Granier A, Cermak J (1998) Sapflow measurements in forest stands: methods and uncertainties. *Annales des Sciences Forestieres*, **55**, 13–27.
- Medlyn BE, Barton CVM, Broadmeadow MSJ, *et al.* (2001) Stomatal conductance of forest species after long-term exposure to elevated CO₂ concentration: a synthesis. *New Phytologist*, **149**, 247–264.
- Meinzer FC, Clearwater MJ, Goldstein G (2001) Water transport in trees: current perspectives, new insights and some controversies. *Environmental and Experimental Botany*, **45**, 239–262.
- Morgan JA, Pataki DE, Körner C, *et al.* (2004) Water relations in grassland and desert ecosystems exposed to elevated atmospheric CO₂. *Oecologia*, **140**, 11–25.
- Morison JIL, Gifford RM (1984) Plant growth and water use with limited water supply in high CO₂ concentrations. II. Plant dry weight, partitioning and water use efficiency. *Aust J Plant Physiol*, **11**, 375–384.
- Niklaus PA, Körner C (2004) Synthesis of a six-year study of calcareous grassland responses to in situ CO₂ enrichment. *Ecological Monographs*, **74**, 491–511.
- Pepin S, Körner C (2002) Web-FACE: a new canopy free-air CO₂ enrichment system for tall trees in mature forests. *Oecologia*, **133**, 1–9.
- R Development Core Team (2004) *R: A language and environment for statistical computing*. R Foundation for Statistical Computing, Vienna, Austria.
- Schäfer KVR, Oren R, Lai CT, Katul GG (2002) Hydrologic balance in an intact temperate forest ecosystem under ambient and elevated atmospheric CO₂ concentration. *Global Change Biology*, **8**, 895–911.
- Stocker R, Leadley PW, Körner C (1997) Carbon and water fluxes in a calcareous grassland under elevated CO₂. *Functional Ecology*, **11**, 222–230.
- Wullschlegel SD, Gunderson CA, Hanson PJ, Wilson KB, Norby RJ (2002) Sensitivity of stomatal and canopy conductance to elevated CO₂ concentration interacting variables and perspectives of scale. *New Phytologist*, **153**, 485–496.
- Wullschlegel SD, Norby RJ (2001) Sap velocity and canopy transpiration in a sweetgum stand exposed to free-air CO₂ enrichment (FACE). *New Phytologist*, **150**, 489–498.
- Zweifel R, Häsler R (2001) Dynamics of water storage in mature subalpine *Picea abies*: temporal and spatial patterns of change in stem radius. *Tree Physiology*, **21**, 561–569.
- Zweifel R, Item H, Häsler R (2001) Link between diurnal stem radius changes and tree water relations. *Tree Physiology*, **21**, 869–877.

Chapter 3

Responses of deciduous forest trees to severe summer drought in Central Europe

Responses of deciduous forest trees to severe drought in Central Europe

published in *Tree Physiology*, 25, 641-650
© 2005 Heron Publishing - Victoria, Canada

Sebastian Leuzinger, Gerhard Zotz, Roman Asshoff and Christian Körner

(original publication included)

Responses of deciduous forest trees to severe drought in Central Europe

SEBASTIAN LEUZINGER,^{1,2} GERHARD ZOTZ,¹ ROMAN ASSHOFF¹ and CHRISTIAN KÖRNER¹

¹ Botanisches Institut der Universität Basel, Schönbeinstrasse 6, CH-4056 Basel, Switzerland

² Corresponding author (sebastian.leuzinger@unibas.ch)

Received September 30, 2004; accepted January 15, 2005; published online April 1, 2005

Summary In 2003, Central Europe experienced the warmest summer on record combined with unusually low precipitation. We studied plant water relations and phenology in a 100-year-old mixed deciduous forest on a slope (no ground water table) near Basel using the Swiss Canopy Crane (SCC). The drought lasted from early June to mid September. We studied five deciduous tree species; half of the individuals were exposed to elevated CO₂ concentration ([CO₂]) (530 ppm) using a free-air, atmospheric CO₂-enrichment system. In late July, after the first eight weeks of drought, mean predawn leaf water potential about 30 m above ground was -0.9 MPa across all trees, dropping to a mean of -1.5 MPa in mid-August when the top 1 m of the soil profile had no plant accessible moisture. Mean stomatal conductance and rates of maximum net photosynthesis decreased considerably in mid-August across all species. However, daily peak values of sap flow remained surprisingly constant over the whole period in *Quercus petraea* (Matt.) Liebl., and decreased to only about half of the early summer maxima in *Fagus sylvatica* L. and *Carpinus betulus* L. (stomatal down-regulation of flux). Although we detected no differences in most parameters between CO₂-treated and control trees, predawn leaf water potential tended to be less negative in trees exposed to elevated [CO₂]. Leaf longevity was greater in 2003 compared with the previous years, but the seasonal increase in stem basal area reached only about 75% of that in previous years. Our data suggest that the investigated tree species, particularly *Q. petraea*, did not experience severe water stress. However, an increased frequency of such exceptionally dry summers may have a more serious impact than a single event and would give *Q. petraea* a competitive advantage in the long run.

Keywords: drought, elevated CO₂ concentration, global climate change, sap flow, Swiss Canopy Crane, tree phenology, water relations, web-FACE.

Introduction

Drought represents a major constraint on plant growth and productivity in most terrestrial plant communities (Hinckley et al. 1979, Churkina and Running 1998). The record-breaking

heat wave and low precipitation that Europe experienced in 2003 highlighted the potential consequences of drought events for temperate European forests. For desert and Mediterranean-type climates with hot dry summers, drought events are common and their impact on species assemblages and productivity has long been acknowledged (e.g., Mouillot et al. 2002). Fewer studies have addressed the role of severe drought in Europe, where such events have been reported in historic times but have been rare during the past century (Lloyd-Hughes and Saunders 2002), with the last severe drought in 1976. However, recent evidence suggests an increase in the frequency of extreme weather conditions in Europe related to global climate change (Schär et al. 2004). Given the economic importance of agriculture and forestry, and the potential impact of climatic change on these industries, the effects of drought have lately evoked interest beyond the scientific community.

Implications of temporal water shortage on temperate forest trees, e.g., with respect to leaf water status (Hinckley et al. 1981), stomatal conductance, photosynthesis (Epron and Dreyer 1993) and hydraulic conductivity (Bréda et al. 1993, Cochard et al. 1996), have been studied extensively. In the course of a drought, gradually decreasing stomatal conductance, predawn leaf water potential, assimilation and growth are commonly observed, accompanied by a stimulation of fine root growth. Tree organs (leaves, roots, stem) generally differ in their sensitivity to drought (Westgate and Boyer 1985, Bréda et al. 1993) and a whole-tree approach is needed rather than one restricted to the leaf level (Leuschner et al. 2001a). Furthermore, when investigating drought responses of plants in general, it is crucial to compare several species, as even closely related species may differ greatly in their drought responses (e.g., Gieger and Thomas 2002). Water relations also need to be studied together with growth because it is well known that cambial activity is much more sensitive to drought than leaf-level gas exchange (e.g., Macfarlane and Adams 1998). Species under investigation have predominantly been those of economic importance (e.g., *Picea abies* (L.) Karst., *Quercus petraea* (Matt.) Liebl., and *Fagus sylvatica* L.; Schwanz et al. 1996, Leuschner et al. 2001a). *Quercus petraea* was generally found to have a higher drought resistance than

F. sylvatica, its main competitor (Epron and Dreyer 1993, Backes and Leuschner 2000). However, *F. sylvatica* seems to outcompete *Q. petraea* over most of Western and Central Europe. Competitive superiority may thus depend rather on canopy architecture and leaf orientation (Leuschner et al. 2001a) or shade tolerance (Küppers and Schneider 1993) than on the ability to maintain growth and vitality under drought stress. The ultimate long-term reproductive success and hence species abundance and distribution is unlikely to depend on individual physiological processes that are impaired during a single drought period. Rather, it will be the duration and frequency of drought events over a number of years that will likely determine changes in community structure.

The combined effect of elevated CO₂ concentration ([CO₂]) and drought is of particular interest as their conjunction forms part of a likely scenario for summers in Europe in the near future (Schär et al. 2004). The multitude of studies on water relations in trees subjected to an elevated [CO₂] has been reviewed by Chaves and Pereira (1992), Saxe et al. (1998), Pospisilova and Čatský (1999), Körner (2000) and Medlyn et al. (2001). These reviews suggest that deciduous trees may be less affected by drought stress when exposed to an elevated [CO₂] and thus may extend their ranges into less favorable areas. Conifers, on the other hand, show little or no measurable stomatal response to an elevated [CO₂] (Ellsworth 1999, Körner 2000), and hence may benefit less from reduced canopy transpiration in response to elevated [CO₂]. In potted *Q. petraea*, Guehl et al. (1994) found greater biomass production during water shortage in elevated [CO₂]. Similarly, greater biomass production was found for cherry and oak seedlings during exposure to drought at elevated [CO₂] (Picon et al. 1996, Centritto et al. 1999). However, unlike their responses to controlled environments, plants in the field can respond to drought by exploring deeper soil horizons or by more intensive rooting in a given soil volume. For example, Chaves et al. (1995) found only a marginal reduction in water-use by *Q. ilex* exposed to drought. A previous study at the Swiss Canopy Crane (hereafter, SCC) site in Hofstetten, Switzerland, revealed a reduction in transpiration of only about 10% in response to drought as measured by sap flow, with *Q. petraea* and *F. sylvatica* showing the least reaction (Cech et al. 2003). These authors also found a reverse (positive) effect of elevated [CO₂] on sap flow under dry conditions. Clearly, more in situ studies are needed, in which tall trees experience simulated atmospheric change under natural conditions. Here we used free-air, atmospheric CO₂-enrichment technology (FACE, Pepin and Körner 2002) in combination with a canopy crane to study the combined effect of [CO₂] and drought on trees in a mature forest.

We took advantage of the unique combination of drought and an exceptional heat wave that occurred in Europe in the summer of 2003, the heat wave having a mean return period of more than 10,000 years (according to traditional climate models, Schär et al. 2004). Drought responses were explored at the SCC site in Hofstetten, Switzerland, where some of the experimental trees are subjected to an elevated [CO₂]. The aims of the study were twofold: (1) to compare drought responses in adult specimens of five common deciduous tree species using

a multilevel approach including measurements of water potential, maximum net photosynthesis, leaf conductance, sap flow, growth and phenology; and (2) to investigate the influence that atmospheric CO₂-enrichment exerts on these parameters in situ.

Materials and methods

Site description and study species

The study site is located in a diverse mixed forest stand about 15 km south of Basel, Switzerland (47°28' N, 7°30' E, 550 m a.s.l.), with the SCC providing access to the canopy. The forest is 80–100 years old; tree height ranges from 30 to 35 m; tree density (diameter = 0.1 m) is 415 trees ha⁻¹; and stem basal area is 46 m² ha⁻¹. The leaf area index (LAI) of the canopy in the experimental area is about 5. The dominant stand species are *F. sylvatica* L. and *Q. petraea*. Deciduous broad-leaved *Carpinus betulus* L., *Tilia platyphyllos* Scop., *Acer campestre* L. and *Prunus avium* L., and three species of conifers (not included in this study), occur as companion species. *Quercus petraea*, *F. sylvatica*, *C. betulus*, *A. campestre* and *T. platyphyllos* were selected for observations, as abundant deciduous species typical of a Swiss lowland forest. Soils are of the rendzina type on calcareous bedrock (a silty loam with an accessible profile depth of about 30 cm and a pH of about 5.8 in the top 10 cm of the profile). The site is situated on a slope with no access to the ground water table and has an essentially rocky subsoil at 40 to 90 cm below the surface.

The typical humid temperate zone climate is characterized by mild winters and moderately warm summers. Mean January and July air temperatures are 2 and 19 °C, respectively. Long-term mean annual precipitation for the region is 990 mm, two thirds of which commonly falls during the growing season. The previous years (2001 and 2002) were average with respect to temperature and precipitation. In the study year (2003), the growing season for deciduous trees lasted from the beginning of April (bud break) to the beginning of November. Most measurements were started on June 1 and ended on September 11.

Canopy access and atmospheric CO₂ enrichment system

Access to the tree canopy was achieved by a 45-m free-standing tower crane equipped with a 30-m jib. Of the 64 trees in the crane area, 14 broad-leaved trees (four *F. sylvatica*, three *Q. petraea*, four *C. betulus*, one *T. platyphyllos*, one *A. campestre* and one *P. avium*, the last not used for this experiment) were selected for the elevated [CO₂] treatment in autumn of 2000 (all within a continuous plot). A similar number of control trees were located in the remaining crane area at a sufficient distance from the CO₂ release zone. Atmospheric CO₂ enrichment of the forest canopy was achieved by a free-air, pure CO₂ release system (Pepin and Körner 2002), which consisted of a web of 4-mm plastic tubes (about 0.5 km per tree) with laser-punched holes emitting pure CO₂ into the tree canopy (web-FACE). The rate at which CO₂ was injected into the tubing system and released around the tree crowns was set by computer-controlled magnetic valves to maintain a target [CO₂]

of 550 ppm as closely as possible (details in Pepin and Körner 2002). The system was set up in late September 2000 and operated in the three subsequent growing seasons (from budbreak until leaf fall) every day from dawn to dusk. The overall mean seasonal daytime $[\text{CO}_2]$ within the canopy deviated slightly from the set point and was 520 ppm in 2001 and 530 ppm in 2002 and 2003.

Environmental data

Rain, throughfall precipitation, air humidity, potential evapotranspiration, temperature and soil humidity were monitored by weather stations located above the tree canopy at the top of the crane and in the understory. Tipping bucket rain gauges (RG1, Delta-T, Cambridge, U.K.) were used to monitor rain, and throughfall precipitation was quantified with 22 evenly spaced funnel-type rainwater collectors. Potential evapotranspiration was measured with two evaporimeters (ET gauge, Spectrum Technologies, Plainfield, IL). Data were recorded as 10-min means with data loggers (DL3000, Delta-T). Soil moisture data were obtained at 15-cm depth from hourly measurements with theta-probes (ML2x, Delta-T) located within and immediately outside of the atmospheric CO_2 -enrichment zone and connected to another data logger (DL2e, Delta-T). Additional soil water content across a 90-cm profile (the lower 50 cm representing eventual water in rock crevices) was monitored every 7–14 days during the 2003 growing season at four locations using time domain reflectometry (MP-917 and probes PRB-F, Environmental Sensor, Victoria, BC, Canada).

Leaf water potential measurements

Predawn leaf water potential was measured with a pressure chamber (SKPM 1400, Skye Instruments, Powys, U.K.) from the canopy crane gondola on 5 days from July to September (July 22, July 23, August 14, August 20 and September 12). The weather was clear on all five days with light availabilities up to $1600 \text{ mmol m}^{-2} \text{ s}^{-1}$. On three occasions, daily courses of water potential were recorded. Samples were taken at similar heights above ground to avoid variability due to hydrostatic water potential and samples were wrapped with scotch tape immediately after cutting to prevent further transpiration. We sampled three to four individuals of *Q. petraea*, *F. sylvatica* and *C. betulus* and two of *A. campestre* and *T. platyphyllos*.

Sap flow measurements

Sap flux density within the xylem was measured by the constant heat-flow technique described by Granier (1985, 1987). Each sensor (UP, Kolkwitz, Germany) consists of two 20-mm-long probes (2 mm in diameter), each equipped with a copper-constantan thermocouple and wrapped with heating wire. The upper probe was inserted radially into the sapwood at breast height into bore holes lined with thin-walled aluminum tubing. The bore holes were separated vertically by about 15 cm. The upper probe was heated at a constant power of 200 mW, while the lower reference probe remained unheated. During conditions of zero sapflow, e.g., at night or during prolonged rain events, the temperature difference, ΔT , between the probes reaches a maximum (about 9–15 K). Sap flow dur-

ing the day causes a decrease in ΔT by cooling the upper probe. Sap flux density within the xylem (J_s) measured in $\text{m}^3 \text{ H}_2\text{O m}^{-2}$ was calculated from an empirical relationship validated for several species by Granier (1985), and recently revalidated by Clearwater et al. (1999). We tested for azimuthal variability in sap flux densities, which revealed differences of up to a factor of three between six sensors in *Q. petraea*, whereas almost no differences were found between sensors in *F. sylvatica*. We also compared sap flux densities among trees and among species. Maximum sap flux density was between 30 and 90 J_s ($10^{-6} \text{ m}^3 \text{ H}_2\text{O m}^{-2} \text{ s}^{-1}$) for *Q. petraea*, between 80 to 140 J_s for *F. sylvatica* and about 60 to 100 J_s in *C. betulus*. Given these large differences in absolute sap flow rates and the difficulty of calibrating and converting sap flow signals of mature trees with uncertain sapwood widths into absolute flow rates, we considered relative values only in the present study.

Measurements of J_s were performed from June 21 to October 1, 2003, on three dominant tree species (*Q. petraea*, *F. sylvatica* and *C. betulus*, $n = 2$, only one tree per species at the beginning of the season) using three to six sensors per tree (equally spaced around the stem). Sensors were protected against rain and external thermal influences by aluminum covers filled with polyester wool. Readings were taken at 30-s intervals and recorded as 10-min means using a multi-channel data logger (DL2e, Delta-T). The signals per tree were averaged over all sensors per stem.

Leaf gas exchange measurements

Instantaneous rates of $\text{CO}_2/\text{H}_2\text{O}$ gas exchange were measured in situ in the first half of the day in early (mid-June), mid- (August) and late summer (early September 2003) on mature leaves fully exposed to the sun in the outer canopy of 25 trees (13 trees exposed to elevated $[\text{CO}_2]$ and 12 controls) with a portable gas exchange system (Li-6400, Li-Cor, Lincoln, NE). From each tree, eight (June), four (August) and four (September) leaves from different branches were selected for gas exchange measurements, which were conducted at saturating photosynthetic photon flux (PPF) ($1200 \mu\text{mol m}^{-2} \text{ s}^{-1}$; from an LED light source; Li-Cor 6400-02). Trees grown in an elevated $[\text{CO}_2]$ were measured at about 530 ppm, control trees at about 360 ppm. Chamber temperature (June: $27.1 \pm 1.5 \text{ }^\circ\text{C}$; August $30.1 \pm 0.9 \text{ }^\circ\text{C}$; September: $20.9 \pm 0.8 \text{ }^\circ\text{C}$; mean \pm SD) and relative humidity (June: $64 \pm 9\%$; August $37 \pm 2\%$; September: $60 \pm 4\%$) tracked ambient conditions. A data set was recorded once the net rate of photosynthesis and stomatal conductance remained constant. Individual measurements lasted less than 5 min.

Growth and phenology data

Each month, from 2001 to 2003, we measured the breast-height diameter of 22 trees randomly distributed within the study site with fixed "Permanent Tree Girth-Tape" (D1-L, UMS GmbH, Munich, Germany; accuracy of measurement 0.1 mm). Trees measured were as follows: *Q. petraea*: $n = 6$, 3 ambient, 3 elevated $[\text{CO}_2]$; *F. sylvatica*: $n = 6$, 3 ambient, 3 elevated $[\text{CO}_2]$; *C. betulus*: $n = 6$, 3 ambient, 3 elevated $[\text{CO}_2]$;

T. platyphyllos: $n = 2$, 1 ambient, 1 elevated [CO_2]; and *A. campestre*: $n = 2$, 1 ambient, 1 elevated [CO_2]. Leaf longevity, defined by the time span from 75% bud break to 75% leaf fall was documented in 2002 and 2003, based on observations on a total of 24 individuals of the dominant tree species (*C. betulus*: $n = 8$; *F. sylvatica*: $n = 6$; *Q. petraea*: $n = 6$; *T. platyphyllos*: $n = 2$; and *A. campestre*: $n = 2$; half of the individuals of each species being subjected to elevated [CO_2]).

Data analysis

Leaf water potential, photosynthesis parameters and sap flow data were evaluated by repeated-measures analysis of variance (ANOVA). Datasets that were not normally distributed (according to the Kolmogorov-Smirnov test for normality) were log-transformed before analysis. Tukey's HSD post hoc test for unequal sample size was used to detect differences between CO_2 treatments. Data analysis was performed with the software package STATISTICA Version 5.0 (Statsoft, Tulsa, OK). Error terms represent standard errors unless otherwise stated.

Results

Environmental data

At the SCC site, total accumulated rain during the study as defined above was less than 50% of the 10-year mean from 1989 to 1999, and spring precipitation was also well below the mean (Figure 1). Moreover, throughfall precipitation amounted to approximately half of the above-canopy precipitation of 188 mm, while potential evapotranspiration was 559 mm, i.e.,

exceeding throughfall precipitation almost sixfold during the same period. Mean monthly temperatures exceeded the long-term mean (1989–1999) dramatically (e.g., +6.8 °C for June). Soil water content at 15-cm depth dropped from around 30 Vol.% in early June to 8 Vol.% within the first five weeks of drought and remained low with no plant accessible moisture throughout the rest of the study (Figure 1). Because of the stony subsoil at the study site, soil water between 15- and 90-cm depth as derived from TDR was low and spatially variable (6 to 18 Vol.%). However, irrespective of the absolute values, the signals remained mostly constant during the drought, indicating that none of the remaining moisture was taken up by trees from the monitored soil horizons. There was no significant difference in soil water between the elevated [CO_2]-treated area and the control area in the explored soil horizon (constant minimum readings; data not shown).

Rate of net photosynthesis and leaf conductance

Both net photosynthesis (A) and leaf conductance (g) decreased significantly, by 60 to 80%, from June to August in all species (Figures 2A and 2B). Intraspecific variation was large in both parameters, but nonsignificant in August when all species were strongly affected. Only *Q. petraea* (and to some extent *T. platyphyllos*) resumed g and A values in September comparable with those of June (Figures 2A and 2B), whereas the other species showed only partial recovery. Elevated [CO_2] had no significant effect on g . In contrast, elevated- $[\text{CO}_2]$ -treated trees (all species pooled) assimilated more ($12.7 \pm 0.9 \mu\text{mol CO}_2 \text{ m}^{-2} \text{ s}^{-1}$) than trees growing in ambient [CO_2] ($8.3 \pm 0.8 \mu\text{mol CO}_2 \text{ m}^{-2} \text{ s}^{-1}$; repeated-measures ANOVA, $P < 0.002$, $F_{1,9} = 18.7$).

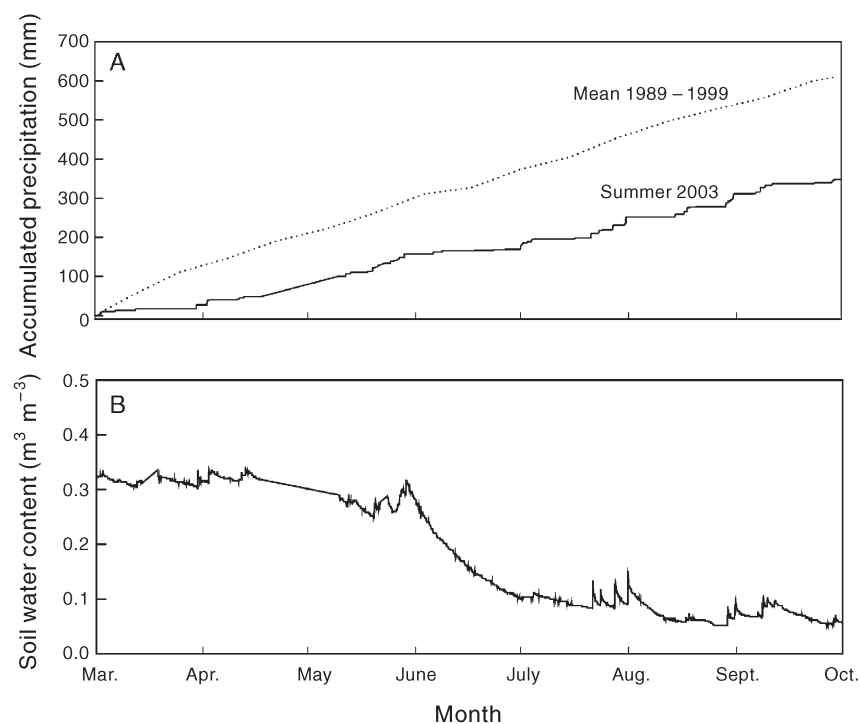


Figure 1. Accumulated seasonal rainfall (mean of 1989 to 1999, dotted line) compared with rainfall during the summer drought of 2003 at the SCC site in Hofstetten, Switzerland (solid line). Total rainfall during the study period (June 1 to September 11) was less than half the 10-year mean (188 versus 415 mm). Subsequently, substantial rainfall caused soil water content to increase as shown in the upper panel (soil water content at a depth of 15 cm).

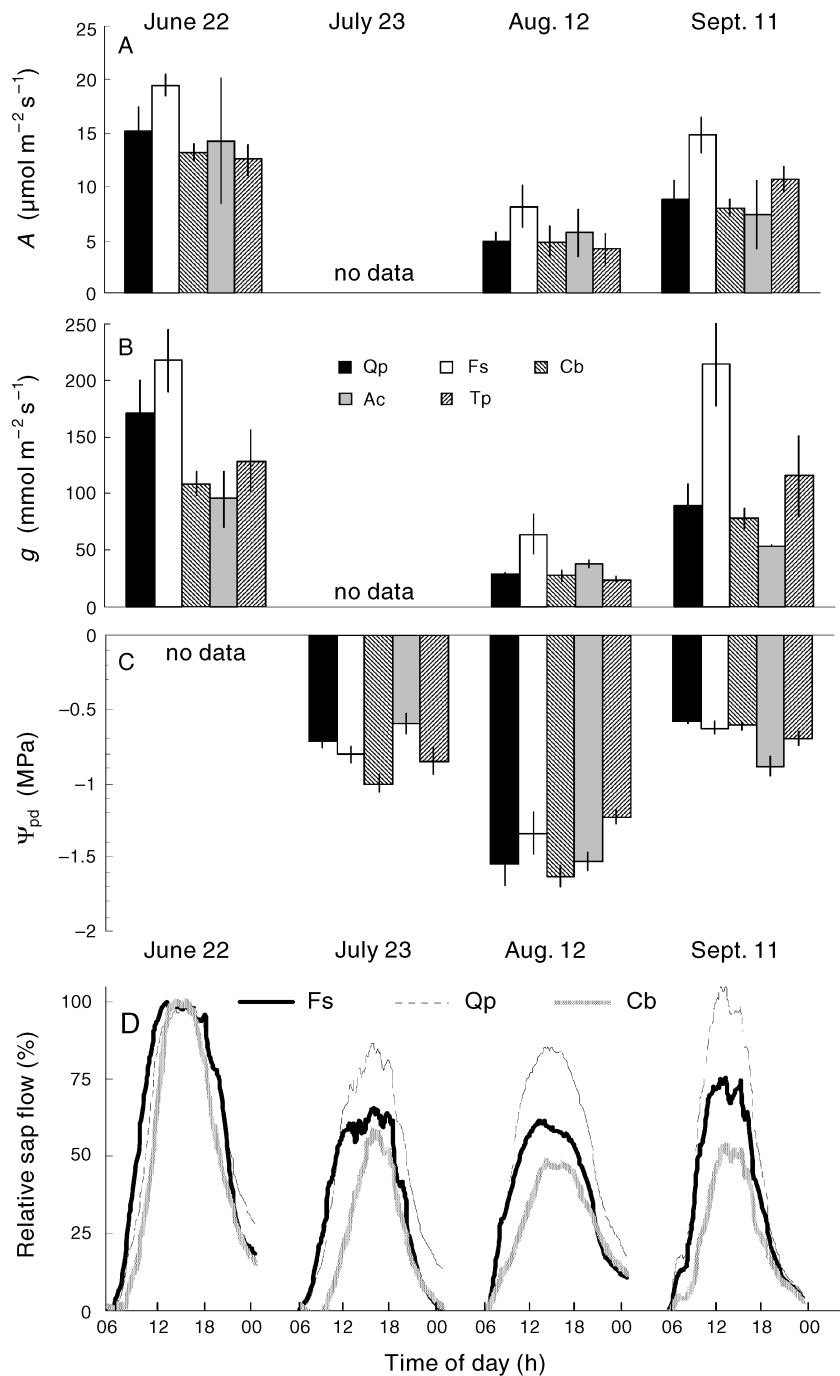


Figure 2. Net rate of maximum photosynthesis, A (A), stomatal conductance, g (B), predawn leaf water potential, Ψ_{pd} (C) and sap flow (relative to initial peak values; D) of three to five species (*Quercus petraea* (Qp), *Fagus sylvatica* (Fs), *Carpinus betulus* (Cb), *Acer campestre* (Ac) and *Tilia platyphyllos* (Tp), all in ambient $[\text{CO}_2]$) at the beginning (22 June), in the middle (23 July and 12 August) and towards the end (11 September) of the 2003 summer drought (means \pm SE). Maximum standard errors for data in panel D are: 12.6 (*Q. petraea*), 18.0 (*F. sylvatica*) and 11.1 (*C. betulus*). All measurements were made on clear days and vapor pressure deficit reached 45, 18, 38 and 12 hPa on the four days shown.

Leaf water potential

At the end of the completely dry period between August 1 and August 14 (Figure 1), predawn leaf water potential (Ψ_{pd}) ranged from -1.7 MPa in *C. betulus* to -1.3 MPa in *Q. petraea* and -1.1 MPa in *T. platyphyllos* (Table 1 and Figure 2C). Over the course of the drought, Ψ_{pd} declined across all species (repeated-measures ANOVA, $P < 0.001$, $F_{4,24} = 82.2$) from a mean of about -0.8 MPa in mid-July to below -1.4 MPa in mid-August, reflecting severe soil desiccation. Mean Ψ_{pd} then

recovered to about -0.9 MPa in the second half of August and about -0.7 MPa in mid-September. Predawn leaf water potential tended to be less negative in elevated $[\text{CO}_2]$ (3-way ANOVA for all species, $P = 0.06$, $F_{1,6} = 5.3$), but there was no significant effect of $[\text{CO}_2]$ on the diurnal minimum of leaf water potential ($P = 0.22$, $F_{1,6} = 1.8$). Trees started the day from different predawn leaf water potentials, but because of differences in daytime flux control, they arrived at similar minima by the afternoon.

Table 1. Leaf water potential (Ψ) of five tree species during the summer drought (2003) in Hofstetten, Switzerland. Shown are means (SE in parentheses) of predawn (Ψ_{pd}) and daily minimum (Ψ_{min} , early afternoon) leaf water potentials for each species. Measurements were on two to four individuals per species and treatment, except for *A. campestre* and *T. platyphyllos*. Abbreviations: A = trees grown under ambient $[\text{CO}_2]$; E = trees subjected to elevated $[\text{CO}_2]$. Different letters indicate significant differences between species (with CO_2 treatment and sampling date pooled, repeated-measures ANOVA, $P < 0.05$).

Ψ_{pd}	<i>F. sylvatica</i> ^a		<i>Q. petraea</i> ^b		<i>C. betulus</i> ^a		<i>T. platyphyllos</i> ^c		<i>A. campestre</i> ^a		All species	
	A	E	A	E	A	E	A	E	A	E	A	E
July 22	-0.83 (0.03)	-0.66 (0.02)	-0.80 (0.03)	-0.79 (0.10)	-1.13 (0.07)	-1.00 (0.24)	-0.80	-0.63	-0.68	-0.56	-0.94 (0.09)	-0.80 (0.08)
July 23	-0.72 (0.06)	-0.70 (0.10)	-0.80 (0.02)	-0.82 (0.12)	-1.10 (0.07)	-0.90 (0.07)	-0.94	-0.76	-0.67	-0.54	-0.86 (0.06)	-0.78 (0.05)
Aug. 14	-1.44 (0.25)	-1.66 (0.14)	-1.42 (0.16)	-1.26 (0.26)	-1.71 (0.08)	-1.54 (0.10)	-1.07 (0.22)	-1.16	-1.54 (0.06)	-1.59	-1.50 (0.08)	-1.47 (0.09)
Aug. 20	-0.82 (0.11)	-0.86 (0.05)	-0.92 (0.03)	-0.89 (0.12)	-1.14 (0.08)	-0.91 (0.04)	-0.95 (0.05)	-0.80	-0.92 (0.03)	-1.01	-0.94 (0.04)	-0.88 (0.03)
Sept. 12	-0.57 (0.04)	-0.58 (0.02)	-0.67 (0.06)	-0.58 (0.05)	-0.61 (0.04)	-0.62 (0.04)	-0.72 (0.10)	-0.68	-0.93 (0.08)	-0.81	-0.68 (0.04)	-0.62 (0.02)
Ψ_{min}	<i>F. sylvatica</i> ^a		<i>Q. petraea</i> ^a		<i>C. betulus</i> ^{bc}		<i>T. platyphyllos</i> ^{ac}		<i>A. campestre</i> ^{ac}		All species	
	A	E	A	E	A	E	A	E	A	E	A	E
July 22	-1.77 (0.14)	-1.76 (0.05)	-2.18 (0.08)	-2.03 (0.06)	-2.27 (0.02)	-2.07 (0.09)	-1.53	-1.32	-2.00	-1.92	-1.95 (0.10)	-1.95 (0.09)
Aug. 20	-1.54 (0.20)	-1.52 (0.06)	-2.20 (0.09)	-2.03 (0.14)	-1.95 (0.13)	-1.88 (0.12)	-1.49 (0.10)	-1.35	-1.94 (0.13)	-1.75	-1.89 (0.09)	-1.82 (0.09)
Sept. 12	-1.21 (0.35)	-1.07 (0.08)	-1.55 (0.08)	-1.63 (0.09)	-1.40 (0.06)	-1.43 (0.16)	-1.29 (0.01)	-1.00	-1.32 (0.01)	-1.40	-1.35 (0.07)	-1.41 (0.10)

Sap flow

Relative sap flow became progressively lower as the drought advanced in *F. sylvatica* and *C. betulus*, although in *Q. petraea*, sap flux density decreased by only 15% on August 12 compared to June 22, versus 40 and 50% in *F. sylvatica* and *C. betulus*, respectively (Figure 2D). In mid-September, sap flux density in *Q. petraea* recovered fully, whereas in *F. sylvatica*, it recovered only slightly, and in *C. betulus*, sap flow continued to decrease. *Quercus petraea* and *C. betulus* reached maximum sap flow rates at higher vapor pressure deficits (around 8 to 9 hPa) than *F. sylvatica* (about 6 hPa), i.e., *F. sylvatica* started to control transpiration at a lower VPD, reducing transpiration by overcompensating stomatal regulation above a VPD of about 18 hPa (Figure 3). *Quercus petraea* showed the smallest decrease in transpiration during conditions of high VPD (flow stabilized by stomatal control), whereas *C. betulus* reduced sap flow considerably (about 50%) above a VPD of 30 hPa. After minor rain events during the drought, relative sap flow rates increased rapidly in *C. betulus* only, decreasing again shortly afterwards, which may explain, in part, the discrepancy between Figures 2D and 3.

Growth and phenology

In 2003, the seasonal increase in tree basal area was reduced by about 25% over all 22 trees monitored compared with the two previous years (2001 and 2002 versus 2003, $P = 0.06$) and basal area growth virtually ceased by early August (Figure 4). Surprisingly, we observed increasing stem diameters late in the year, which was most likely caused by wetting of the bark after the first extensive rainfalls. There were clear differences between species: *F. sylvatica* and *T. platyphyllos* were affected most, whereas *A. campestre*, *C. betulus* and *Q. petraea* did not differ as much in growth rates from the two previous years. In 2003, leaf longevity was prolonged by a mean of 22 days across all trees compared with the previous year (one-way ANOVA, $P < 0.001$). This difference was mainly due to delayed discoloration and leaf fall, whereas earlier bud break in spring 2003 accounted for only about 5 days of the increased leaf longevity. Although leaves looked more yellow than normal in some species (mainly *C. betulus*) at the peak of the drought in August, they became green again after the September rains and none of the monitored species showed signs of accelerated senescence or leaf fall. There was also no mid-season leaf shedding.

Discussion

Our study yielded three major findings: (1) *Q. petraea* maintained a consistently better water status during the drought than the other four species. Despite the high interspecific variability in drought response, no species showed signs of drought-induced leaf mortality; (2) across all trees, the summer drought of 2003 caused reduced basal stem area growth of all investigated species compared with growth in the two previous years; and (3) elevated $[\text{CO}_2]$ resulted in less negative predawn leaf water potentials. However, we observed neither significantly lower stomatal conductance in trees exposed to elevated $[\text{CO}_2]$ during the drought (though there was a small

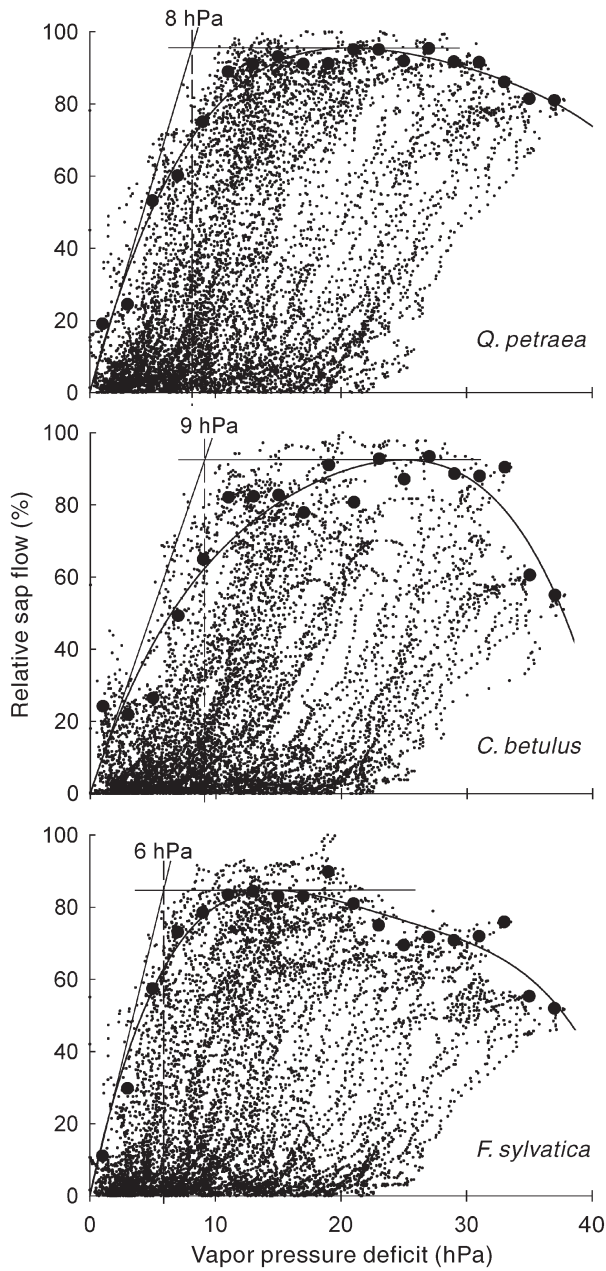


Figure 3. Vapor pressure deficit (VPD) plotted against relative sap flow for *Q. petraea*, *C. betulus* and *F. sylvatica*. Bold lines show best 4th order polynomial fit (least squares) for 95 percentiles of classes of 2 hPa VPD (bold dots). R^2_{adj} values are 0.97, 0.90 and 0.94 for *Q. petraea*, *C. betulus* and *F. sylvatica*, respectively, $P < 0.001$ for all three species, $n = 2$ (except for June and July $n = 1$).

trend in this direction) nor a significant $[CO_2]$ -related increase in diameter growth across all species compared with controls.

Water relations during drought

The effect of severe drought as experienced in 2003 was aggravated by the heat wave which reduced the ratio of precipitation to evaporation further. Subtracting mean throughfall precipitation (about 100 mm) from potential evapotranspiration

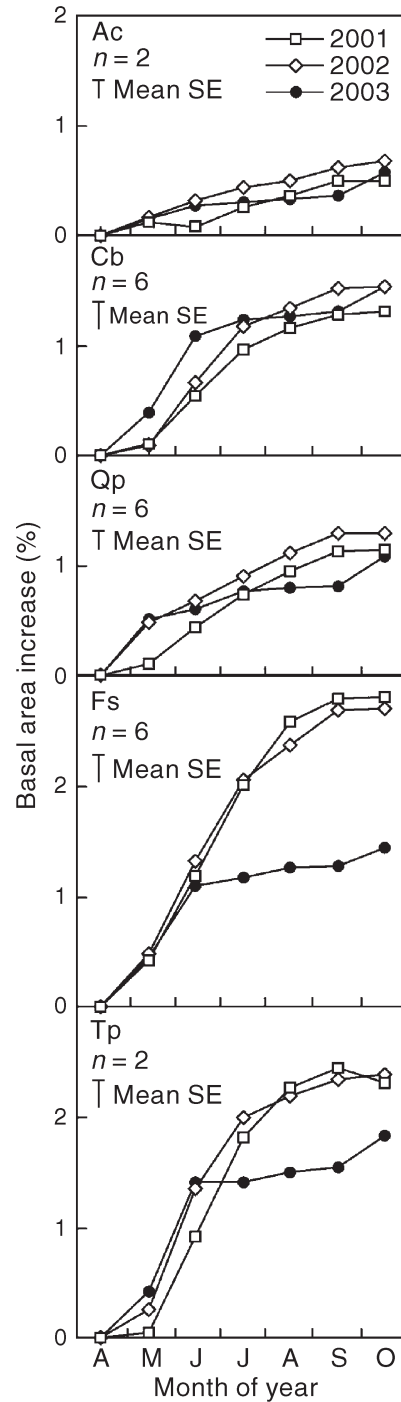


Figure 4. Stem basal area increase (%) in the drought year 2003 compared with the two previous years with mean precipitation (2001 and 2002) for the five species *Acer campestre* (Ac), *Carpinus betulus* (Cb), *Fagus sylvatica* (Fs), *Tilia platyphyllos* (Tp) and *Quercus petraea* (Qp). For clarity, the SE is averaged over the vegetation period (mean SE). Differences between trees grown under elevated CO_2 and ambient conditions were not significant, hence data were pooled for analysis.

(559 mm) results in a negative water budget of about 460 mm during the study period, or a potential water loss of 4.5 mm per day. Even if actual evapotranspiration was substantially lower

because of stomatal down-regulation, we estimate severe soil desiccation down to at least 2.5 to 3 m, given the extremely rocky subsoil. In fact, many understory plants such as *Mercurialis perennis* L. wilted permanently. Canadell et al. (1996) reviewed the rooting depths of 21 temperate deciduous forest trees and arrived at 1.8 to 4.3 m, with a mean of 3.0 ± 0.2 m. *Quercus petraea* was found to have somewhat deeper rooting (max. 1.5 m) than *F. sylvatica* (1.1 m) (Leuschner et al. 2001b). Based on the estimates above, we expected much more severe signs of water shortage in the study trees. Surprisingly, this was not the case. This suggests that trees had access to deeper soil water through deep-reaching fine root systems, which may have been overlooked in excavation studies.

Overall, we found important differences in drought response among species, particularly between the co-dominant species *Q. petraea* and *F. sylvatica*. In essence, *Q. petraea* maintained surprisingly high transpiration rates (estimated by sap flow) although assimilation and stomatal conductance were depressed substantially (but were still twice as high as in *F. sylvatica* and *C. betulus* at the peak of the drought). There are two possible explanations for this: (1) both *F. sylvatica* and *Q. petraea* had access to deep water, but *F. sylvatica* did not tolerate such high flux rates and thus down-regulated transpiration by stomatal closure, or (2) *Q. petraea* had access to deep water that was inaccessible to *F. sylvatica*. We favor the first explanation, as we measured minimum leaf water potentials (Ψ_{\min}) of -2.2 MPa in *Q. petraea* but values no lower than -1.8 MPa in *F. sylvatica* under the same conditions (Table 1).

According to Hacke and Sauter (1995), embolism occurs at leaf water potentials below -1.9 MPa in *F. sylvatica*, and Bréda et al. (1993) state that both beech and oak can be considered water stressed when leaf water potential drops below -2.0 MPa. Although there is one study reporting Ψ_{\min} values below -3.0 MPa for both *F. sylvatica* and *Q. petraea* in Greece (Raftoyannis and Radoglou 2002), such low leaf water potentials have never been reported from Central or Western Europe. We argue that with a minimum predawn leaf water potential (Ψ_{pd}) of -1.66 MPa at the peak of drought, *F. sylvatica* trees were considerably water stressed, as such low Ψ_{pd} values have never been found previously in tall adult trees (Aranda et al. 2002, Peuke et al. 2002). However, *Q. petraea* showed higher Ψ_{pd} together with lower Ψ_{\min} values, which suggests that this species suffered less from water shortage. The greater abundance of *F. sylvatica* across most of Central and Western European lowlands contrasts with the higher drought resistance of *Q. petraea*, indicating that drought has not been the dominant selective force so far. This issue has been amply discussed by Leuschner et al. (2001a, 2001b). These authors observed drought-stimulated fine root growth as well as generally high competitive ability in fine root growth in *F. sylvatica* but not in *Q. petraea*. The diffuse-porous *F. sylvatica* also seems to operate at lower sap flux densities than the ring porous *Q. petraea*, possibly because of its higher Huber-value (Lösch 2001). Nevertheless, we observed *F. sylvatica* trees down-regulating transpiration by stomatal closure at atmospheric vapor pressure deficits above about 10 hPa, thereby mitigating cavitation risk. Cavitation risk is higher in *F. sylvatica* than in *Q. pubescens*, an oak species closely related to the one studied

here (Lösch 2001). Lower cavitation risk may thus explain the greater drought resistance of oak.

Carpinus betulus raised sap flow rates quickly after even minor rain events with little throughfall precipitation. This suggests that *C. betulus* features an effective fine root system in the shallowest soil horizon, allowing it to rapidly use small quantities of water that become available during otherwise dry periods (Figure 3). *Acer campestre* did not differ in *A* and *g* from the more drought-sensitive species *F. sylvatica* and *C. betulus*, whereas *T. platyphyllos* seemed to recover particularly well in September reaching pre-drought *A* and *g* values. Thus, *T. platyphyllos* may be a relatively drought-tolerant species, not previously recognized as such, whereas *A. campestre* seems to be more susceptible to drought.

The surprisingly low sap flow rates in all species at high VPD (e.g., almost zero flow at 20 hPa VPD; Figure 3) were a consequence of many extraordinarily hot nights (flow approaches 0) in August when predawn temperatures remained well above 20 °C and relative humidity was as low as 30%.

Growth and phenology

Intraspecific differences in physiological responses to drought matched patterns of basal stem area increase quite well. As expected, *Q. petraea* showed the least difference in growth reduction compared with the two previous years, whereas in *F. sylvatica*, water shortage had an unambiguous effect on basal area increase (Figure 4). *Carpinus betulus* showed rapid basal area growth during the spring when soil water availability was still high, but ceased growth almost completely during the drought. For *A. campestre* and *T. platyphyllos*, sample sizes are too low to allow interpretation of growth responses. Drought has generally been associated with reduced leaf longevity in deciduous species (Jonasson et al. 1997), depending on length and severity of the drought. In contrast, increases in leaf longevity as in our particular case have rarely been reported (but see Casper et al. 2001). The increase in stem basal area in October following the first autumn rains (Figure 4) is unlikely to have been caused by late season growth. The difference in thickness of fresh and air-dried bark samples (compare Zweifel et al. 2000, Asshoff et al., unpublished data) indicates that the apparent increase in basal area can be fully explained by bark swelling after rain.

Drought–CO₂ interactions

Elevated CO₂ in combination with drought caused less negative predawn leaf water potentials. As predawn leaf water potential is the sum of the (constant) hydrostatic potential plus the soil matrix potential, this indicates water savings of trees exposed to a high [CO₂] during drought. However, trees exposed to an elevated [CO₂] showed no measurable reduction in stomatal conductance during the drought, but small reductions may have escaped our assessment. A study by S.G. Keel et al. (Laboratory of Atmospheric Chemistry, Paul Scherrer Institute, Villigen, Switzerland, personal communication), which was conducted at the same site, indicated that there is such a difference, but the mean reduction across species is small (about 10–15%) compared with the variation in the data.

We conclude that a drought as severe as that in Europe during 2003 exerts no damage on the tested tree species. The visual impression during this summer suggests that this applies to most lowland forests in this area, where obvious drought damage was restricted to hill tops, ridges or rock escarpments. However, we identified a pronounced differentiation in the impact of the drought on water consumption, leaf photosynthesis and growth across the studied species. Adult *Q. petraea*, it appears, copes best with drought events, but it is too early to predict a possible shift in species composition in mixed forests of the kinds studied.

Acknowledgments

We thank Olivier Bignucolo and Erwin Amstutz for crane operations, the Swiss Federal Office of the Environment (BUWAL) and the University of Basel. Financial support came from the Swiss National Science Foundation (Grant 3100–059769.99 to C. Körner and project P 3.2 of J. Fuhrer).

References

- Aranda, I., L. Gil and J.A. Pardos. 2002. Physiological responses of *Fagus sylvatica* L. seedlings under *Pinus sylvestris* L. and *Quercus pyrenaica* Willd. overstories. *For. Ecol. Manage.* 162:153–164.
- Backes, K. and C. Leuschner. 2000. Leaf water relations of competitive *Fagus sylvatica* and *Quercus petraea* trees during 4 years differing in soil drought. *Can. J. For. Res.* 30:335–346.
- Bréda, N., H. Cochard, E. Dreyer and A. Granier. 1993. Water transfer in a mature oak stand (*Quercus petraea*)—seasonal evolution and effects of a severe drought. *Can. J. For. Res.* 23:1136–1143.
- Canadell, J., R.B. Jackson, J.R. Ehleringer, H.A. Mooney, O.E. Sala and E.-D. Schulze. 1996. Maximum rooting depth of vegetation types at the global scale. *Oecologia* 108:583–595.
- Casper, B.B., I.N. Forseth, H. Kempenich, S. Seltzer and K. Xavier. 2001. Drought prolongs leaf life span in the herbaceous desert perennial *Cryptantha flava*. *Funct. Ecol.* 15:740–747.
- Cech, P.G., S. Pepin and C. Körner. 2003. Elevated CO₂ reduces sap flux in mature deciduous forest trees. *Oecologia* 137:258–268.
- Centritto, M., H.S.J. Lee and P.G. Jarvis. 1999. Interactive effects of elevated CO₂ and drought on cherry (*Prunus avium*) seedlings. I. Growth, whole-plant water use efficiency and water loss. *New Phytol.* 141:129–140.
- Chaves, M.M. and J.S. Pereira. 1992. Water stress, CO₂ and climate change. *J. Exp. Bot.* 43:1131–1139.
- Chaves, M.M., J.S. Pereira, S. Cerasoli, J. Clifton Brown, F. Miglietta and A. Raschi. 1995. Leaf metabolism during summer drought in *Quercus ilex* trees with lifetime exposure to elevated CO₂. *J. Biogeogr.* 22:255–259.
- Churkina, G. and S.W. Running. 1998. Contrasting climatic controls on the estimated productivity of global terrestrial biomes. *Ecosystems* 1:206–215.
- Clearwater, M.J., F.C. Meinzer, J.L. Andrade, G. Goldstein and N.M. Holbrook. 1999. Potential errors in measurement of nonuniform sap flow using heat dissipation probes. *Tree Physiol.* 19: 681–687.
- Cochard, H., N. Bréda and A. Granier. 1996. Whole tree hydraulic conductance and water loss regulation in *Quercus* during drought: evidence for stomatal control of embolism? *Ann. Sci. For.* 53: 197–206.
- Ellsworth, D.S. 1999. CO₂ enrichment in a maturing pine forest: are CO₂ exchange and water status in the canopy affected? *Plant Cell Environ.* 22:461–472.
- Epron, D. and E. Dreyer. 1993. Long-term effects of drought on photosynthesis of adult oak trees *Quercus petraea* (Matt) Liebl. and *Quercus robur* L. in a natural stand. *New Phytol.* 125:381–389.
- Gieger, T. and F.M. Thomas. 2002. Effects of defoliation and drought stress on biomass partitioning and water relations of *Quercus robur* and *Quercus petraea*. *Basic Appl. Ecol.* 3:171–181.
- Granier, A. 1985. Un nouvelle méthode pour la mesure du flux de sève brute dans le tronc des arbres. *Ann. Sci. For.* 42:193–200.
- Granier, A. 1987. Mesure du flux de sève brute dans le tronc du Douglas par une nouvelle méthode thermique. *Ann. Sci. For.* 44: 1–14.
- Guehl, J.M., C. Picon, G. Aussenac and P. Gross. 1994. Interactive effects of elevated CO₂ and soil drought on growth and transpiration efficiency and its determinants in two European forest tree species. *Tree Physiol.* 14:707–724.
- Hacke, U. and J.J. Sauter. 1995. Vulnerability of xylem to embolism in relation to leaf water potential and stomatal conductance in *Fagus sylvatica*, *F. purpurea* and *Populus balsamifera*. *J. Exp. Bot.* 46:1177–1183.
- Hinckley, T.M., P.M. Dougherty, J.P. Lassoie, J.E. Roberts and R.O. Teskey. 1979. Severe drought—impact on tree growth, phenology, net photosynthetic rate and water relations. *Am. Midl. Nat.* 102: 307–316.
- Hinckley, T.M., R.O. Teskey, F. Duhme and H. Richter. 1981. Temperate hardwood forests. In *Water Deficits and Plant Growth*. Ed. T.T. Kozlowski. Academic Press, New York, pp 153–208.
- Jonasson, S., H. Medrano and J. Flexas. 1997. Variation in leaf longevity of *Pistacia lentiscus* and its relationship to sex and drought stress inferred from leaf δ¹³C. *Funct. Ecol.* 11:282–289.
- Körner, C. 2000. Biosphere responses to CO₂ enrichment. *Ecol. Appl.* 10:1590–1619.
- Küppers, M. and H. Schneider. 1993. Leaf gas-exchange of beech (*Fagus sylvatica* L.) seedlings in lightflecks—effects of fleck length and leaf temperature in leaves grown in deep and partial shade. *Trees* 7:160–168.
- Leuschner, C., K. Backes, D. Hertel, F. Schipka, U. Schmitt, O. Terborg and M. Runge. 2001a. Drought responses at leaf, stem and fine root levels of competitive *Fagus sylvatica* L. and *Quercus petraea* (Matt.) Liebl. trees in dry and wet years. *For. Ecol. Manage.* 149:33–46.
- Leuschner, C., D. Hertel, H. Coners and V. Buttner. 2001b. Root competition between beech and oak: a hypothesis. *Oecologia* 126: 276–284.
- Lloyd-Hughes, B. and M.A. Saunders. 2002. A drought climatology for Europe. *Int. J. Climatol.* 22:1571–1592.
- Lösch, R. 2001. Wasserhaushalt der Pflanzen. Quelle und Meyer, Wiebelsheim, Germany, 595 p.
- Macfarlane, C. and M.A. Adams. 1998. δ¹³C of wood in growth-rings indicates cambial activity of drought-stressed trees of *Eucalyptus globulus*. *Funct. Ecol.* 12:655–664.
- Medlyn, B.E., C.V.M. Barton, M.S.J. Broadmeadow et al. 2001. Stomatal conductance of forest species after long-term exposure to elevated CO₂ concentration: a synthesis. *New Phytol.* 149: 247–264.
- Mouillot, F., S. Rambal and R. Joffre. 2002. Simulating climate change impacts on fire frequency and vegetation dynamics in a Mediterranean-type ecosystem. *Glob. Change Biol.* 8:423–437.
- Pepin, S. and C. Körner. 2002. Web-FACE: a new canopy free-air CO₂ enrichment system for tall trees in mature forests. *Oecologia* 133:1–9.
- Peuke, A.D., C. Schraml, W. Hartung and H. Rennenberg. 2002. Identification of drought-sensitive beech ecotypes by physiological parameters. *New Phytol.* 154:373–387.

- Picon, C., J.M. Guehl and G. Aussenac. 1996. Growth dynamics, transpiration and water-use efficiency in *Quercus robur* plants submitted to elevated CO₂ and drought. *Ann. Sci. For.* 53:431–446.
- Pospisilova, J. and J. Čatský. 1999. Development of water stress under increased atmospheric CO₂ concentration. *Biol. Plant.* 42: 1–24.
- Raftoyannis, Y. and K. Radoglou. 2002. Physiological responses of beech and sessile oak in a natural mixed stand during a dry summer. *Ann. Bot.* 89:723–730.
- Saxe, H., D.S. Ellsworth and J. Heath. 1998. Tree and forest functioning in an enriched CO₂ atmosphere. *New Phytol.* 139:395–436.
- Schär, C., P.L. Vidale, D. Luthi, C. Frei, C. Haberli, M.A. Liniger and C. Appenzeller. 2004. The role of increasing temperature variability in European summer heatwaves. *Nature* 427:332–336.
- Schwanz, P., K.H. Haberle and A. Polle. 1996. Interactive effects of elevated CO₂, ozone and drought stress on the activities of antioxidative enzymes in needles of Norway spruce trees (*Picea abies*, L. Karsten) grown with luxurious N-supply. *J. Plant Physiol.* 148:351–355.
- Westgate, M.E. and J.S. Boyer. 1985. Osmotic adjustment and the inhibition of leaf, root, stem and silk growth at low water potentials in maize. *Planta* 164:540–549.
- Zweifel, R., H. Item and R. Häsler. 2000. Stem radius changes and their relation to stored water in stems of young Norway spruce trees. *Trees* 15:50–57.

Chapter 4

Stomatal conductance in mature deciduous forest trees exposed to elevated CO₂

Stomatal conductance in mature deciduous forest trees exposed to elevated CO₂

Trees, in revision

Sonja G. Keel¹, Steeve Pepin^{2,3}, Sebastian Leuzinger² and Christian Körner²

Abstract Stomatal conductance (g_s) of mature trees exposed to elevated CO₂ concentrations was examined in a diverse deciduous forest stand in NW Switzerland. Measurements of g_s were carried out on upper canopy foliage before noon, over four growing seasons, including an exceptionally dry summer (2003). Across all species reductions in stomatal conductance were smaller than 25% most likely around 10%, with much variation among species and trees. Given the large heterogeneity in light conditions within a tree crown, this signal was not statistically significant, but the responses within species were surprisingly consistent throughout the study period. Except during a severe drought, stomatal conductance was always lower in trees of *Carpinus betulus* exposed to elevated CO₂ compared to *Carpinus* trees in ambient air, but the difference was only statistically significant on two out of fifteen days. In contrast, stomatal responses in *Fagus sylvatica* and *Quercus petraea* varied around zero with no consistent trend in relation to CO₂ treatment. During the 2003 drought in the third treatment year, the CO₂ effect became reversed in *Carpinus*, resulting in higher g_s in trees exposed to elevated CO₂ compared to control trees, most likely due to better water supply because of the previous soil water saving_s. This was supported by less negative predawn leaf water potential in CO₂ enriched *Carpinus* trees, indicating an improved water status. These findings_s illustrate (1) smaller than expected CO₂-effects on stomata of mature deciduous forest trees, and (2) the possibility of soil moisture feedback on canopy water relations under elevated CO₂.

Introduction

Reduction of stomatal aperture is a common response of plants exposed to elevated CO₂ concentrations (Morison & Gifford, 1984). In canopies well-coupled to the atmosphere, such reductions in stomatal conductance (g_s) result in a corresponding decrease in leaf transpiration. Hence, a large number of studies have been carried out during the last few decades to determine the effect of rising atmospheric CO₂ on g_s and water consumption of dominant forest tree species (for reviews see Curtis & Wang 1998, Saxe *et al.* 1998 Medlyn *et al.* 2001).

Most of the work examining stomatal responses to CO₂ in tree species has been confined to seedling_s and sapling_s, with little research on mature forest trees. These experiments have demonstrated that g_s in young woody individuals is generally reduced in response to elevated CO₂ (mean reduction of 21%, Medlyn *et al.* 2001). This has led to the prediction that water use in most forest trees will be reduced as the CO₂ concentration in the atmosphere increases. Similarly to herbaceous species, the stomatal responses of sapling_s exposed to elevated CO₂ were found to vary among species and to be less pronounced under environmental conditions that reduce maximum g_s (e.g. drought, high temperature, high evaporative demand; Heath 1998; Wullschlegel *et al.* 2002). Furthermore, there is now solid evidence that plant responses to CO₂ may change with experimental conditions such as the duration of exposure and plant age (Medlyn *et al.* 2001), soil characteristics (Bucher-Wallin *et al.*, 2000) and biotic interactions (Körner, 2002). Conifer species seem to make an exception, as stomata appear less responsive to CO₂ enrichment in this group of species (Teskey 1995; Ellsworth 1999). For all these reasons it is unrealistic to predict the long-term water relation responses of mixed forests to rising CO₂ concentrations from data obtained in sapling_s of certain species grown in artificial substrates for a short period of time. These uncertainties have led to a growing consensus that forest tree research must be carried out on mature individuals under natural forest conditions (Körner,

¹ Laboratory of Atmospheric Chemistry, Paul Scherrer Institute, CH-5232 Villigen, Switzerland

² Institute of Botany, University of Basel, Schönbeinstrasse 6, CH-4056, Basel, Switzerland

³ Current address: Département des sols et de génie agroalimentaire, Université Laval, Pavillon Paul-Comtois, Québec (Québec) G1K 7P4, Canada

1995).

Nevertheless, exploring the effects of elevated CO₂ on the water relations of tall forest trees has always presented a considerable challenge given the large size and complex structure of their canopy. Hence, investigations conducted on trees growing near natural CO₂ springs (Jones *et al.* 1995; Tognetti *et al.* 1998; Tognetti *et al.* 1999) and experiments performed with branch-bags (Dufrene *et al.* 1993; Teskey 1995; Roberntz and Stockfors 1998; Barton and Jarvis 1999) have provided most of the data currently available on mature trees. Although branch-bags offer a useful alternative to growth chambers for the investigation of mature trees, there is little, if any, possibility of feedback effects from the soil because only a small portion of the whole crown is exposed to elevated CO₂. Based on sap flow measurements carried out in a mature forest in NW Switzerland, Cech *et al.* (2003) presented evidence that tree responses to elevated CO₂ may be influenced by soil moisture feedback. They reported that during a relatively dry period, CO₂-enriched trees showed increased sap flow density compared to control trees. This reverse CO₂-effect, where an increased rather than a reduced transpirational flux (and hence, g_s) was observed in response to elevated CO₂, suggests that daily water savings by CO₂-enriched trees may have contributed to an improved water status by the time when control trees fell short in soil moisture. These results highlight the importance of large-scale observations, in which coupled plant-soil systems are studied (Wullschleger *et al.*, 2002).

Using free-air CO₂ enrichment (FACE) technology, major advances have been made towards a large-scale approach of studying forest trees under more realistic growth conditions (Ellsworth 1999; Wullschleger *et al.* 2002; Herrick *et al.* 2004). Yet for reasons of practicability, long-term field CO₂ experiments with trees have mainly been conducted in relatively young (10-20 years) forest plantations with no (or little) natural interspecific competition for light and water. To our knowledge, no large-scale investigation has examined the effect of CO₂ enrichment on a natural, diverse forest. However, a study conducted on *Liquidambar styraciflua* L. trees emerging through gaps in the Duke *Pinus taeda* L. forest provides support to the significance of species identity (Herrick *et al.*, 2004a). While the stomata of *P. taeda* showed no significant CO₂ response (Ellsworth, 1999), those of *L. styraciflua* do. Given the evidence that stomatal responses to elevated CO₂ are species-specific, it is essential to account for tree species diversity when investigating the responses of whole forest stands to elevated CO₂.

In this paper, we present stomatal data from the first FACE experiment exposing the canopy of mature broad-leaved trees from six different species in a

natural temperate forest ecosystem to elevated CO₂ concentrations (ca. 540 ppm). Stomatal conductance was measured in all species on eleven days over the first full growing season of CO₂ exposure to test the hypothesis that stomatal aperture is reduced under elevated CO₂ and to determine whether CO₂ responses are species-specific. Further measurements were carried out during three additional growing seasons in the three dominant species only. Our main objective was to provide realistic experimental data on g_s of adult deciduous trees exposed to CO₂ enrichment for model-based predictions on the water consumption of forests in a high CO₂ atmosphere.

Materials and Methods

Site description

The experiment was conducted in a diverse forest stand located 15 km south of Basel, Switzerland (47° 28' N, 7° 30' E; elevation: 550 m a.s.l.). The forest is approximately 100 years old with canopy tree heights between 30 and 35 m. The stand has a stem density of 415 trees ha⁻¹ (diameter ≥ 10 cm), a total basal area of 46 m² ha⁻¹ and a leaf area index of approximately 5 in the experimental area. It is dominated by *Fagus sylvatica* L. and *Quercus petraea* (Matt.) Liebl., with *Carpinus betulus* L., *Tilia platyphyllos* Scop., *Acer campestre* L. and *Prunus avium* L. present as companion species. In addition, the site has a strong presence of conifers (*Abies alba* Mill., *Picea abies* L., *Pinus sylvestris* L. and *Larix decidua* Mill.) outside the CO₂-enriched area. Among the species included in the experiment, *Fagus* and *Quercus* contribute 24% and 18%, respectively, to the total basal area under the crane, whereas the other four species contribute less than 6%.

The climate is a typical humid temperate zone climate, characterised by mild winters and moderately warm summers. During the four study years (2001-2003, 2005), the growing season of deciduous trees lasted from the end of April to the end of October (ca. 180 days). Mean January and July temperatures are 2.1 and 19.1° C. Total annual precipitation for the region averages 990 mm, of which two-thirds fall during the growing season. The soil is a silty-loamy rendzina and is characterised by a 15 cm deep rock-free topsoil and a 15-30 cm deep rocky subsoil (approximately 40% of the subsoil volume are stones) underlain by fragmented limestone bedrock. In the upper 10 cm, the soil has a pH of 5.8 (measured in distilled water extracts).

CO₂ enrichment system (web-FACE)

A 45-m freestanding tower crane equipped with a 30-m jib and a working gondola provided access to 62 dominant trees in an area of about 3000 m². A group

of 14 adult broad-leaved trees (3 *Fagus*, 4 *Quercus*, 4 *Carpinus*, 1 *Tilia*, 1 *Acer* and 1 *Prunus*), covering a canopy area of roughly 550 m² were selected for CO₂ enrichment, whereof one slim individual of *Quercus* died. Control trees (3 *Fagus*, 2 *Quercus*, 2 *Carpinus*, 2 *Tilia*, 2 *Acer* and 1 *Prunus*) were located in the remaining crane area at sufficient distance from the CO₂ release zone (mainly in the SW area of the plot). CO₂-enrichment of the forest canopy was achieved by a free-air, pure CO₂ release system that consisted of a web of 4 mm plastic tubes (approximately 0.5 km per tree) with 0.5 mm laser punched holes (spaced at 30-cm intervals) emitting pure CO₂ into the tree canopy. For a more detailed description, see Pepin & Körner (2002).

Stomatal conductance and meteorological measurements

Stomatal conductance to water vapour (g_s , mmol m⁻² s⁻¹) was measured on upper canopy foliage of 13 trees in elevated CO₂ (ca. 540 ppm) and 12 trees in ambient CO₂ (ca. 375 ppm) during eleven sunny days in summer 2001 (12 June-25 Aug). In subsequent years measurements were restricted to *Fagus*, *Quercus*, and *Carpinus* (26 June, 8 July and 14 August 2002; 24 June, 22 July [all six species measured], 22 August 2003; 18 August 2005). Measurements of g_s were carried out in the morning (8:00-12:00) on three fully sunlit leaves per tree (1-4 trees per treatment and species) using a transient state diffusion porometer (AP4, Delta-T Devices, Cambridge, UK). The sampling procedure on each measurement day was designed to compare treatments under relatively similar weather conditions. Hence, a tree was randomly selected first, and then an individual of the same species but opposite treatment was randomly chosen. This procedure was subsequently extended to the other trees. In the drought summer 2003 (14 August, 20 August) predawn leaf water potential was measured with a pressure chamber (SKPM 1400, Skye Instruments, Powys, U.K.) from the canopy crane gondola on the same species where stomatal conductance was measured.

Occasional parallel studies with a steady-state photosynthesis system (LI-6400, Li-Cor, Lincoln, NE, USA) recalled consistently lower leaf conductances, a difference for which we found no explanation and which we consider intrinsic to the two devices. Since the LI-6400 system is based on measurements of mass flow and gas concentrations, whereas the AP4's conductance data rely on an indirect calibration procedure with pore plates and does not ventilate leaves, we rather trust the absolute LI-6400 readings. A literature comparison of g_s values by Körner et al. (1979) and results from a study on non-ventilated porometers by Verhoef (1997) point in the same direction. Concurrent measurements performed with

the AP4 porometer and the LI-6400 gas exchange system under different environmental conditions indicated that readings from both instruments are linearly related ($g_s(\text{LI-6400}) = 0.623 * g_s(\text{AP4}) - 2.09$, $R^2 = 0.972$). Hence, the difference is systematic and the AP4 produces signals proportional to the LI-6400. Subsequent measurements of g_s were, nonetheless, carried out with the AP4 porometer for its far better suitability for such a canopy survey, in which much of the 'true' precision comes from good coverage of the natural variability. Such canopy coverage requires rapid measurement in many leaves across all trees in a daily course. Perhaps even more importantly, the AP4 readings are so fast that they capture the momentary stomatal status in a leaf, whereas the time it takes to achieve readings with the LI-6400 will incur stomatal responses to conditions in the cuvette. Since we are exploring treatment differences rather than absolute values for their own sake, any systematic error would not affect our analysis.

Environmental data

Wind speed, photon flux density, rainfall, air temperature and relative humidity were measured above the tree canopy using a weather station located at the top of the crane (anemometer AN1, quantum sensor QS, tipping bucket rain gauge RG1, shielded temperature and relative humidity probe RHA 1, Delta-T, Cambridge, UK). Measurements were performed every 30 s (except for wind speed which was measured as wind run) and data were recorded as 10-min means using a data logger (DL3000, Delta-T, Cambridge, UK). Vapour pressure deficit (VPD) was calculated from 10-min averages of relative humidity and air temperature. Soil water content was measured using time domain reflectometry (TDR). Six point probes were buried at approximately 10 cm depth, two of which in the CO₂ enriched area and four in the surrounding control area (ML2x, Delta-T, Cambridge, UK). Three additional probes were installed in 2004 and all probes were recalibrated. In addition we used three profile probes to determine moisture content between 0 and 90 cm depth which provided some indication of relative moisture trends in the sub soil (MP-917 and probes PRB-F, Environmental Sensor Inc., Victoria, BC, Canada).

Data processing and statistical analysis

We analysed mean g_s per tree using a repeated measures analysis of variance (RM-ANOVA) with species and CO₂ treatment as fixed factor effects (type I sums of squares, factors in the same order as listed) and time (measurement day or year) as the repeated factor. Our tree sample consisted of 13 treated trees and 12 controls. The unreplicated species *Tilia*,

Acer and *Prunus* were pooled and treated as ‘other’ species, hereafter referred to as ‘TAP’. To test the effect of elevated CO₂ on g_s of all six species, a repeated measures ANOVA was carried out for the first year only (2001; in the following years, measurements have been performed on the three dominant species only). To determine whether CO₂-effects on g_s differed among years, a subsample of the three main species (*Carpinus*, *Fagus*, and *Quercus*) which were measured throughout the four study years was analysed using averages for each tree and year. Furthermore, a RM-ANOVA was computed for each species separately. In the case of dominant species, a seasonal average was calculated for each tree and year, and analysed by a repeated measures ANOVA with treatment as a fixed factor and year as a repeated factor. A similar RM-ANOVA was also carried out for each species and year separately using measurement day as a repeated factor. Additionally, one-way ANOVAs with CO₂ treatment as a fixed factor effect were performed for each species and day separately and for all trees together. CO₂-induced reductions in stomatal conductance (in % of g_s under ambient conditions) were calculated for each species and year. A weighted average reduction was calculated for the years with no exceptional weather conditions (2001, 2002, and 2005) giving the first year a weight of 11/15, the second a weight of 3/15 and the fifth year a weight of 1/15 based on the different number of measurement days (Fig.2 ‘All’). In the case of ‘TAP’, the overall mean is identical with the first year mean, since no additional data were obtained in subsequent years with no exceptional weather conditions. All statistical analyses were computed using R version 2.0.1 with a level of significance of P < 0.05.

Results

Weather conditions

The years 2001, 2002 and 2005 were characterised by average weather conditions (Tab. 1), with the exception of a relatively dry period in August 2001 (Fig. 1). In the first three years there were only two TDR probes which produced inconsistent differences between the CO₂ enriched area and the control area, most likely due to the large spatial heterogeneity of soils. After reinstallation and calibration of the probes in 2004, soil moisture was slightly and consistently higher in the CO₂ enriched area. In summer 2003, central Europe experienced a severe drought with precipitation less than half of normal and air temperatures 2 - 4°C higher than the 10-year average (1989-1999). Towards the end of June, soil water content dropped to approximately 10% (no plant available moisture) in the top 30 cm measured at our study site and

remained at this level throughout July and August (Fig. 1). Similarly low readings were recorded at 60-90 depth with the profile TDR probes during the peak of the drought in August. Hence, during this period, soils were desiccated down to 90 cm depth of the profile and trees depended on deeper moisture reserves (no ground water table on these slopes).

Table 1: Mean air temperature (T), and vapour pressure deficit (VPD) for each measurement day (8:00-12:00). Due to instrument failure data of 31 July 2001 are missing.

Date	T (°C)	VPD (hPa)
12 June 01	12.2	5.1
13 June 01	15.6	6.9
21 June 01	18.5	11.0
26 June 01	21.5	12.1
27 June 01	23.0	12.9
4 July 01	19.0	9.1
26 July 01	21.3	9.5
28 July 01	22.3	7.2
31 July 01	-	-
12 August 01	14.7	5.8
25 August 01	22.2	7.8
26 June 02	18.1	7.6
8 July 02	20.8	8.9
14 August 02	16.8	5.7
24 June 03	23.4	12.6
22 July 03	22.0	10.4
22 August 03	20.5	12.2
18 August 05	18.5	2.8

Stomatal conductance

There was, over all six species, a tendency towards lower stomatal conductance in trees exposed to elevated CO₂ compared to trees under ambient CO₂ conditions (-10%, Tab. 2, Fig. 2). Conductances differed significantly among species and between measurement days leading to a lot of noise in the data set. Furthermore, a significant species x day effect indicated that different species responded differently to changing weather conditions, which added to the observed variation. Although we found species-specific reductions in g_s ranging from -4% in *Quercus* to -21% in *Carpinus*, the species x CO₂-treatment factor was clearly not significant (Tab. 2). Only on one single day in 2001 all species showed a slightly reduced g_s in elevated CO₂ (Fig. 2). To eliminate the large differences in g_s among species, the data were standardised with respect to the maximum daily average g_s of each tree. This, however, did not lead to a significant CO₂ effect either. We calculated the reduction of g_s which could still be detected with the given variation using a power t-test with a significance level of 0.05 and a power of 0.8. A one-sided power t-test was used since we did not expect an increase in g_s in response to elevated CO₂ under regular weather condition. The power test revealed that given the observed variation, a reduction of 25% in stomatal conductance in CO₂-enriched trees would be detectable across all species.

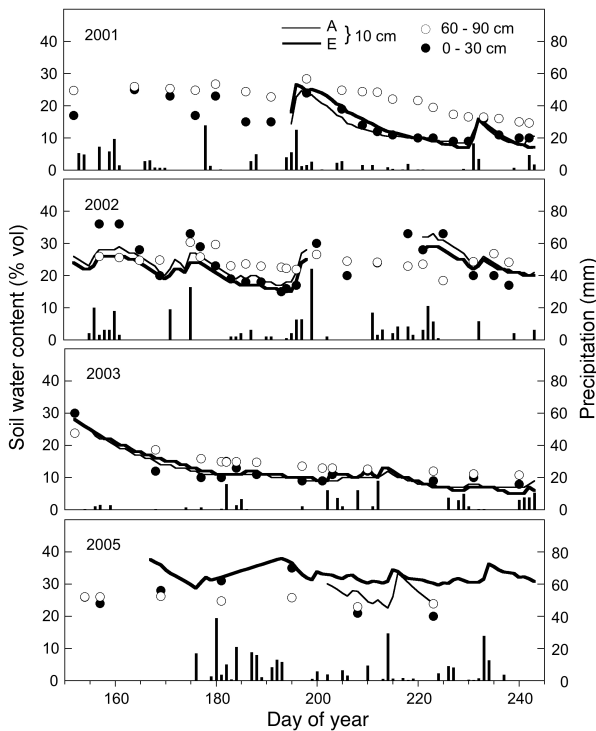


Figure 1: Soil water content at 10 cm depth in the area exposed to ambient CO_2 (A, thin line, $n=2$) and elevated CO_2 (E, thick line, $n=4-7$), at 60-90 cm depth (open symbols) and 0-30 cm depth (closed symbols) both in the ambient CO_2 area ($n=3$) and precipitation (bars) during four growing seasons.

The dominant tree species (*Carpinus*, *Fagus*, and *Quercus*) were sampled over all four study years to examine whether stomatal responses to elevated CO_2 persisted in the long term. Results were very similar to those obtained in the first year when all six tree species were considered. There were no significant CO_2 -effects on g_s , but significant differences in g_s among species and years (Tab. 3), the latter being driven by the lower conductances measured in 2003 during the exceptional drought. These differences in g_s between years were no longer statistically significant after exclusion of the drought year's data. Among species, *Carpinus* showed the largest and most consistent reduction in stomatal conductance in response to CO_2 enrichment which however was only statistically significant on two single days in the first experimental year (Fig. 2). Over the four year period the CO_2 effect was not significant (Tab. 4). Test results were also not significant when considering the growing seasons with no extraordinary weather conditions only or each year separately. For the 'TAP' species, there were no significant differences between treatments (test results not shown). In contrast, *Fagus* and *Quercus* showed much smaller (to negligible) and inconsistent stomatal responses (Fig. 2).

Table 2: Results of repeated measures ANOVA for stomatal conductance of four tree species (*Carpinus*, *Fagus*, *Quercus*, 'TAP' species) exposed to elevated CO_2 over 11 measurement days from June to August 2001.

Factor	df	F	P
Species	3	3.8	0.03
CO_2	1	2.4	0.14
Species x CO_2	3	0.2	0.91
Day	10	12.1	<0.001
Species x Day	30	3.0	<0.001
CO_2 x Day	10	1.0	0.47
Species x CO_2 x Day	30	0.5	0.98

Table 3: Results of repeated measures ANOVA for stomatal conductance of trees exposed to elevated CO_2 of three species (*Carpinus*, *Fagus*, and *Quercus*) during four growing seasons (2001, 2002, 2003, 2005).

Factor	df	F	P
Species	2	6.71	0.014
CO_2	1	0.50	0.49
Species x CO_2	2	0.13	0.88
Year	3	18.38	<0.001
Species x Year	6	2.07	0.09
CO_2 x Year	3	0.93	0.44
Species x CO_2 x Year	6	0.64	0.70

Stomatal responses to elevated CO_2 during a severe drought

During a prolonged drought period in summer 2003 (Fig. 1), g_s of CO_2 -enriched trees and control trees were strongly reduced in most species compared to previous years (Fig. 2). There was, however, considerable variability in stomatal responses to drought among tree species. Mean seasonal g_s at ambient CO_2 during the drought year were only slightly reduced in *Quercus* (6%) compared to 2001, whereas in *Fagus*, the 'TAP' species and *Carpinus*, moderate to pronounced reductions were found (52% - 68%; see 'Year'-effect in Tab. 4). Towards the end of this severe drought, we observed significantly higher conductances in CO_2 -enriched *Carpinus* trees compared to control trees ($P=0.004$, Fig. 2). A trend towards higher g_s values under elevated CO_2 was also observed in the 'TAP' species. At the same time, predawn leaf water potentials tended to be higher in CO_2 -enriched *Carpinus* trees (-1.14 MPa in ambient CO_2 vs. -0.91 MPa in elevated CO_2 , $P=0.053$) but not in trees belonging to the 'TAP' species). In *Fagus* and *Quercus*, g_s was not altered by CO_2 enrichment under these dry soil conditions, in line with the data for other years with no extraordinary weather conditions when no significant CO_2 effect was detected on g_s .

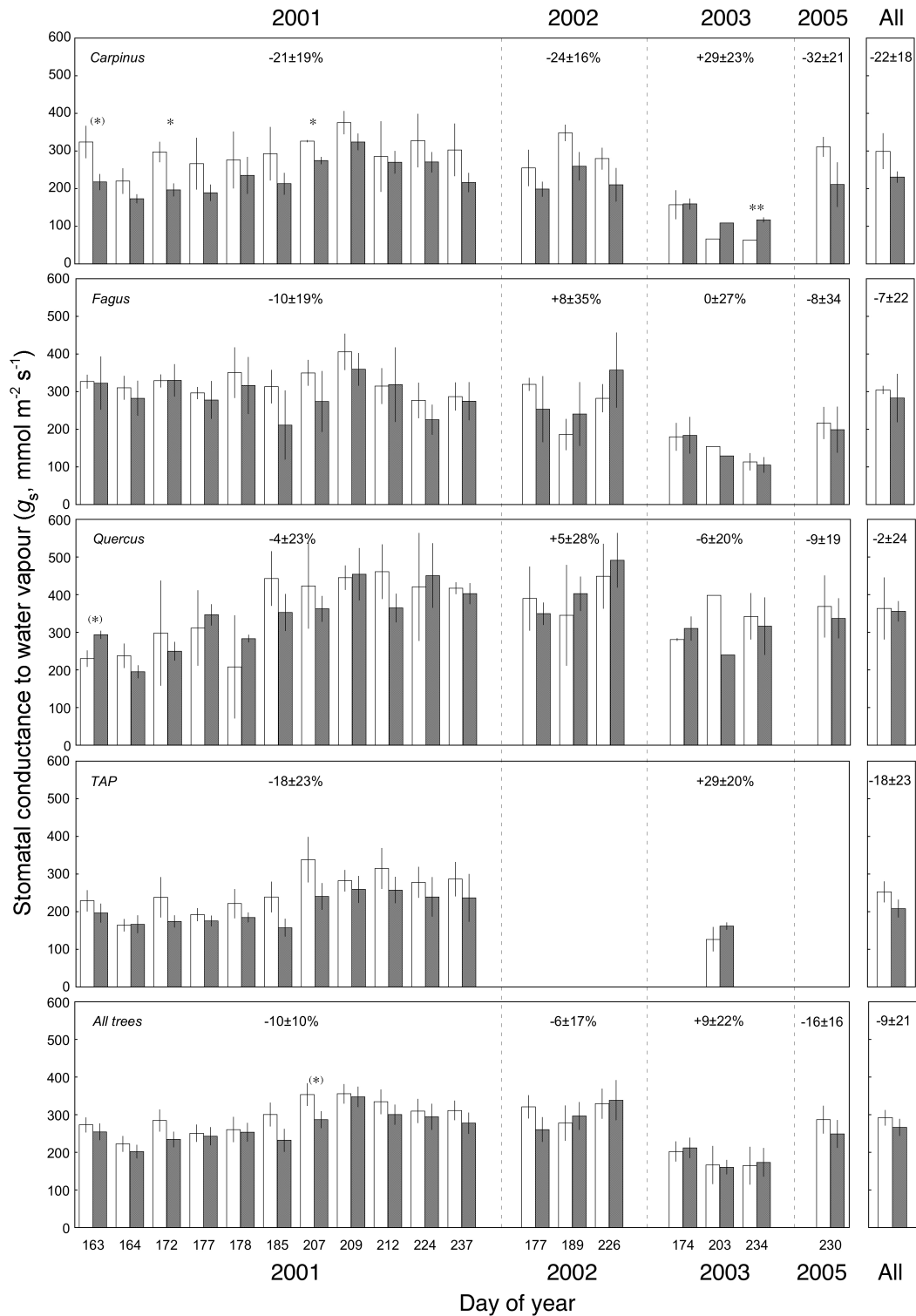


Figure 2: Stomatal conductance (g_s , mean \pm SE) of upper canopy foliage in six deciduous tree species ($n=2-4$ trees) exposed to ambient (A , open bars; ca. 375 ppm) and elevated CO_2 (E , dark bars; ca. 540 ppm) during four growing seasons (8:00-12:00). 'TAP' refers to *Tilia*, *Acer*, and *Prunus*, three species that were pooled because they were not replicated (E , $n=3$; A , $n=5$). The 'All' column refers to average g_s for three years with no exceptional weather conditions (2001, 2002, 2005) weighted by measurement days per year. In the bottom panel, 'All trees' refers to six species in the year 2001 and on day 203 in 2003 (E , $n=13$; A , $n=12$) and the three main species (*Carpinus*, *Fagus*, *Quercus*) in 2002, 2003 and 2005 (E , $n=10$; A , $n=7$). Percent numbers represent mean CO_2 signals \pm SE across season. The summer of 2003 was exceptionally dry. Note, the AP4 porometer produces somewhat high absolute g_s values, which, however, does not affect differences between CO_2 treatments (see Material and Methods). (* $P < 0.1$; * $P < 0.05$; ** $P < 0.01$; *** $P < 0.001$)

Table 4: Results of repeated measures ANOVA for stomatal conductance of three species exposed to elevated CO₂ over four growing seasons (2001, 2002, 2003, 2005).

Factor	df	Carpinus		Fagus		Quercus	
		F	P	F	P	F	P
CO ₂	1	3.11	0.18	0.02	0.91	0.02	0.89
Year	3	7.77	0.005	12.7	0.0005	2.73	0.11
CO ₂ x Year	3	1.58	0.25	0.34	0.80	0.20	0.90

Discussion

This study documents responses of stomatal conductance in a diverse natural forest to elevated CO₂. The four year data reveal that reductions in conductance in response to 540 ppm CO₂ are certainly smaller than 25%. Despite the large number of readings_s and four years of data collection, we were unable to demonstrate the occurrence of a statistically significant reduction of stomatal conductance and only found a tendency towards reduced g_s of around 10% when averaged across all species and trees. As can be seen in Fig. 2 *Carpinus* and the ‘TAP’ species (*Tilia*, *Acer* and *Prunus*) consistently show more pronounced reductions of g_s compared to other species which is in full agreement with sap flow data from the same trees in 2001 (Cech et al. 2003). This makes us believe that significant reductions of g_s in response to CO₂ enrichment would most likely have been found in *Carpinus* and the ‘TAP’ species if there were more trees under the crane area. The reversed responses (increased g_s in CO₂-enriched trees) measured in *Carpinus* and the same tendency observed in the ‘TAP’ species during a severe drought in 2003 reflect the consequences of soil moisture savings_s. Higher predawn leaf water potentials in *Carpinus* under elevated CO₂ and drought adds a piece of evidence that this species is more sensitive to CO₂ than the other species. The size of the responses seen in *Carpinus* and the ‘TAP’ species over the four years, though not significant, are well in line with the mean 21% reduction reported by Medlyn et al. (2001) using a meta analysis for long-term experiments carried out in the field and are also consistent with measurements carried out on *Liquidambar styraciflua* in two FACE experiments (-24%, Gunderson et al. 2002; -28%, Herrick et al. 2004b). The responses in *Fagus* and *Quercus* were much smaller and less uniform, hence CO₂ effects at leaf level are much less likely even if we had more trees. In line with our findings_s Dufrêne et al. (1993), using branch-bags_s in mature *Fagus*, also found no CO₂-effect on g_s in this most common European deciduous tree species. A number of full grown tree species, noteworthy conifers, also have shown no stomatal response to elevated CO₂ (Teskey 1995; Ellsworth 1999).

Our data therefore support that stomatal responses to elevated CO₂ are most likely species-specific. The presence or absence of a certain species in a catch-

ment would thus have hydrological consequences. Our data illustrate the risk of drawing general conclusions from a single species’ response. In this sense, our results match studies conducted on sapling_s and potted trees, which also reported great species specificity in stomatal responses to CO₂ (Picon et al. 1996; Heath 1998).

The study of g_s in this natural, highly diverse, mature forest exposed to elevated CO₂ suffered from the common experimental and analytical difficulties when realistic test conditions come into play (Körner, 2001). To comply with the height requirement of the study trees (between 30 and 35 m) and the complex structure of the canopy, a new CO₂ enrichment system was designed (web-FACE, Pepin and Körner 2002). However, the need of a canopy crane did not permit randomisation of the treatment units (it would require several cranes) and therefore, we employed a detailed investigation of a priori differences in physiology and morphology between control trees and those later exposed to CO₂. The analysis performed by Cech et al. (2003) revealed no systematic differences between the two groups of trees, hence the prerequisites for the experiment were fulfilled. Given the stature of the forest, the large size of the CO₂-enriched area exerted a further constraint, namely that not all species could be measured at the same time despite rapid crane operation. On the other hand, the area was still not large enough to permit replication in both treatments to a desirable extent. One way to handle this was to consider the CO₂ response of ‘trees’ only, irrespective of species (13 treated trees and 12 control trees). We performed such tests, but these revealed no significant CO₂ effect either, possibly due to the large variation in absolute g_s among species (at full stomatal opening g_s in *Quercus* is roughly 2 times that of the other species).

Despite these inevitable problems, it is still remarkable that the trend towards reduced stomatal conductance in the six deciduous tree species exposed to elevated CO₂ was sustained throughout the summers of 2001, 2002 and 2005 (with no exceptional weather conditions as opposed to 2003). This is in agreement with earlier studies which have shown small but consistent responses in g_s of *Liquidambar styraciflua* trees over 3 - 4 years of CO₂ enrichment (Gunderson et al. 2002; Herrick et al. 2004). Bearing in mind that trees in this study are of considerable

age, height, and size, the consistency of the responses over several years (particularly in *Carpinus*) leads to our confidence in the data, although differences were rarely statistically significant. Very good correspondence between these leaf level stomatal conductance data and sap flow density carried out on the same trees in 2001 adds to this confidence. Reductions in mean daily sap flow density of CO₂-enriched trees averaged approximately 11% across all days of the growing season in 2001 (Cech et al. 2003), a value close to the non significant overall 10% reduction in g_s (mean of all six tree species) reported here for the first year, although the stomatal signal does not include a boundary layer component. Furthermore, the same species were found to be more responsive to elevated CO₂ (*Carpinus* and the 'TAP' species).

In plant systems with high stomatal control over transpiration, CO₂-induced reductions in g_s can lead to a decrease in water consumption and result in higher soil moisture content Hungate *et al.* (2002). During a period of relatively high evaporative demand and decreasing soil water content in summer 2001, Cech et al. (2003) observed greater sap flow density in CO₂-enriched trees than in control trees. Although the differences in sap flow density between the two groups of trees were not statistically significant, treatment differences increased over time, providing support to the hypothesis that soil moisture savings in the CO₂-enriched area could reverse the effect of elevated CO₂ on stomatal conductance and transpiration. Based on the findings of Cech et al. (2003), we expected similar soil moisture feedback to appear during the drought conditions of summer 2003 and, indeed we did observe such a reversal of CO₂ effects on g_s of *Carpinus* and a tendency in this direction in the 'TAP' species.

These results suggest that small, at the leaf level hardly measurable, CO₂-induced decreases in g_s are sufficient to translate into a cumulative soil water enrichment in the area exposed to elevated CO₂. There are insufficient data for the rocky subsoil to verify this for roots at greater depth, but a higher predawn leaf water potential under elevated CO₂ and drought suggests water savings throughout all rooted soil horizons (Leuzinger et al. 2005). During the summer drought of 2003, these water savings must have occurred at much deeper soil layers, because soil moisture dropped to 10% at 60-90 cm depth (corresponding to air dry soil moisture). Manual TDR readings, at high spatial frequency in 2002 confirmed that soil water content at approximately 10 cm was significantly increased in the CO₂-enriched area (Cech et al. 2003). Yet, during the extreme summer drought, this method was not applicable since the top soil was completely dry.

During the severe drought of summer 2003, g_s decreased considerably in all investigated species, with

the exception of *Quercus* (a deep rooted, drought-tolerant genus which might have access to soil moisture at greater depth, Epron & Dreyer 1993; Epron & Dreyer 1993). Again, the results matched sap flow measurements showing nearly constant sap flow density in *Quercus* throughout the summer months, whereas in *Carpinus* and *Fagus* sap flow density decreased to half of the early summer maxima (Leuzinger et al. 2005).

In conclusion, we showed that stomatal responses to elevated CO₂ in these mature forest trees are certainly smaller than 25%, most likely in the range of about 10% across species. Globally, even small CO₂-driven reductions in stomatal conductance could have a significant impact on the water balance. Using gas exchange theory only, Gedney *et al.* (2006) speculated that such trends influenced run-off in the twentieth century in a continental specific way. But based on our and other field data (those for conifers in particular) and accounting for atmospheric feedback, we believe that theory based signals are likely to overestimate actual effects substantially. Although we were unable to detect significant reductions in any species, the combined trends in leaf conductance and leaf water potential point at a great sensitivity of *Carpinus* to elevated CO₂ and no leaf level response in *Fagus* and *Quercus*. Based on gas exchange theory (Farquhar & Wong, 1984) no species specificity would be expected. In the long run, such species specific differences may lead to a change in species abundance driven by soil moisture (and nutrient) effects. Our results clearly demonstrate the need to account for biodiversity and both soil moisture and atmospheric humidity feedback on CO₂ responses of stomata in order to arrive at a realistic picture of the hydrological and biological consequences of ongoing atmospheric CO₂-enrichment.

Acknowledgements We thank Erwin Amstutz and Olivier Bignucolo for crane operations and on site support. The CO₂-enrichment experiment was funded by the Swiss National Science Foundation projects No. 3100-059769.99, No. 3100-067775.02, No. 5005-65755 (Swiss NCCR Climate) and the Swiss Canopy Crane by the Swiss Agency for the Environment, Forest and Landscape. We thank two anonymous reviewers for helpful suggestions on the manuscript.

References

- Bucher-Wallin IK, Sonnleitner MA, Egli P, Gunthardt-Goerg MS, Tarjan D, Schulin R, Bucher JB (2000) Effects of elevated CO₂, increased nitrogen deposition and soil on evapotranspiration and water use efficiency

- of spruce-beech model ecosystems. *Phyton - Annales Rei Bonanicae*, **40**, 49–60.
- Cech PG, Pepin S, Körner C (2003) Elevated CO₂ reduces sap flux in mature deciduous forest trees. *Oecologia*, **137**, 258–268.
- Curtis PS, Wang XZ (1998) A meta-analysis of elevated CO₂ effects on woody plant mass, form, and physiology. *Oecologia*, **113**, 299–313.
- Dufrene E, Pontailler JY, Saugier B (1993) A branch bag technique for simultaneous CO₂ enrichment and assimilation measurements on beech (*Fagus sylvatica* L.). *Plant Cell and Environment*, **16**, 1131–1138.
- Ellsworth DS (1999) CO₂ enrichment in a maturing pine forest: are CO₂ exchange and water status in the canopy affected? *Plant Cell and Environment*, **22**, 461–472.
- Epron D, Dreyer E (1993) Long-term effects of drought on photosynthesis of adult oak trees [*Quercus petraea* (Matt) Liebl. and *Quercus robur* Liebl.] in a natural stand. *New Phytologist*, **125**, 381–389.
- Farquhar GD, Wong SC (1984) An empirical model of stomatal conductance. *Australian Journal of Plant Physiology*, **11**, 191–220.
- Gedney N, Cox PM, Betts RA, Boucher O, Huntingford C, Stott PA (2006) Detection of a direct carbon dioxide effect in continental river runoff records. *Nature*, **439**, 835–838.
- Gunderson CA, Sholtis JD, Wullschleger SD, Tissue DT, Hanson PJ, Norby RJ (2002) Environmental and stomatal control of photosynthetic enhancement in the canopy of a sweetgum (*Liquidambar styraciflua* L.) plantation during 3 years of CO₂ enrichment. *Plant Cell and Environment*, **25**, 379–393.
- Heath J (1998) Stomata of trees growing in CO₂-enriched air show reduced sensitivity to vapour pressure deficit and drought. *Plant Cell and Environment*, **21**, 1077–1088.
- Herrick JD, Maherali H, Thomas RB (2004a) Reduced stomatal conductance in sweetgum (*Liquidambar styraciflua*) sustained over long-term CO₂ enrichment. *New Phytologist*, **162**, 387–396.
- Herrick JD, Maherali H, Thomas RB (2004b) Reduced stomatal conductance in sweetgum (*Liquidambar styraciflua*) sustained over long-term CO₂ enrichment. *New Phytologist*, **162**, 387–396.
- Hungate BA, Reichstein M, Dijkstra P, *et al.* (2002) Evapotranspiration and soil water content in a scrub-oak woodland under carbon dioxide enrichment. *Global Change Biology*, **8**, 289–298.
- Jones MB, Brown JC, Raschi A, Miglietta F (1995) The effects on arbutus unedo L. of long-term exposure to elevated CO₂. *Global Change Biology*, **1**, 295–302.
- Körner C (1995) Towards a better experimental basis for upscaling plant responses to elevated CO₂ and climate warming. *Plant, Cell and Environment*, **18**, 1101–1110.
- Körner C (2001) Biosphere responses to CO₂ enrichment. *Ecol. Appl.*, p. in press.
- Körner C (2002) Grassland in a CO₂-enriched world. In: *Multi-function Grasslands* (eds Durand JL, Emile JC, Huyghe C, Lemaire G), pp. 611–624. Versailles cedex, France.
- Medlyn BE, Barton CVM, Broadmeadow MSJ, *et al.* (2001) Stomatal conductance of forest species after long-term exposure to elevated CO₂ concentration: a synthesis. *New Phytologist*, **149**, 247–264.
- Morison JIL, Gifford RM (1984) Plant growth and water use with limited water supply in high CO₂ concentrations. II. Plant dry weight, partitioning and water use efficiency. *Aust J Plant Physiol*, **11**, 375–384.
- Pepin S, Körner C (2002) Web-FACE: a new canopy free-air CO₂ enrichment system for tall trees in mature forests. *Oecologia*, **133**, 1–9.
- Picon C, Guehl JM, Ferhi A (1996) Leaf gas exchange and carbon isotope composition responses to drought in a drought-avoiding (*Pinus pinaster*) and a drought-tolerant (*Quercus petraea*) species under present and elevated atmospheric CO₂ concentrations. *Plant Cell and Environment*, **19**, 182–190.
- Saxe H, Ellsworth DS, Heath J (1998) Tree and forest functioning in an enriched CO₂ atmosphere. *New Phytol.*, **139**, 395–436.
- Teskey RO (1995) A field-study of the effects of elevated CO₂ on carbon assimilation, stomatal conductance and leaf and branch growth of *Pinus taeda* trees. *Plant Cell and Environment*, **18**, 565–573.
- Tognetti R, Longobucco A, Miglietta F, Raschi A (1998) Transpiration and stomatal behaviour of *Quercus ilex* plants during the summer in a Mediterranean carbon dioxide spring. *Plant Cell and Environment*, **21**, 613–622.
- Tognetti R, Longobucco A, Miglietta F, Raschi A (1999) Water relations, stomatal response and transpiration of *Quercus pubescens* trees during summer in a Mediterranean carbon dioxide spring. *Tree Physiology*, **19**, 261–270.
- Wullschleger SD, Gunderson CA, Hanson PJ, Wilson KB, Norby RJ (2002) Sensitivity of stomatal and canopy conductance to elevated CO₂ concentration interacting variables and perspectives of scale. *New Phytologist*, **153**, 485–496.

Chapter 5

Tree species diversity affects canopy leaf temperatures in a mature temperate forest

Tree species diversity affects canopy leaf temperatures in a mature temperate forest

Agricultural and Forest Meteorology, submitted

Sebastian Leuzinger and Christian Körner

Abstract Forest canopies play a major role in the biosphere - atmosphere interaction. Their actual temperature may deviate substantially from ambient atmospheric conditions as reported by weather stations. While there is a long tradition of false-colour imagery, new digital technologies in combination with IR transmission lenses and autocalibration routines permit unprecedented insight into the actual temperature regimes in canopies. We report canopy leaf temperature distribution over space and time assessed over a 35 m tall mixed deciduous forest in NW Switzerland by means of a construction crane and a high resolution thermal camera. At an air temperature of 25° C, conifers (*Picea abies*, *Pinus sylvestris* and *Larix decidua*) and deciduous broad-leaved trees with exceptionally high transpiration (*Quercus petraea*) or very open, low density canopies (*Prunus avium*) exhibited mean canopy leaf temperatures close to air temperature (0.3 to 2.7 K above ambient) and the maximum amplitude within a given crown reached 6 to 9 K. In contrast, broad-leaved deciduous species with dense canopies (*Fagus sylvatica*, *Carpinus betulus* and *Tilia platyphyllos*) were 4.5 to 5 K warmer than air temperature and showed within canopy temperature amplitudes of 10 to 12 K. Calculated leaf boundary resistance was clearly lower for conifers (3 to 24 ms⁻¹) than for broad-leaved trees (33 to 64 ms⁻¹). The study illustrates that mean leaf temperatures in forest trees are not adequately explained by either stomatal conductance or leaf dimensions, but strongly depend on canopy architecture (leaf area density, branching habits) in combination with leaf traits. Aerodynamic leaf and canopy characteristics lead to strongly enhanced vapour pressure gradients (evaporative forcing) and leaf temperatures vary enormously over short distances, calling for statistical T-models (frequency distribution) rather than the use of means in any flux calculations. The presence/absence of certain tree taxa plays a key role in forest surface temperature.

Introduction

The leaf energy balance and the resulting leaf temperature are central themes of biometeorology. Transpiration, sensible heat flux, photosynthesis, respiration and other metabolic activities are driven by leaf temperature. The leaf, on the other hand, also influences its temperature through stomatal control of transpiration and traits which affect heat exchange (size, shape, angle, pubescence, length of petiole etc.). On top of these, canopy architecture (height, density, roughness) control heat and water exchange and thus effective temperatures (Grace 1977, Jones 1992). These characteristics may change rapidly (after minutes) in the case of stomatal conductance, at seasonal scales in the case of leaf angle or leaf position (heliotropism, seasonal shoot growth) or canopy density (seasonal loss of foliage). Long-term changes (many years to centuries) operate through community dynamics, i.e. the abundance of taxa with certain leaf or canopy characteristics (leaf morphology, size, surface properties, canopy architecture) as well as reflectance and specific leaf water relations. Seasonal phenology also plays a key role. All these features may either increase or reduce canopy temperature, which is then further influenced by dynamic interactions with the atmosphere (Jarvis & McNaughton, 1986). To some extent, trees can engineer their thermal environment and thereby avoid excessive heat or enhance temperatures at otherwise cool conditions. One of the first detailed studies on leaf temperatures across a wide range of taxa and leaf morphologies using thermocouples was undertaken by Ansari & Loomis (1959). They state that generally, sunlit thin leaves warm ca. 6 to 10 K above air temperature in still air and ca. 3 to 5 K with moderate wind speed (5 m/s), a rule of thumb that is still widely valid.

Leaf temperatures are key to many aspects of functional plant ecology. Their significance for plant water relations was acknowledged already in the early 20th century (see review by Raschke 1960), irrigation scheduling by means of canopy temperature surveys has been used in agri- and horticulture since the 1960s (e.g. Fuchs & Tanner 1966, Jackson *et al.* 1977, Fuchs

1990, Jones 2004). More recently, methods have been developed to accurately estimate stomatal conductance from leaf temperatures (Jones 1999, Jones *et al.* 2002, Leinonen *et al.* 2006). Other applications reach from land-surface climate modelling (Dai *et al.*, 2004) to highly topical issues of increasing land surface temperatures caused by global warming (Zaitchik *et al.*, 2006). McElwain *et al.* (1999) even explain the great turnover of the Triassic-Jurassic megafloora with a selection for smaller leaves better adapted to high leaf temperatures.

Large-scale vegetation surveys became possible using satellite infrared images (e.g. Soer 1980). Various vegetation-related parameters can be estimated from such data, including transpiration (Zhang *et al.*, 2003), plant water stress (Mahey *et al.*, 1991), NDVI (Nemani & Running, 1989) and of course, canopy temperature in their own right (Matsushima & Kondo, 2000).

While surveying vegetation temperatures from aircrafts or satellites can cover vast surface areas in short time, such data are too coarse to account for within-canopy variation and differences between species. Rather than the mean, it is the fine-scale temperature distributions and diurnal variation in temperature which determine heat and gas fluxes. In particular for broad-leaved trees in temperate and tropical forests, canopy temperature may differ substantially among species (Grace, 1977). The use of canopy cranes have made it possible to carry out IR-measurements from close enough distance and with the needed temporal and spatial resolution to provide the species-specific leaf temperatures that are actually experienced under given environmental conditions.

The immediate coupling of leaf temperature with its latent heat loss (Jones & Leinonen, 2003) calls for a description of plant water status parameters, particularly when water supply is highly variable. Temperate forests, however, were found to be the least sensitive low elevation vegetation type to the prolonged 2003 summer drought and heatwave over Europe in terms of canopy temperature and NDVI (Zaitchik *et al.* 2006). This is in line with concurrent water relations data, showing that at the present study site, it takes over three weeks of continuous drought to significantly reduce daily sap flow peaks (Leuzinger *et al.*, 2005). Therefore, leaf temperature characteristics of deciduous temperate forests are expected to be relatively robust and less dependent on short-term variation in soil moisture than other types of vegetation such as grassland and crops.

The aim of this study was to provide basic data on species specific spatial and temporal canopy temperature distributions of tall temperate zone forest trees. In particular, we juxtapose coniferous and broad-leaved species and 'open' versus 'compact' tree

canopies to explore the significance of forest species composition on canopy heat accumulation. We substantiate our discussion by accounting for leaf morphology and leaf diffusive conductance.

Materials and Methods

Site description and studied species

We used a diverse mixed forest stand located 15 km south of Basel, Switzerland (47° 28' N, 7° 30' E; elevation: 550 m a.s.l.). The forest is approximately 100 years old with canopy tree heights between 30 and 38 m. The stand has a stem density of 415 trees ha⁻¹ (diameter ≥ 10 cm), a total basal area of 46 m² ha⁻¹ and a leaf area index of ca. 5 in the experimental area (Pepin & Körner, 2002). It is dominated by *Fagus sylvatica* L. and *Quercus petraea* (Matt.) Liebl., with *Carpinus betulus* L., *Tilia platyphyllos* Scop., *Acer campestre* L. and *Prunus avium* L. present as companion species. In addition, the site has a strong natural presence of conifers (*Abies alba* Mill., *Larix decidua* Mill., *Picea abies* L., *Pinus sylvestris* L.). We henceforth refer to the genus only. A 45-m freestanding tower crane equipped with a 30-m jib and a working gondola provided access to 64 dominant trees in an area of ca. 3000 m². Fourteen adult trees have been subjected to a CO₂ treatment since 2001 (Pepin and Körner 2002). Although these trees showed a mean ca. 15 % reduction in whole canopy transpiration (sap flow), this did not lead to measurable canopy warming (>0.3 K) at the scale at which measurements were taken (Leuzinger and Körner, submitted). Part of the sap flow response resulted from downward adjustment in LAI (in *Fagus*). Therefore, CO₂-treated and non-treated trees were not further distinguished in the current analysis.

The climate is a typical humid temperate zone climate, characterised by mild winters and moderately warm summers. Mean January and July temperatures are 2.1 and 19.1° C. Total annual precipitation at the study site was 950 mm in 2004 and 910 mm in 2005, which is close to the expected long-term average at that site (990 mm), of which two-thirds normally falls during the growing season. The soil is a silty-loamy rendzina that developed on calcareous bedrock. In terms of moisture regime, the two years during which the present study was conducted were average years, and all measurements were carried out at ample soil moisture and clear sky.

Environmental data and soil moisture

Wind speed, photon flux density, rainfall, air temperature and relative humidity were measured above the tree canopy using a weather station located at the top of the crane (anemometer AN1, quantum

sensor QS and a tipping bucket rain gauge RG1, all from Delta-T, Cambridge, UK). Measurements were performed every 30 s and data were recorded as 10-min means using a data logger (DL3000, Delta-T, Cambridge, UK). Vapour pressure deficit (henceforth referred to as vpd) was calculated from wet and dry bulb, self-made aspiration psychrometer (10-min averages) located at canopy height. Net radiation was measured separately with a net radiometer located ca. 10 m above the canopy (CRN1, Kipp and Zonen, Delft, The Netherlands). Soil water content was measured at ca. 10 cm depth using seven time domain reflectometry probes (ML2x probes, Delta-T, Cambridge, UK) logged hourly in order to provide high time resolution. Soil water in fine substrate around 4 TDR profile probes (PRB-F time domain reflectometry, Environmental Sensor, Victoria, BC, Canada) was approximately uniformly distributed between 0 and 90 cm throughout the 2004 and 2005 growing season. With an increasing rock density at depth, this means that soil moisture per unit soil volume is much lower at deeper soil horizons, while the actual concentration per unit fine substrate in rock crevices may even increase with depth.

Thermal imaging

We used a state-of-the-art thermal camera (Vario-Cam, Infratec, Dresden, Germany) with a resolution of 240 x 320 pixels, providing 76'800 temperature readings with a 0.1 K resolution. For the type of closed vegetation considered here, a constant emissivity of 98 % was assumed (Rubio et al. 1996). For the spatial distribution, we scanned the whole canopy under the crane jib during stable clear sky conditions in midsummer. Canopy regions of similar size and sun exposure were selected for frequency distribution analysis (see Figure 2). Approximately 5-10 such frames per tree, taken at 5 to 50 s intervals, were averaged to obtain a temporally and spatially robust pattern of temperature distribution per tree. For the temporal temperature distributions, we took IR-pictures at a frequency of 0.2 Hz (5 s intervals) on two cloud-free days with little wind. We scanned a defined part of the canopy from the counter jib of the crane from 7.30 am to 10 am (true local time) and from 7.30 until 2 pm respectively. Similarly exposed and sized canopy surface polygons were selected to track mean temperature. Both for spatial and temporal analyses, thermal images were filtered from what was clearly identified as background and non-leaf temperatures (e.g. branches, forest soil). For temperature series, the mean values were smoothed with an automatic spline function (R Development Core Team, 2004) to facilitate graphic representation.

Data processing and statistical analysis

For analyses of thermal images, Irbis professional (In-

fratec, Dresden, Germany) was used. The free software package 'R', version 2.1.0 (R Development Core Team, 2004) was used for all data processing, statistical analyses and graphics.

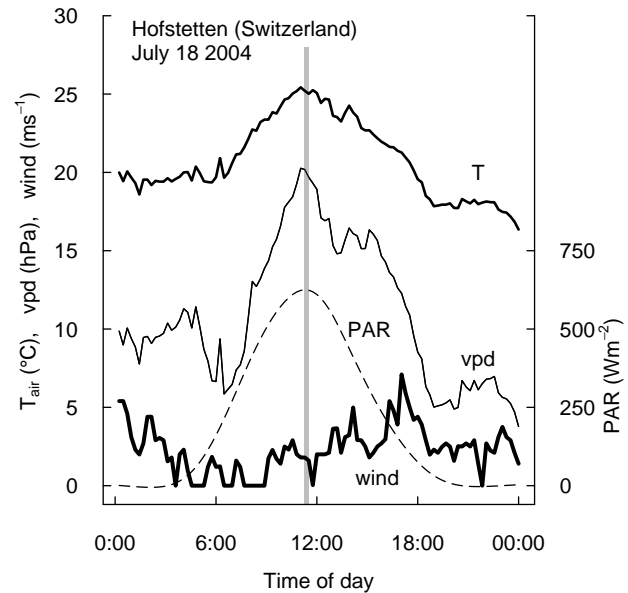


Figure 1: Vapour pressure deficit (vpd), PAR (Wm^{-2}), wind (ms^{-1}) and air temperature ($^{\circ}\text{C}$) during the canopy temperature measurements in 2004 (see Figure 3). The grey bar indicates the time period when measurements took place.

Results

Water status

The water status of plants is intimately coupled with their foliage temperature. Thus, the interpretation of leaf temperature data requires data on the plants' water supply. For the present study, all leaf temperature measurements were made at ample forest water supply. During the 2004 measurements, mean soil moisture at 10 cm depth was 31 Vol. % while during the 2005 measurements, mean soil moisture was 35 Vol. %. For the present soil type and climatic conditions, this is a very high soil moisture content (field capacity) and means that trees operated far from shortage of soil moisture and exhibited close to maximum transpiration. From previous studies during the 2003 summer drought, we know that the deciduous species studied here are not very sensitive to even prolonged drought as rated by their stomatal downregulation and sap flow, possible because of deep water storage (no ground water table on these calcareous slopes, Leuzinger et al. 2005). Hence, the leaf temperatures of the studied trees here can be expected to reflect

conditions of unrestricted evaporative cooling. Maximal stomatal conductance of the investigated deciduous species ranged from 70 to 340 $\text{mmolm}^{-2} \text{s}^{-1}$ (Figure 1, Table 1 and Keel et al. 2006, Sellin and Kupper 2004, Handa et al. 2005, Willert et al. 1995).

Spatial temperature distribution

Canopies were scanned on July 18 2004 from 11.30 to 11.40 true local time at 25.0°C air temperature and a vpd of 19.7 hPa (Figure 1). Figure 2 shows an example of a thermal image with parts of a *Larix* (dark blue, ca. 25°C), *Quercus* (light blue, ca. 27.5°C) and *Carpinus* (red, ca. 30°C) canopy and some selected frames used to compute mean temperatures and temperature ranges shown in Table 1. The false colours also illustrate the wider temperature range seen in the broad-leaved trees opposed to the very narrow range of *Larix*. Except for the very open canopies of *Prunus* (26.7°C) and the highly transpiring *Quercus* (27.4°C), all deciduous species showed higher mean leaf temperatures (29.5 to 29.8°C) than the coniferous species (25.3 to 27.0K , Table 1, Figure 3). With the exception of *Prunus* (7.3K) and *Quercus* (8.9K), the temperature ranges found across a given tree canopy were distinctly narrower in coniferous species (6 to 8.9K) than in the broad-leaved deciduous species (10.0 to 11.8K). Except for the data of *Pinus*, all frequency distributions were slightly skewed to the upper temperature range. *Larix*, the only deciduous coniferous species, showed by far the lowest canopy temperature, approximately equal to the ambient air temperature.

Temporal temperature distribution

We measured mean leaf to air temperature difference (ΔT_{L-A}) on June 24 and 28 2005, two meteorologically similar days (from 07:30 to 10:00 on day 1, left panels in Figure 4, and from 07:00 to 14:00 on day 2, right panels in Figure 4). Temperature series in Figure 4 were smoothed with a cubic spline function (R Development Core Team, 2004) for the sake of clear visualisation of the rapidly fluctuating signals. Day 1 had a less smooth increase in radiation (some cirrus clouds) which was mirrored by lower ΔT_{L-A} in all species. The three species that were monitored on both days showed very similar patterns of ΔT_{L-A} . With up to 6 K, *Tilia* had consistently the highest ΔT_{L-A} followed by *Fagus* (up to 4.5 K) and *Quercus* (up to 3 K). *Carpinus* was not measured on the second day, but remained ca. 1 K below *Tilia* on the first day. This ranking of ΔT_{L-A} among species confirms approximately the one from the instantaneous ΔT_{L-A} measurements shown in Figure 3.

As a measure for the short-term temporal variability of the above temperature series $\Delta T_{L-A,t}$, where t annotates time, we calculated the standard errors (s.e.) of the first order differenced time series, i.e. $\Delta^1 \Delta T_{L-A,t} = \Delta T_{L-A,t} - \Delta T_{L-A,t-1}$ (K) where Δ^1 stands for first order differencing characterising the deviation of $\Delta T_{L-A,t}$ from $\Delta T_{L-A,t-1}$. The time step was 5 seconds, i.e. the frequency 0.2 Hz. Day one (left panel of Figure 4, only morning hours) showed more short-term variation than day two (right panel of Figure 4), but there was no significant difference between species within the respective days. On day one, s.e. ($\Delta^1 \Delta T_{L-A,t}$) was $3.0 \cdot 10^{-3} \text{K}$ for *Tilia*, $2.1 \cdot 10^{-3} \text{K}$ for *Fagus*, $2.8 \cdot 10^{-3} \pm 0.2 \cdot 10^{-3} \text{K}$ for *Carpinus* and $2.3 \cdot 10^{-3} \pm 0.1 \cdot 10^{-4} \text{K}$ for *Quercus*. On day two, s.e. ($\Delta^1 \Delta T_{L-A,t}$) was $2.0 \cdot 10^{-3} \text{K}$ for *Tilia*, $1.6 \cdot 10^{-3} \pm 0.2 \cdot 10^{-4} \text{K}$ for *Fagus* and $1.4 \cdot 10^{-3} \pm 0.1 \cdot 10^{-4} \text{K}$ for *Quercus*.

Estimation of aerodynamic leaf boundary layer resistance

The energy balance equation for a leaf, solved for leaf to air temperature difference ΔT_{A-L} , reads

$$\Delta T_{A-L} = \frac{r_{HR}(r_{aW} + r_{lW})\gamma\Phi_{ni}}{\rho_a c_p (\gamma(r_{aW} + r_{lW}) + sr_{HR})} - \frac{r_{HR}\delta e}{\gamma(r_{aW} + r_{lW}) + sr_{HR}},$$

with the density of air ρ_a , the thermal conductivity of air c_p , the psychrometer constant γ , the isothermal net radiation Φ_{ni} and the slope s of the linearised relationship between the leaf to air temperature difference and the vapour pressure deficit of the air δe (Jones 1992). When solved for r_{aW} , the leaf boundary layer resistance to water vapour, we obtain

$$r_{aW} = \frac{\rho_a c_p r_{HR} (\delta e + \Delta T_{A-L} s)}{\gamma (r_{HR} Q_{ni} - \Delta T_{A-L} \rho_a c_p)} - r_{lW}.$$

Net radiation Φ_{ni} as measured with a net radiometer was 642Wm^{-2} and r_{HR} was varied from 5 to 200sm^{-1} but since it did not change resistances substantially, it was fixed at 50sm^{-1} . A constant leaf area index (LAI) of 5 was assumed. The thus calculated leaf boundary resistances r_{aW} were higher for the broad-leaved (33 to 65sm^{-1}) than for the coniferous trees (3 to 24sm^{-1} , Table 1).

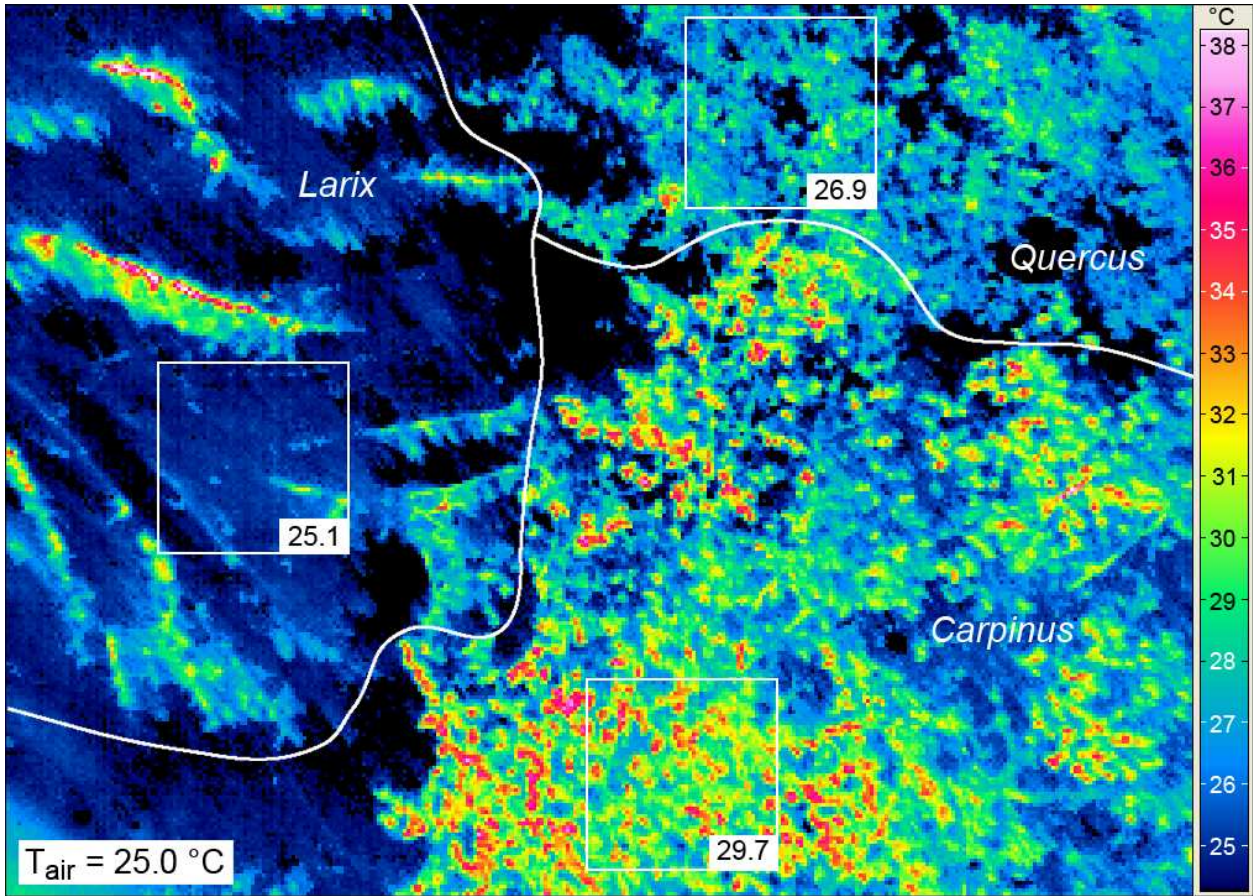


Figure 2: False colour thermal image taken on August 18 2004, 11.30, showing parts of a *Larix* (left, ca. 25° C), *Quercus* (top right, ca. 27.5° C) and *Carpinus* (right, ca. 30° C) canopy. The squares show some selected frames that have been used to compute mean canopy temperatures shown in Figure 3. Areas that were clearly showing branch (note for example the linear structures above the left frame which are the monopodial branches of *Larix*) or shaded understory temperatures (black colour) were either avoided or excluded in the calculations. The *Carpinus* canopy is divided into three major crowns, the centre of the tree is lower and not fully sun-exposed.

Table 1: Mean Canopy temperature with number of replicates n , leaf to air temperature difference, T-range, minimum and maximum, leaf width and the standard error (where applicable) of three coniferous and five deciduous forest trees. The two right-most columns indicate the maximum conductances g_s ($\text{mmolm}^{-2}\text{s}^{-1}$) of 15 bright summer days during 2001 to 2005 (measurements from the drought year 2003 were excluded) and the difference between theoretical leaf to air temperature difference ($\Delta_{L-A,i}$) and the measured one (Δ_{L-A} , see text). Constants used were: $\gamma = 66.5 \text{ Pa K}^{-1}$ (at 25° C), $\rho = 1.175 \text{ kg m}^{-3}$ and $s = 189 \text{ PaK}^{-1}$. Stomatal conductances are cited from the indicated references where unavailable from the present study site.

species	n	T_{mean}	ΔT_{L-A}	T-range	T_{min}	T_{max}	leaf width (mm)	g_s	r_{aW} (sm^{-1})
Larix	1	25.3	0.3	6.0	23.4	29.5	0.4±0.04	250 ²	24.2
Prunus	2	26.7±0.20	1.7	7.3±0.55	24.0±0.25	31.4±0.30	41.2±1.2	237	33.4
Pinus	2	27.0±0.17	2.0	6.3±0.85	23.9±0.70	30.4±0.15	1.3±0.06	120 ³	2.8
Quercus	12	27.4±0.22	2.4	8.9±0.37	23.3±0.11	32.2±0.36	49.1±1.2	343	49.9
Picea	2	27.8±0.07	2.8	8.9±0.05	24.9±0.10	33.8±0.15	1.2±0.05	125 ¹	12.5
Carpinus	5	29.5±0.21	4.5	10.3±0.24	25.1±0.19	35.6±0.17	36.8±0.8	240	59.9
Fagus	9	29.6±0.34	4.6	10.0±0.37	24.9±0.11	34.9±0.37	45.2±1.0	272	64.9
Tilia	2	29.8±0.88	4.8	11.8±0.30	25.1±0.25	37.0±0.55	72.3±2.0	207	57.8

¹(Sellin & Kupper, 2004), ²Handa *et al.* (2005), ³Willert *et al.* (1995)

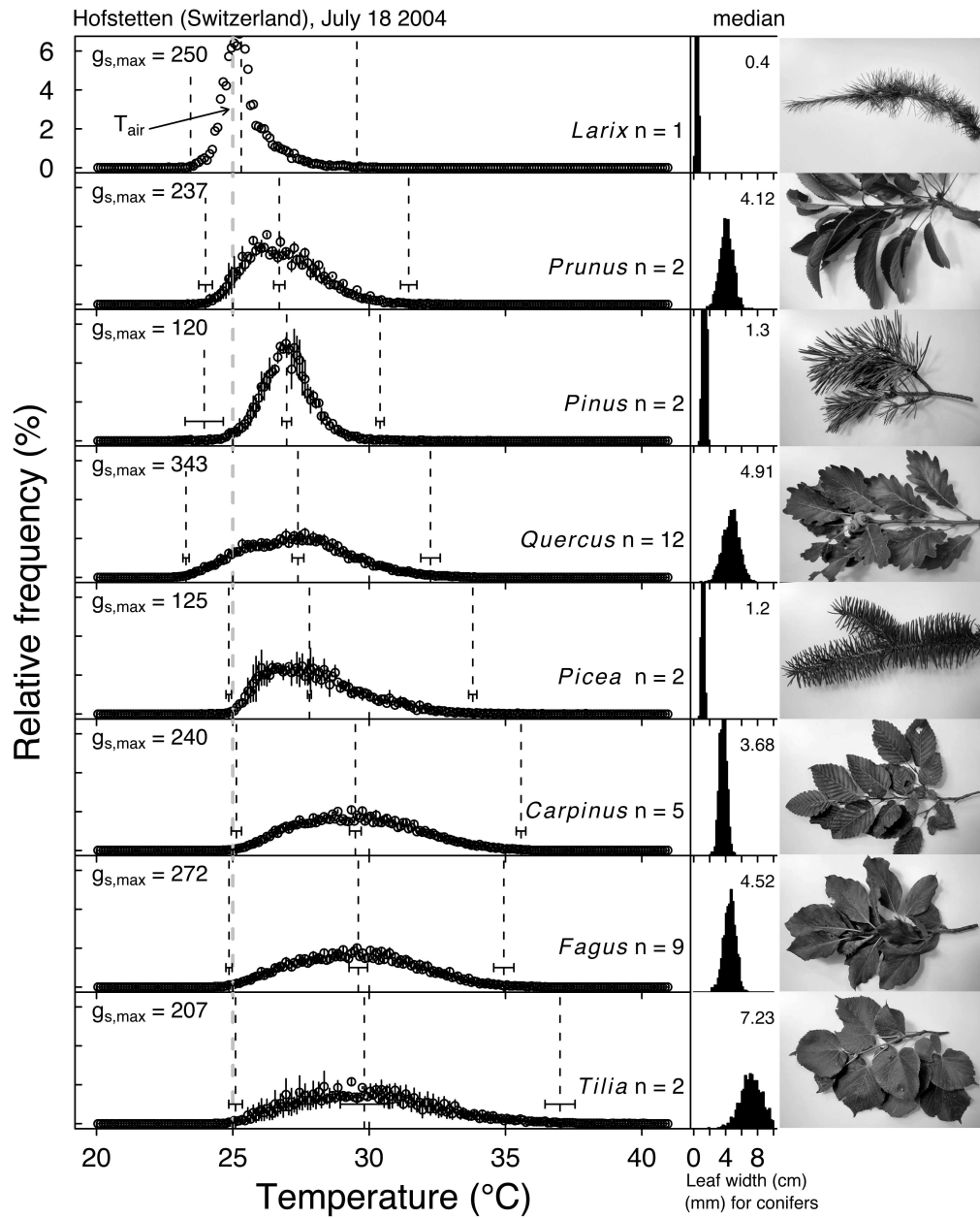


Figure 3: Leaf temperature distributions (left) and leaf width (right) of the eight different species shown (photos) at an ambient air temperature of 25° C with standard errors where applicable. Broken vertical lines show minimum, mean and maximum with the according standard errors (horizontal bars). Maximum g_s values are inserted (see Table 1). Note the different scales for coniferous and broad-leaved leaf widths. The mean is indicated in cm in the top right corner.

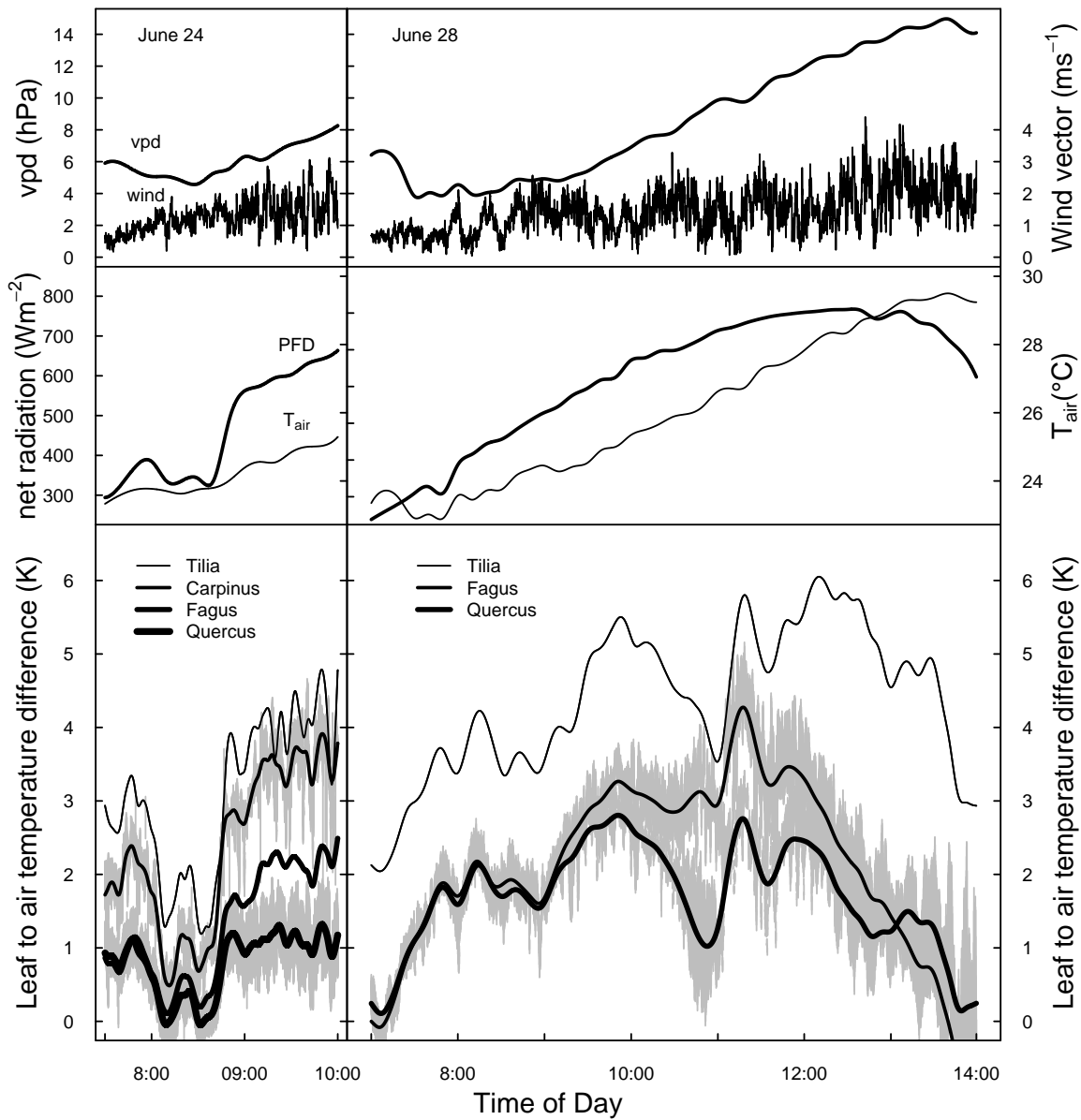


Figure 4: Leaf to air temperature difference and four environmental parameters at the Swiss Canopy Crane site in Hofstetten during two days in 2005 (Day 1: June 24, left panel; day 2: June 28, right panel). *Tilia*, *Fagus*, *Carpinus* and *Quercus* with grey vertical bars as standard errors where replication was available (Day 1: *Carpinus* n=2, *Quercus* n=4. Day 2: *Fagus* n=3, *Quercus* n=3).

Discussion

This study demonstrates that mean canopy temperatures of temperate forest trees deviate substantially from air temperature, but in a highly species-specific manner. On an average summer day, ΔT_{L-A} reached from nearly 0 K in the aerodynamically well coupled *Larix* to 5 K for *Tilia* with its exceptionally dense canopy structure. Further, canopy temperature ranges became generally wider with mean leaf width, probably because within-leaf temperature ranges also increased with leaf width. Neither mean canopy temperature nor canopy temperature ranges are explained in a straight-forward manner by leaf width, maximum stomatal conductance or their combination. It rather appears that canopy characteristics (branching, leaf density, canopy roughness) are causing the final canopy temperature pattern, which can only be determined empirically.

Mean canopy temperature tracked over time at a frequency of 0.2 Hz for a subset of species confirmed the T-patterns found in the analysis of individual pictures (*Tilia* > *Fagus* > *Carpinus* > *Quercus*), except for *Fagus*, which was cooler than *Carpinus* on one day (Figure 4 left panel). This shows that under stable weather conditions, several single images adequately describe mean canopy temperature distribution, and that long time series may not be necessary. The analysis of the differenced time series as a measure of temporal variability did not show consistent differences between species, although *Tilia* had the highest short-term variability on both days. This may be explained by its (compared to the other species) rather decoupled canopy (see below), which is strongly influenced by the short-term radiation regime and only little buffered by the air temperature (Jarvis & McNaughton 1986, McNaughton & Jarvis 1991). The average difference between temperature means of two subsequent images (5 s intervals) was approximately $1 \cdot 10^{-3}$ K for all species. This means that average leaf cooling or warming under these fully sunlit conditions occurred at a rate of ca. 0.12 K per minute.

We find the variability of the T-ranges (nearly doubling from *Larix* to *Tilia*) within the different canopies remarkable. A canopy-dwelling spider for example would only be exposed to 23 to 30° C in a *Larix* canopy, while if it sat on a *Tilia* canopy, it would be exposed to 25 to 37° C.

The calculation of the leaf boundary layer resistance r_{aW} combines the cooling effect of transpiration (latent heat loss) and the measured leaf to air temperature difference ΔT_{L-A} . Because we did not estimate the parallel resistance of air to heat and radiation (r_{HR}), our calculated r_{aW} values are to be interpreted in relative rather than in absolute terms. They convincingly separated the more coupled broad-leaved (around 50 sm^{-1}) from the less coupled conif-

erous trees (between 3 and 30 sm^{-1}).

Our results illustrate the importance of tree species composition for the local climate. While the net energy budget for the canopy would perhaps stay the same, a beech-dominated vegetation type would exhibit a surface temperature ca. 5 K higher than for example a larch forest. Such glaring differences in surface temperature may have consequences for vegetation - atmosphere modelling. Moorcroft (2006) for example recently pointed out the importance of the inclusion of species diversity in dynamic global vegetation models.

References

- Ansari AQ, Loomis WE (1959) Leaf Temperatures. *American Journal of Botany*, **46**, 713–717.
- Dai YJ, Dickinson RE, Wang YP (2004) A two-big-leaf model for canopy temperature, photosynthesis, and stomatal conductance. *Journal of Climate*, **17**, 2281–2299.
- Fuchs M (1990) Infrared measurement of canopy temperature and detection of plant water-stress. *Theoretical and Applied Climatology*, **42**, 253–261.
- Fuchs M, Tanner CB (1966) Infrared Thermometry of Vegetation. *Agronomy Journal*, **58**, 597–&.
- Grace J (1977) *Plant response to wind*. London ; New York ; San Francisco, Academic Press.
- Handa IT, Korner C, Hattenschwiler S (2005) A test of the tree-line carbon limitation hypothesis by in situ CO₂ enrichment and defoliation. *Ecology*, **86**, 1288–1300.
- Jackson RD, Reginato RJ, Idso SB (1977) Wheat canopy temperature - A practical tool for evaluating water requirements. *Water Resources Research*, **13**, 651–656.
- Jarvis PG, McNaughton SJ (1986) Stomatal control of transpiration: scaling up from leaf to region. *Advances in Ecological Research*, **15**, 1–49.
- Jones HG (1992) *Plants and microclimate*. Cambridge University Press.
- Jones HG (1999) Use of thermography for quantitative studies of spatial and temporal variation of stomatal conductance over leaf surfaces. *Plant Cell and Environment*, **22**, 1043–1055.
- Jones HG (2004) Irrigation scheduling: advantages and pitfalls of plant-based methods. *Journal of Experimental Botany*, **55**, 2427–2436.
- Jones HG, Leinonen I (2003) Thermal Imaging for the Study of Plant Water Relations. *Journal of Agricultural Meteorology*, **53** (3), 205–217.
- Jones HG, Stoll M, Santos T, de Sousa C, Chaves MM, Grant OM (2002) Use of infrared thermography for monitoring stomatal closure in the field: application to grapevine. *Journal of Experimental Botany*, **53**, 2249–2260.

- Leinonen I, Grant OM, Tagliavia CPP, Chaves MM, Jones HG (2006) Estimating stomatal conductance with thermal imagery. *Plant Cell and Environment*, **29**, 1508–1518.
- Leuzinger S, Zotz G, Asshoff R, Korner C (2005) Responses of deciduous forest trees to severe drought in Central Europe. *Tree Physiology*, **25**, 641–650.
- Mahey RK, Singh R, Sidhu SS, Narang RS (1991) The use of remote-sensing to assess the effects of water-stress on wheat. *Experimental Agriculture*, **27**, 423–429.
- Matsushima D, Kondo J (2000) Estimating regional distribution of sensible heat flux over vegetation using satellite infrared temperature with viewing angle correction. *Journal of the meteorological society of Japan*, **78**, 753–763.
- McElwain JC, Beerling DJ, Woodward FI (1999) Fossil plants and global warming at the Triassic-Jurassic boundary. *SCIENCE*, **285**, 1386–1390.
- McNaughton KG, Jarvis PG (1991) Effects of spatial scale on stomatal control of transpiration. *Agr. Forest Meteorol.*, **54**, 279–302.
- Moorcroft P (2006) How close are we to a predictive science of the biosphere? *Trends in Ecology and Evolution*, **21** (7), 400–407.
- Nemani RR, Running SW (1989) Estimation of regional surface-resistance to evapotranspiration from NDVI and thermal-IR AVHRR data. *Journal of applied meteorology*, **28**, 276–284.
- Pepin S, Körner C (2002) Web-FACE: a new canopy free-air CO₂ enrichment system for tall trees in mature forests. *Oecologia*, **133**, 1–9.
- R Development Core Team (2004) *R: A language and environment for statistical computing*. R Foundation for Statistical Computing, Vienna, Austria.
- Raschke K (1960) Heat transfer between the plant and the environment. *Annual review of plant physiology and plant molecular biology*, **11**, 111–126.
- Sellin A, Kupper P (2004) Within-crown variation in leaf conductance of Norway spruce: effects of irradiance, vapour pressure deficit, leaf water status and plant hydraulic constraints. *Annals of Forest Science*, **61**, 419–429.
- Soer GJR (1980) Estimation of regional evapotranspiration and soil-moisture conditions using remotely sensed crop surface temperature. *Remote Sensing of Environment*, **9**, 27–45.
- Willert DJ, Matyssek R, Herppich W (1995) *Experimentelle Pflanzenökologie*. Georg Thieme Verlag Stuttgart New York.
- Zaitchik BF, Macalady AK, Bonneau LR, Smith RB (2006) Europe's 2003 heat wave: A satellite view of impacts and land-atmosphere feedbacks. *International Journal of Climatology*, **26**, 743–769.
- Zhang RH, Sun XM, Liu JY, Su HB, Tang XZ, Zhu ZL (2003) Determination of regional distribution of crop transpiration and soil water use efficiency using quantitative remote sensing data through inversion. *Science in China Series D-Earth Sciences*, **46**, 10–22.

Chapter 6

A sensitivity analysis of leaf temperature to changes in transpiration

A sensitivity analysis of leaf temperature to changes in transpiration

Introduction

The question whether a CO₂-effect on plant transpiration can be detected by way of decreased latent heat flux and subsequent leaf warming can be answered theoretically. To do so, we need a measure of the natural variation occurring in leaf temperature over time. This variation depends on the specific canopy and leaf morphological properties and will be different for every vegetation type. Before carrying out leaf temperature measurements, I tried to assess the sensitivity of leaf temperature to changing transpiration in an on/off-experiment (switching off the CO₂-supply during short periods, see chapter 2) with varying canopy resistance. The aim was in particular to work out an optimal on/off schedule for the SCC site with maximum likelihood of detecting the CO₂-effect on transpiration. H. G. Jones pioneered the use of thermal cameras to quantify plant transpiration (e.g. Jones 1999), but the method has never been applied to forest trees in the context of elevated CO₂. Here I first present my sensitivity analysis and later discuss possible reasons of why the effect was not consistently found in the experiments (see chapter 2).

The net short- and longwave radiation energy that a leaf is exposed to (Φ_n) can essentially be partitioned between latent heat flux λE and sensible heat flux C :

$$\Phi_n = \lambda E + C \quad (1)$$

This statement is true only if we allow metabolic storage to be of negligible order of magnitude and if the system is in steady state, i.e. there is no radiative energy involved in changing tissue temperature. These are reasonable for short term investigations.

The sensible heat flux C is a function of ρ_a (the density of air), c_p (thermal conductivity of air), the leaf-to-air temperature difference ΔT and the resistance of air to heat r_{aH} :

$$C = \rho_a c_p \Delta T / r_{aH} \quad (2)$$

Latent heat flux on the other hand can be expressed as

$$\lambda E = (\rho_a c_p / \gamma) (e_{s(T_l)} - e_a) / (r_{aW} + r_{lW}) \quad (3)$$

where γ is the psychrometer constant ($=66.5 \text{ Pa K}^{-1}$ at 25° C). r_{aW} and r_{lW} are the resistances to water of the leaf boundary layer and the leaf. The leaf to air vapour pressure deficit ($e_{s(T_l)} - e_a$) is dependent on the leaf surface temperature, but this dependence can be avoided by using the Penman transformation (Penman, 1948)

$$e_{s(T_l)} - e_a = (e_{s(T_a)} - e_a) - s \Delta T \quad (4)$$

which assumes a linear relationship between the leaf to air temperature difference and the vapour pressure deficit of the air δe . The slope of this linear relationship is called s and simplifies the energy balance equation substantially. Combining (1) to (4) yields:

$$\Delta T = \frac{r_{aH}(r_{aW} + r_{lW})\gamma\Phi_n}{\rho_a c_p [\gamma(r_{aW} + r_{lW}) + sr_{aH}]} - \frac{r_{aH}\delta e}{[\gamma(r_{aW} + r_{lW}) + sr_{aH}]} \quad (5)$$

If we now look at what happens to ΔT , it is important to note that Φ_n itself depends on leaf temperature. It is possible to allow for this effect using the concept of isothermal net radiation (Φ_{ni} , see Jones 1992), which is the net radiation that would be absorbed by the leaf if it were at air temperature. We further replace the term r_{aH} by r_{HR} , the parallel sum of resistance of air to heat (r_H) and radiation (r_R). We thus obtain

$$\Delta T = \frac{r_{HR}(r_{aW} + r_{lW})\gamma\Phi_{ni}}{\rho_a c_p [\gamma(r_{aW} + r_{lW}) + sr_{HR}]} - \frac{r_{HR}\delta e}{[\gamma(r_{aW} + r_{lW}) + sr_{HR}]} \quad (6)$$

The constants used are: $\rho_a = 1.175 \text{ kg m}^{-3}$, $c_p = 1010 \text{ J kg}^{-1} \text{ K}^{-1}$ and $\lambda = 2.442 \cdot 10^{-6} \text{ J kg}^{-1}$.

These equations form the basis of the following analyses. The questions of interest are the following:

1. If evaporation E changes under elevated CO₂, how does this affect leaf temperature? That is, how large a decrease in E will cause a measurable increase in leaf surface temperature, given the variation of this particular canopy?

2. How sensitive is leaf temperature to other parameters than E , especially to those that cannot be measured accurately?
3. How likely are these environmental parameters going to change and how can these effects be minimised by choosing appropriate on/off schedules and climatic conditions?

Results from a pilot study in 2004

The various methods of thermal scanning used in the pilot study revealed the following:

- Average canopy temperature of the treated plot was 21.91°C versus $21.88 \pm 0.15^\circ\text{C}$ of the surrounding control area (measured from ca. 200 m above ground, see chapter 2). While there was no difference, this result shows that over large areas ($>100\text{m}^2$), variability is small and average temperatures are consistent.
- In a 50 min scan, I found a significant difference in canopy temperature between a CO_2 -enriched and an non-treated canopy of beech (confidence interval = 0.27 to 1.26°C increase in leaf temperature of treated tree, see chapter 2) but there was no difference in oak.
- Variability of leaf temperature over time under favourable conditions: I saw a marked decrease in leaf temperature already in the presence of small wind gusts. However, the maximum temperature range over time under stable conditions was roughly within 1 K (Figure 1).

Sensitivity of leaf temperature to reduced evaporation

Combining equations (1) and (2) and using the concept of isothermal net radiation, we obtain ΔT as a function of evaporation:

$$\Delta T = \frac{(\Phi_{ni} - \lambda E)r_{HR}}{\rho_a c_p} \quad (7)$$

The terms ρ_a , c_p and λ are constants, so if the isothermal net radiation Φ_{ni} and the resistance of air to heat and radiation r_{HR} are assumed constant, we have a linear relationship between evaporation and ΔT , the leaf to air temperature difference. In a first approximation, r_{HR} should remain constant as leaf temperature changes. Technically, there could also be a feedback loop on evaporation itself because leaf temperature changes, but this is probably minor and will be ignored for the moment.

Typical values for the parameters in equation (5)

for a sunny day in summer are: $\Phi_{ni} = 400\text{Wm}^2$, $r_{HR} = 10\text{sm}^{-1}$, $E = 4.5 \cdot 10^{-5}\text{ms}^{-1}$, which yields a leaf to air temperature difference of approximately 2.5 K. Certainly, the most variable factor is the resistance to heat and radiation r_{HR} of air, which largely depends on the uncontrollable turbulent wind patterns around the leaf. However, we may assume that while the variability of r_{HR} is large (causing leaf temperature to fluctuate within about 1 K, see Figure 1), it is constant over time, thus not affecting leaf temperature *on average* (timescale $> 30\text{min}$). Table 1 shows how ΔT changes as r_{HR} , Q_{ni} and E increase. Consequently, when a 10 % increase in E takes place, I would expect ΔT to increase by about 0.1 K and a maximum of 0.2 K at an increase in E of 20 %

Table 1: Sensitivity of leaf to air temperature difference to changes in r_{HR} , Q_{ni} and E

10 % increase in	causes change in ΔT of
r_{HR}	+10 %
Q_{ni}	+14 %
E	-3.7 %

It thus becomes clear that leaf surface temperature is over 3 times more sensitive to changes in net radiation than to changes in leaf transpiration. On the other hand, net radiation can be measured rather accurately. Also, it should only be a function of daytime in stable weather conditions, and can thus be corrected for.

Sensitivity of leaf temperature to other factors

For the investigation of how leaf temperature reacts to other factors than evaporation, I make use of equation (6) and subsequently change individual factors in order to observe the behaviour of ΔT . Let us look at each individual term and its influence on ΔT as the other factors remain constant.

Resistance to heat and radiation of air

r_{HR}

The simultaneous resistance to heat and radiation of air r_{HR} depends on the complex air flow patterns around the leaf and cannot be controlled for as mentioned earlier. However, I rely on its variance being constant under constant weather conditions, which seems to be a valid assumption (Figure 1). As expected, changes in r_{HR} entail major changes in ΔT (Figure 2). At high net radiation, the changes are more pronounced (top panel). At low stomatal resistance to water vapour, changes in ΔT become less,

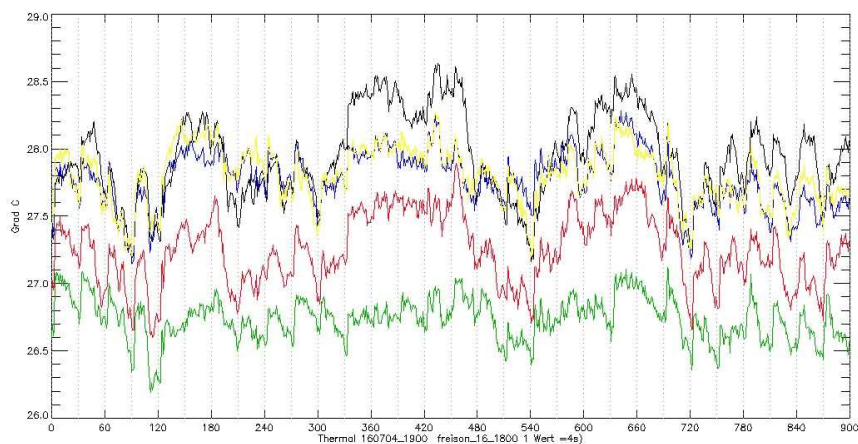


Figure 1: Five time series of an average of 100 pixels (each ca. 15x15cm) of a fully sunlit beech canopy. Length of x-axis corresponds to one hour.

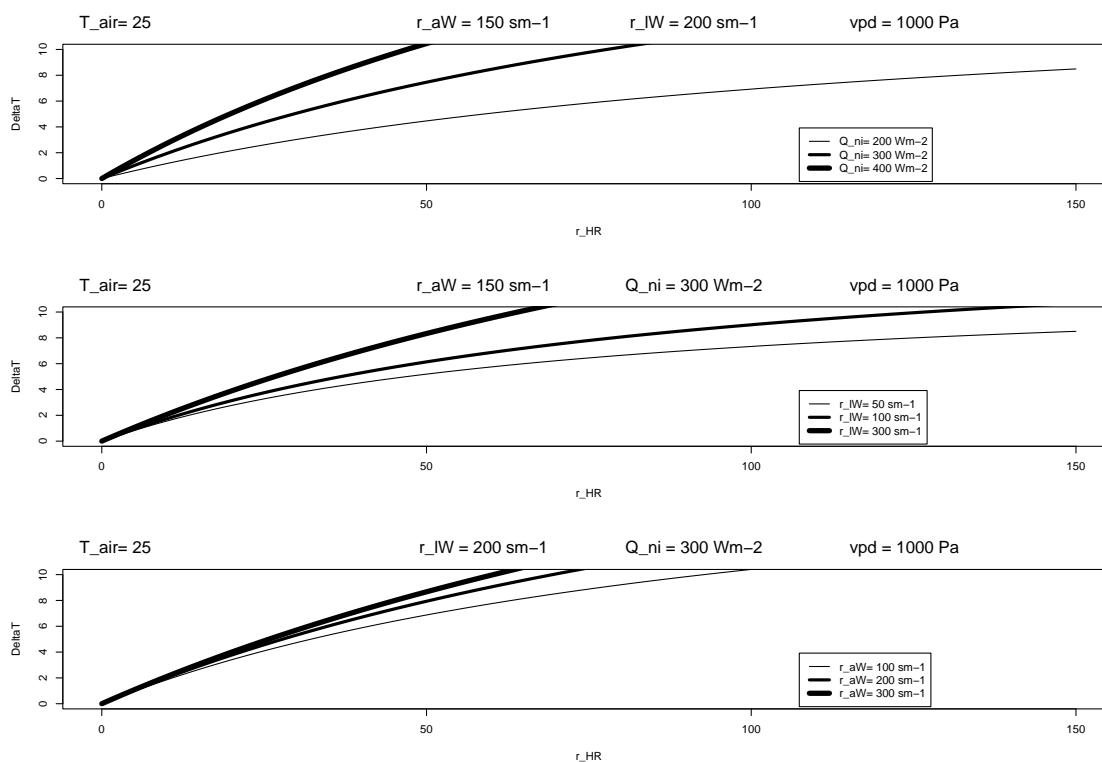


Figure 2: Variation of ΔT in relation to changes in r_{HR} and Q_{ni} (top panel), r_{IW} (middle panel) and r_{aW} (lower panel)

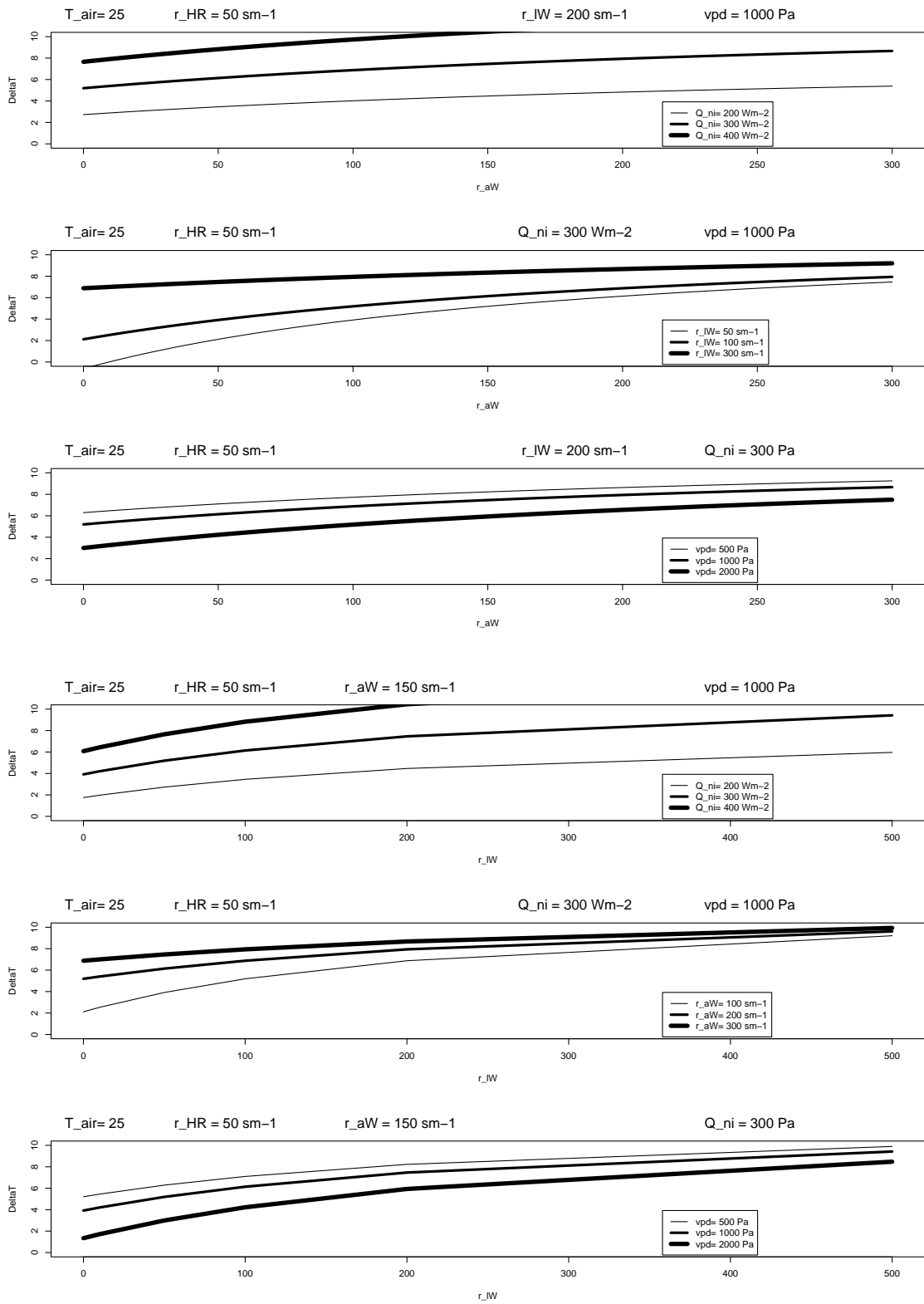


Figure 3: Variation of ΔT in relation to changes in r_{aW} , the boundary layer resistance, with different values for Q_{ni} , r_{IW} and vpd (upper panel), and the equivalent plots with varying r_{IW} , the leaf resistance to water vapour (lower panel)

e.g. at 50 sm^{-1} (corresponding to 20 mms^{-1}) and relatively high r_{HR} , changes in the latter do not cause substantial changes in ΔT any more. r_{aW} does seem relatively unimportant to the relationship between r_{HR} and ΔT . Increasing vpd lowers the sensitivity of r_{HR} to ΔT , but vpd is not changing fast under stable conditions.

Resistance to water vapour of air r_{aW}

The resistance of the air to water vapour immediately above the leaf, the boundary layer resistance r_{aW} , not only depends on the highly irregular air flow regime around the leaf, it is also involved in feedback loops when transpiration changes. From Figure 3, I conclude that ΔT is far less sensitive to changes in boundary layer resistance r_{aW} than to changes in resistance to heat and radiation r_{HR} .

Resistance to water vapour of the leaf

r_{lW}

This term comprises the cuticular resistance plus the stomatal resistance. ΔT is increasingly sensitive to r_{lW} the boundary layer resistance r_{aW} becomes smaller (3). ΔT is more sensitive to r_{lW} the higher Q_{ni} and vpd. For mesophytes, minimum stomatal resistance is around 80 to 250 sm^{-1} , which is higher than r_{aW} in most cases. Thus, r_{lW} is immediately linked to λE , and it is easier to consider λE comprising both r_{aW} and r_{lW} directly.

Vapour pressure deficit

Increasing vapour pressure deficit causes a linear decrease in ΔT , because - all other factors assumed constant - this causes an increase in transpiration. This term can be expected to be reasonably constant and can be determined accurately during the experiment.

Net radiation Q_{ni}

Increasing isothermal net radiation results in linearly increasing leaf to air temperature difference ΔT . The effect is only slightly attenuated by lower resistances in the soil-plant-atmosphere continuum.

Canopy temperature simulation

One crucial question concerns the length of the period during which the elevated CO_2 should be turned off. In order to answer this question, I simulated a time series to match the experimentally measured one shown in Figure 1. I found that a standardised first order autoregressive series with a standard deviation of 0.08 adequately simulates the series shown in Figure 1 (Figure 4, top panel). If the temperature shift

of 0.2 K in Figure 4 shall be detected, I can now infer a minimal (or optimal) period during which the CO_2 supply should be switched off. If the statistical test for the shift is carried out by fitting an autoregressive time series model and subsequently testing the significance of the intercept (which stands for the mean as there is no trend), I enter the statistically safe area only after about 80 minutes (Figure 4, bottom panel).

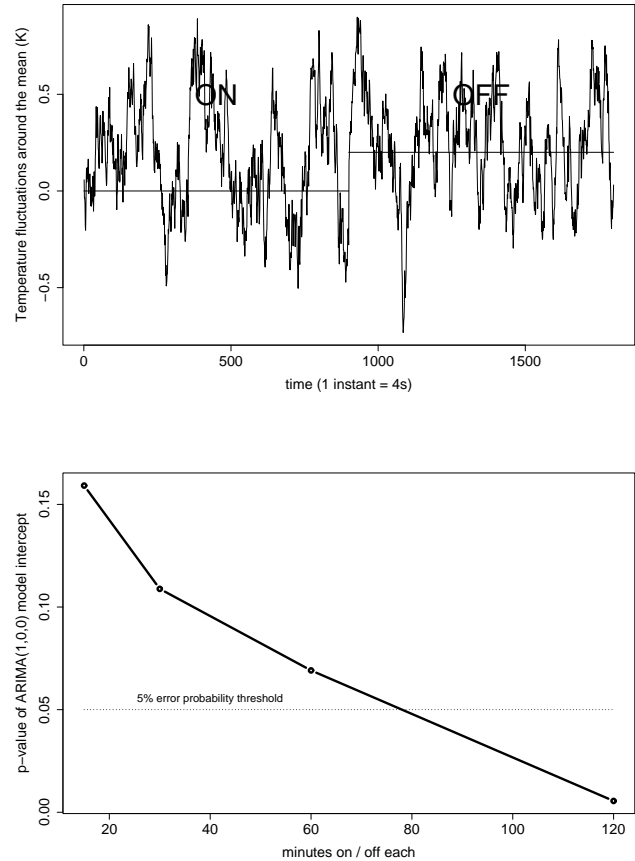


Figure 4: Simulated time series of canopy temperature during a "on/off" experiment, assuming a shift of 0.2 K in the average temperature (upper panel). On/off periods correspond to 30 min each. Lower panel: The p-value of the ARIMA model intercept as the "off" period increases from 15 to 120 minutes.

Conclusion and outcome of experiments

Although the resistances r_{HR} and r_{aW} may have been chosen to be too high in the plotted examples, rendering leaf to air temperature difference ΔT too large, the general patterns became obvious: The most promising conditions to detect reduced transpiration via leaf temperature changes are when net radiation

is high, resistances in the soil-plant-atmosphere continuum on the other hand are small, corresponding to a canopy with low aerodynamic coupling. This is certainly most likely in the late morning. Further, the switch-off period should be at least 80 minutes, as the signal-noise ratio will be too small otherwise. However, if meteorological data (above all wind speed or the wind vector) explain the relatively large variation, temperature shifts due to reduced evaporation could be detected much more easily and shorter switch-off periods may suffice.

Based on these results, experiments were carried out as reported in chapter 2. However, no leaf cooling effect following the interruption of the CO₂-supply was found in any of the on/off experiments (see Results section of chapter 2). The signal was also not seen in the sap flow signal. While the absence of the signal in sap flow could potentially be explained by a buffering of the signal by stem water storage, the absence of the leaf cooling is difficult to explain. One reason could be that the top branches were not adequately supplied with CO₂ in the year of the experiment. It is further possible that aerodynamic coupling was much higher than expected (as reported in chapter 5). In that case, the leaf boundary resistance r_{aW} was underestimated in this analysis and dominated leaf resistance r_{lW} , so that differences in r_{lW} would not have resulted in significant changes in transpiration E . This however would generally question the water savings found with other methods (chapter 2). Comparison of within-image CO₂-treated/non-treated canopies only showed a significant difference of the expected amplitude (ca. 0.4 K) only at the smallest scale, ca. 5 m above the canopy. Close examination of the leaf morphology of the replicas of *Quercus*, *Fagus* and *Carpinus* revealed obvious differences in both leaf size and colour, which may have influenced and confounded the effect of reduced latent heat flow due to elevated CO₂.

References

- Jones HG (1992) *Plants and microclimate*. Cambridge University Press.
- Jones HG (1999) Use of thermography for quantitative studies of spatial and temporal variation of stomatal conductance over leaf surfaces. *Plant Cell and Environment*, **22**, 1043–1055.
- Penman HL (1948) Natural evaporation from open water, bare soil and grass. *Proceedings of the Royal Society of London Series A-Mathematical And Physical Sciences*, **193**, 120–&.

Chapter 7

A model predicting sap flow from
environmental data

A model predicting sap flow from environmental data

Introduction

For the prediction of future climatic conditions, we first need to be able to predict relative sap flow given certain environmental conditions. Second, the quantification of water transpired by plants as a function of the level of CO₂ is essential. Conventional land-surface climate models predict sap flow from mechanistic models of photosynthesis, which become increasingly unrealistic as we move away from controlled greenhouse conditions to natural ecosystems. A statistical model for predicting sap flow as a function of the driving environmental variables is not only a novel research area, it is a much needed missing link between vegetation and climate models. The aim of this study is to build a model for relative sap flow (irrespective of the CO₂-treatment) as a function of several environmental parameters which can then be used to parametrise land-surface climate models.

Methods

The data were collected in a forest stand in Hofstetten, ca. 15 km south of Basel, Switzerland using the Swiss Canopy Crane (45 m free-standing tower crane), providing access to the canopy. Of the 64 trees in the crane area, 14 broad-leaved trees (3 *Fagus sylvatica*, 3 *Quercus petraea*, 4 *Carpinus betulus*, 1 *Tilia platyphyllos*, 1 *Acer campestre* and 1 *Prunus avium*, the last three not used for this experiment) were selected for the CO₂ treatment in autumn of 2000 (all within a continuous plot). Eleven control trees were located in the remaining crane area at sufficient distance from the CO₂ release zone. CO₂ enrichment of the forest canopy was achieved by a free-air, pure CO₂ release system Pepin & Körner (2002). Rain, throughfall precipitation, air humidity, vapour pressure deficit, temperature, and soil humidity were monitored by weather stations located above the tree canopy at the top of the crane and in the understorey. The method of measuring tree sap flow is the so-called ‘constant heat flow’ technique of Granier (1985). For details on the set-up of the experiment and the sap flow measurements see Materials and Methods section of chapter 2. Given the difficulties in inferring size corrected absolute sap flow (for

which tree size, sapwood width and total leaf area are needed), I standardised the time series for each tree to its own maximum (=100%) of the period of interest. Once calibrated with absolute data, the model can then be used for absolute predictions. Measurements of sap flow were performed from June to October 2005 on 3 dominant tree species (*Quercus petraea*, *Fagus sylvatica* and *Carpinus betulus*, $n = 3 - 5$) using 2 sensors per tree. A period which covers a wider range of weather conditions was used (July 20 to August 10, 22 days) for the predictive model. Readings were taken at 30s intervals and recorded as 10-min means (yielding 144 time steps per day) using a multi-channel data logger (DL2e, Delta-T, Cambridge, UK). The signals per tree were averaged over all sensors per stem.

Table 1: Variables in the dataset. The response variable is flux, $n = 40371$ observations (both period 1 and 2).

Variable	Unit	Description
flux	%, 0-1	Relative sap flow averaged across all species and trees, response variable
T	Celcius	ambient temperature
RH	%	relative air humidity
vpd	<i>hPa</i>	vapour pressure deficit
light	mmol $m^{-2}s^{-1}$	photosynthetic active radiation
wind	ms^{-1}	windspeed
winddir	0-360	wind direction (0 = North)
SMA	Vol.%	soil moisture content (ambient plot)
grav	mgal	gravitation
period	integer	1-4, 1: 00:00-06:00 etc.
doy	integer	day of year
season	integer	1: 5-10 Jun, 2: 4-8 Aug '04
mod	min	minute of day

Table 1 contains a list of all 13 variables in the dataset. An overview of the correlations and frequency distributions of the data (one random tree selected) is given in Figure 1. It is easily seen that the variable ‘light’ correlates very well with ‘flux’, so this will certainly be an important predictor in any model. It is obvious that most continuous variables are not normally distributed. In particular, the distribution of the response variable ‘flux’ is skewed to the left. A series of possible transformations was applied to the data and is summarised in Figure 2. The logit transformation ($f(x) = \log(x/(1-x))$) performs

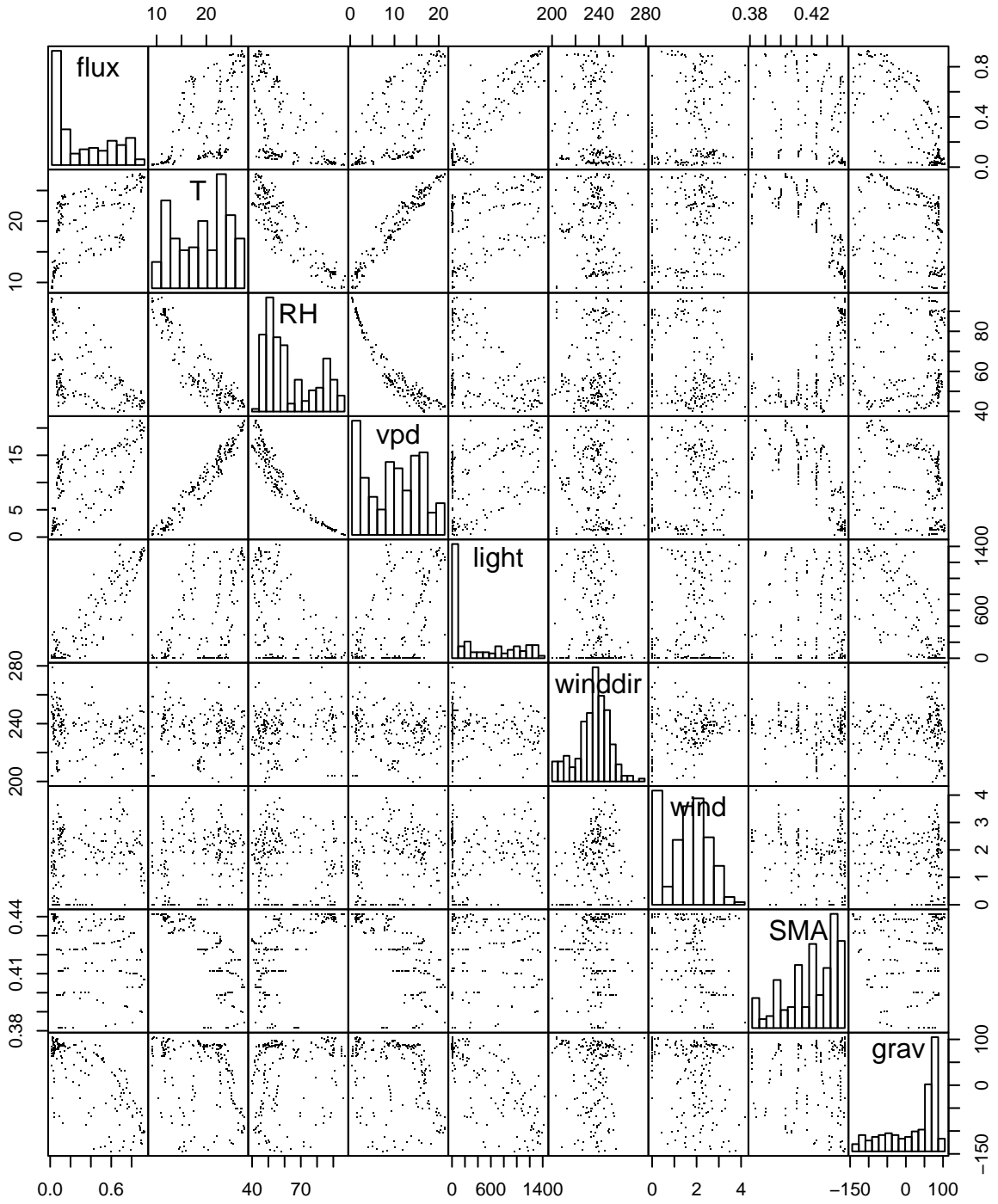


Figure 1: Histograms and pairs plots of some variables in the dataset. The diagonal cases show the respective histograms. Variable abbreviations see Table 1

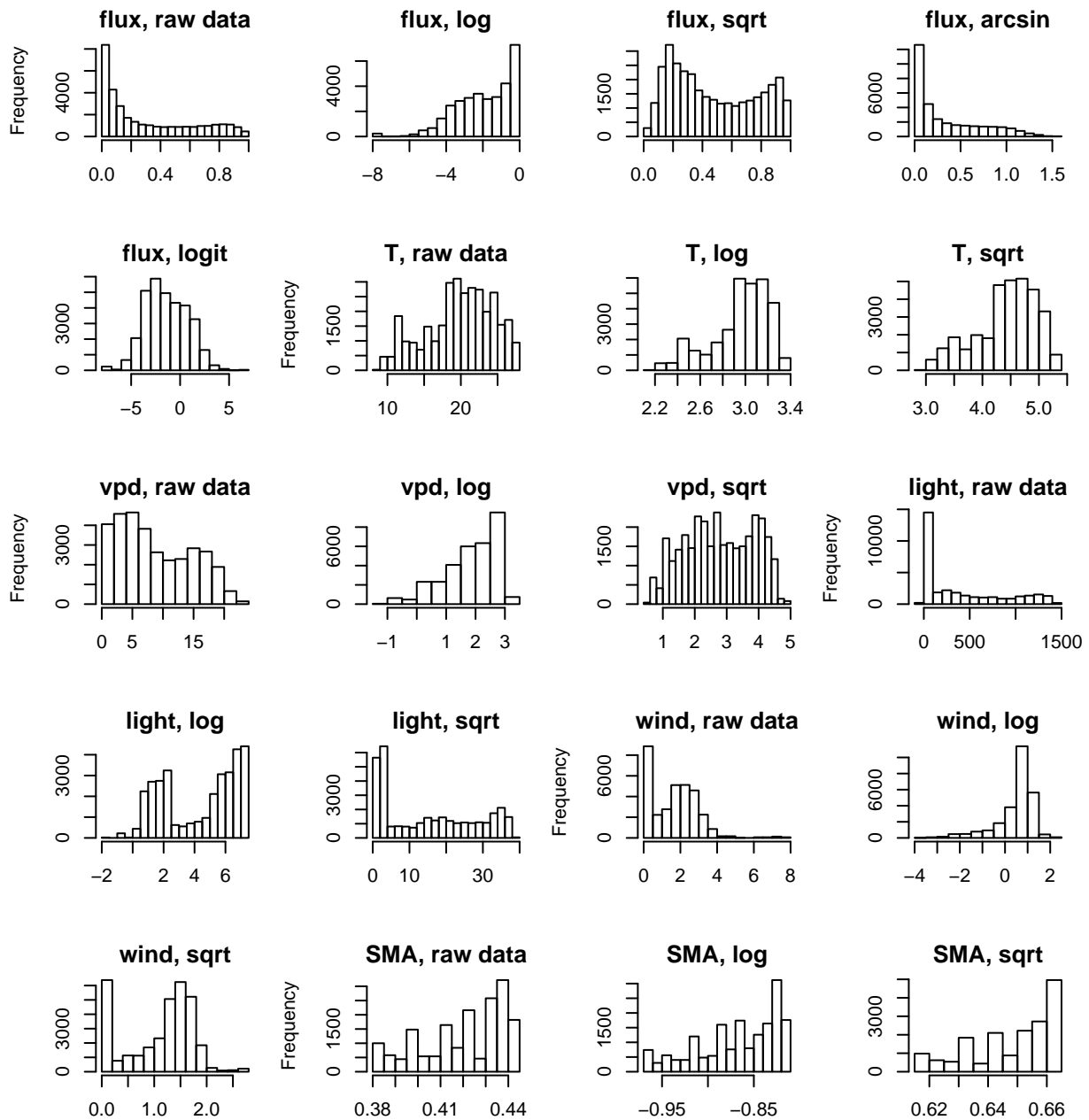


Figure 2: Histograms of response variable flux as well as some important predictor variables and their transformations (sqrt = square root).

best in normalising the response variable, thus a new variable ‘fluxt’ (flux logit transformed) is added to the dataset. The problem then arises of what to do with values equal to zero or one. I decided to set them equal to 0.005 and 0.999 (reasoning with an adequate gap to the closest value smaller than 1 and larger than 0 respectively). For the simple linear model I omitted these values in order to obtain normally distributed numbers. As for the predictor variables, the shown transformations do not improve the normality of the data substantially, even the square root transformation for the variable vpd is not appropriate when looking at the corresponding QQ-plot (not shown). Thus, the original predictor variables were kept. All statistical analyses were carried out using the open source software package R (Version 2.0.1, 2005).

Predictive modelling of sap flow

An exploratory model (linear full model with all predictor variables included, not shown) revealed that some variables such as ‘grav’ and ‘winddir’ are probably not important in predicting flux as they have not been selected by the BIC model selection. The autocorrelation function (ACF) and partial autocorrelation function (PACF) of the variable ‘flux’ (which is identical to the one of ‘fluxt’, data not shown) point out the need for a model with either autoregressive or time-lagged predictors. But before moving on to such models, I apply a more parsimonious linear model with predictive character, based on the results of the exploratory model fit. It is particularly important to note at this point that it is completely irrelevant (and often trivial) whether any of the predictors are significantly contributing to the model. The only criterion is the model’s predictive accuracy, as this model will then be used to parametrise a local land-surface climate model, replacing the mechanistic component based on plant physiological kinetics. The criterion I use for model selection is the residual sum of squares (RSS), meaning the sum of squares between the real data and the model prediction. The analysis is organised as follows: first, a simple predictive linear model (model 1) is fitted, then follow two models with autoregressive (model 2) and/or time lagged (model 3) regressors. Finally, a model on seasonally decomposed series is explored (model 4). The same training (first 16 days of the period) and test set (last 6 days of the period) is used for all models.

Predictive simple linear model

Due to the strong correlation above all between ‘RH’, ‘T’ and ‘vpd’ (Figure 1), it is better to include only one of these variables to avoid collinearity problems. Moreover, the predictive qualities will not improve

by adding correlated variables. Since biologically, ‘vpd’ is the most relevant, it is included in this model (model 1). The variables ‘light’ and ‘wind’ are not or only very weakly correlated (Figure 1) and can thus be included in the model. The variables ‘winddir’, ‘SME’ and ‘grav’ were not contributing significantly in the exploratory model and are thus left out. Taking ‘fluxt’ as the response variable, model 1 reads:

$$fluxt = \beta_0 + \beta_1 T + \beta_2 vpd + \beta_3 light + \beta_4 wind + \beta_5 SMA + \epsilon.$$

The model chosen by BIC (forward and backward) model selection reduces to:

$$fluxt = \beta_0 + \beta_1 T + \beta_2 vpd + \beta_3 light + \beta_4 wind + \epsilon.$$

If however the raw variable ‘flux’, instead of the logit transformed variable ‘fluxt’ is used as the response variable, the model fit improves and the BIC model selection suggests the even simpler model:

$$flux = \beta_0 + \beta_1 vdp + \beta_2 light + \epsilon, \quad (\text{model 1}).$$

The model predictions for the test period are shown in Figure 3. The final model (model 1) predicts better with fewer predictors and untransformed response variable (sum of squared residuals = 12.5) than the model using the logit transformed response variable (sum of squared residuals = 17.8). The fit is further improved by running a cubic spline function over the model output in order to remove some noise (sum of squared residuals = 9.5). Neither the full model output nor the diagnostic plots for model 1 are shown: for the purpose of prediction, the predictive quality measured by the sum of squared residuals is of importance. It is certain however, that the residuals are autocorrelated as was the case for the exploratory model. In the next step, autoregressive models and models with time-lagged predictors are used, trying to improve the predictions further.

ARIMA model with external predictors

We not only know a priori that there is autocorrelation present in the sap flow dataset, but we also know that there is seasonality, the frequency being 24 hours, i.e. 144 time steps as we have 10 min intervals. The use of seasonal ARIMA (SARIMA) models proved not to be useful for predicting sap flow, as the seasonal autoregressive term tends to propagate a seasonal component that is too dominant over the more important external regressors. Furthermore, each seasonal time step shortens the prediction by one season (i.e. one day). It is thus more appropriate to use simple ARIMA models. An ARIMA-model

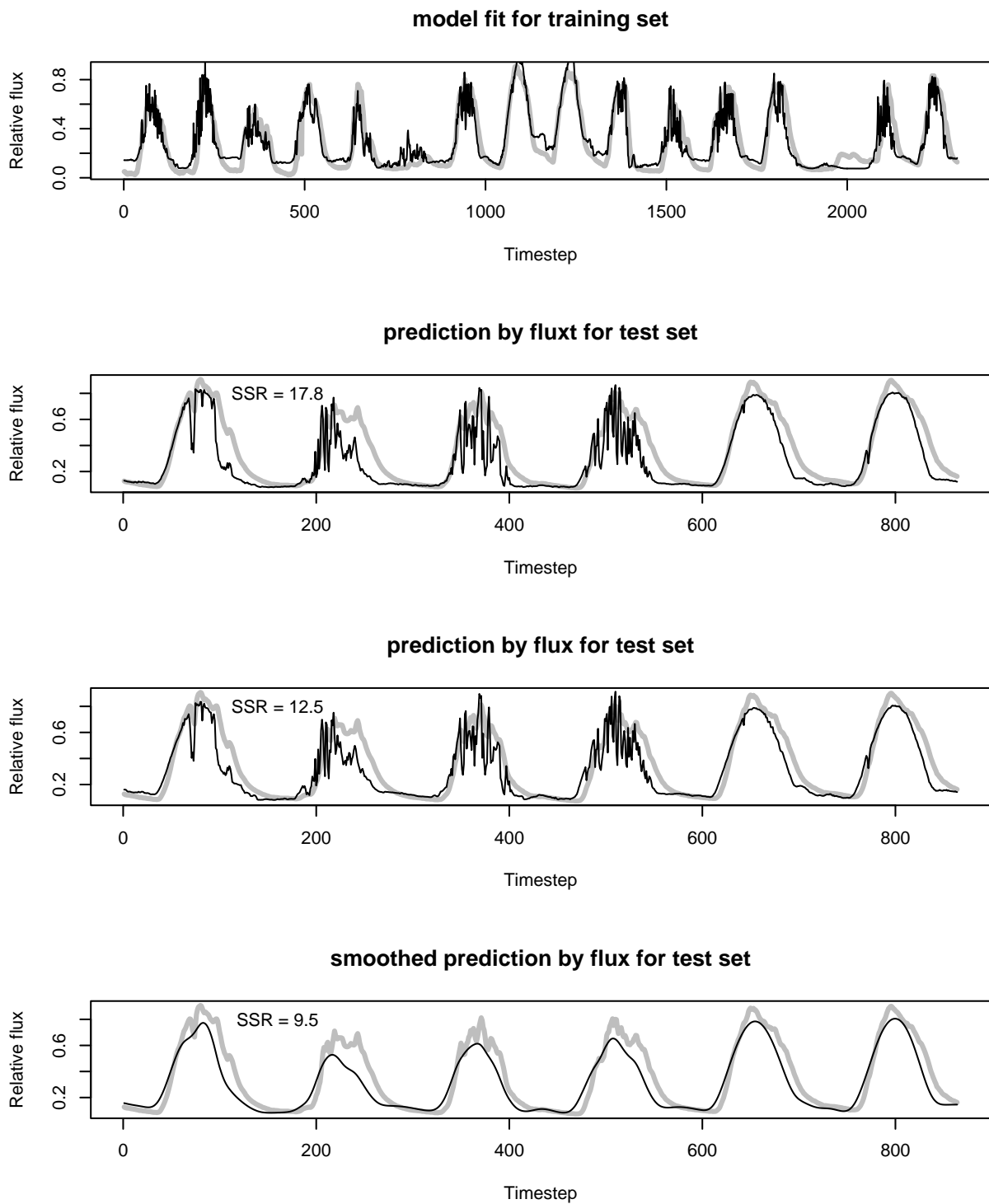


Figure 3: Model fit for training period with 'fluxt' as a response variable (top panel), prediction for the test period of this model (second from top) and prediction of model 1 for the test period (using 'flux' as the response variable and only two predictors, second from bottom). Bottom panel: same as above but predictions are smoothed by a cubic spline function with smoothing parameter = 0.4. For the lower three panels, the residual sums of squares are indicated. Bold grey line = real data, fine line = model prediction.

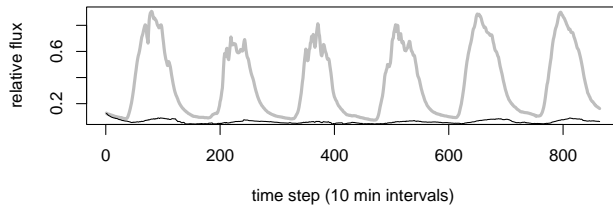


Figure 4: Model predictions for the $ARIMA(5,2,2)$ model with ‘light’ and ‘vpd’ as external regressors. Bold grey line: real data, fine line: model predictions. The fit completely unsatisfactory, but an immediate explanation is lacking.

of the form $ARIMA(p, d, q)$ with external predictors can be written as

$$\nabla^d Y_t = \nabla^d \phi_1 y_{t-1} + \nabla^d \phi_2 y_{t-2} + \dots + \nabla^d \phi_p y_{t-p} + \epsilon_t + \delta_1 \epsilon_{t-1} + \delta_2 \epsilon_{t-2} + \dots + \delta_q \epsilon_{t-q} + \beta_0 + \beta_1 X_1 + \beta_2 X_2 + \dots + \beta_n X_n,$$

where d is the number of times the series is differenced, p is the number of autoregressive terms and q the number of moving average terms. Differencing d times is used to eliminate a possible trend in the series and render it stationary. I use the original variable ‘flux’ instead of the logit transformed variable ‘fluxt’, arguing with the results of the last section, where the model using ‘flux’ performed better. As is already known that the raw flux series is non-stationary, I explored the ACF and PACF plots of the one and two times differenced raw data in order to determine the order of the AR and MA-terms (data not shown). The (not so abrupt) decline of the autocorrelation function for the two times differenced series suggest an $ARIMA(5, 2, 7)$ or possibly an $ARIMA(5, 2, 2)$ model. I tried the more simple model, including ‘light’ and ‘vpd’ as external predictors:

$$\begin{aligned} \nabla^2 flux_t = & \nabla^2 \phi_1 flux_{t-1} + \nabla^2 \phi_2 flux_{t-2} + \\ & \nabla^2 \phi_3 flux_{t-3} + \nabla^2 \phi_4 flux_{t-4} + \nabla^2 \phi_5 flux_{t-5} + \\ & \epsilon_t + \delta_1 \epsilon_{t-1} + \delta_2 \epsilon_{t-2} + \beta_0 + \beta_1 light + \beta_2 vpd \end{aligned} \quad (\text{model 2}).$$

The model fit seems faulty (Figure 4), but there is no immediate explanation. One cause could be the external regressors that are heavily autocorrelated. On the other hand, the prediction gives the impression that the autoregressive terms dominate over the external regressors. It would probably be advisable to try such models using different software packages, but I am doubtful whether ARIMA models are at all useful for the present purpose.

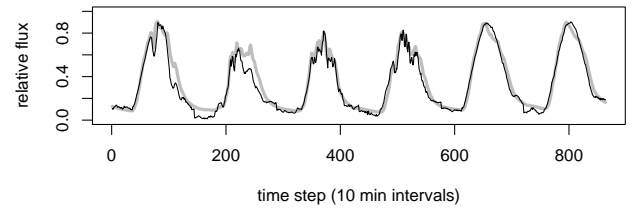


Figure 5: Model fit of linear model with time lagged regressors (model 3). Bold grey line: real data, fine line: model fit. The residual sum of squares is 3.5, the lowest of all models developed so far.

Linear model with time lagged predictors

It is reasonable to assume that there is a time lag between a given set of environmental parameters and the tree’s reaction to these particular circumstances. Biologically, a plausible reaction time for most parameters should not exceed 30 minutes, i.e. 3 time steps in our case, which corresponds approximately to the maximum time needed for leaf pores to get from a fully closed to a fully open status. However, the history even before this time threshold might be of importance for relative sap flow at any time. For example, sap flow rate might depend on the vapour pressure deficit (‘vpd’) of the previous hour: if ‘vpd’ was very high then, we might expect stomatal down-regulation by the tree, regardless of how favourable the conditions are now. Hence, I start with a linear model that includes all of the following variables including their time lags up to lag 6 (60 minutes into the past): ‘T’, ‘RH’, ‘vpd’, ‘light’ ‘wind’ and ‘SMA’. Consequently, I chose a model using the BIC model selection in forward and backward selection mode. The model selected reads:

$$\begin{aligned} flux_t = & \beta_0 + \beta_1 T_t + \beta_2 SMA_t + \beta_3 light_t + \beta_4 wind_t + \\ & \beta_5 per_t + \beta_6 RH_{t-1} + \beta_7 light_{t-1} + \beta_8 light_{t-2} + \\ & \beta_9 light_{t-3} + \beta_{10} light_{t-4} + \beta_{11} light_{t-5} + \\ & \beta_{12} T_{t-6} + \beta_{13} light_{t-6} + \beta_{14} SMA_{t-6} + \epsilon \end{aligned} \quad (\text{model 3}).$$

The model fit as shown in Figure 5 is very satisfying. Both the shape and the relative changes from day to day are predicted very accurately. Only the nightly flux seems to be a little too low and unstable at times. Despite the fact that the longest lags are important, the model is not improved significantly by including even longer time lags.

Decomposition into season, trend and remainder

The STL-decomposition (seasonal-trend loess decomposition, (Cleveland *et al.*, 1990)) allows to extract seasonality and trend from the data in order to allow to analyse these components (plus the remainder) separately. I did this for the training set:

$$flux = sea + tre + rem$$

where *sea* = season, *tre* = trend and *rem* = remainder. Ideally, the remainder consists of gaussian white noise only, so that it can be interpreted as a random error term. When applying the stl decomposition, the period is usually known so that the mean of each time step is computed (e.g. mean of all December values in a yearly series). On the other hand, we can influence the way the trend is calculated by setting a time window for loess smoothing. Logically, if this window is chosen to be very small (only a couple of lags at a period of 144 as in our example), the autocorrelation of the remainder series can be decreased. On the other hand, this increases the variation in the trend which then becomes more difficult to interpret or model. The question in tree sap flow is, whether we want to extract a daily trend (smoothing span of 144 time lags) or for example an hourly trend (smoothing span of 7 time lags). When trying to model sap flow irrespective of the CO₂ effect, I believe the daily trend is of interest only. The plant physiological advantage of this decomposition is that the factors that influence the three distinct parts (season, trend and remainder) of the series can better be assigned to certain predictor variables. The seasonality for example might be a function of daylength only and taken out of the model completely. The trend on the other hand is probably mainly a function of soil moisture (as the soil is drying out there is a tendency to lower sap flow). The remainder would then be explained by factors changing rather fast over time such as wind, light and vpd.

The result of the stl decomposition is shown in Figure 6; the autocorrelation in the remainder series is still considerable. I used a smoothing window for the trend of 288 lags (=two days) in order to extract a long-term trend. Inspecting the ACF and the PACF of the trend and remainder series, I choose an ARIMA(1,1,0) model for both the trend and the remainder of the training set. The trend does not correlate well with any of the predictors, I thus use a wider range of regressors as the ones that are biologically plausible: ‘T’, ‘light’, ‘vpd’ and ‘SMA’ for the trend and ‘wind’, ‘light’, ‘vpd’ and ‘SMA’ for the remainder:

$$\nabla^1 tre(y) = \beta_0 + \nabla^1 \phi tre(y-1) + \beta_1 T + \beta_2 light + \beta_3 vpd + \beta_3 SMA,$$

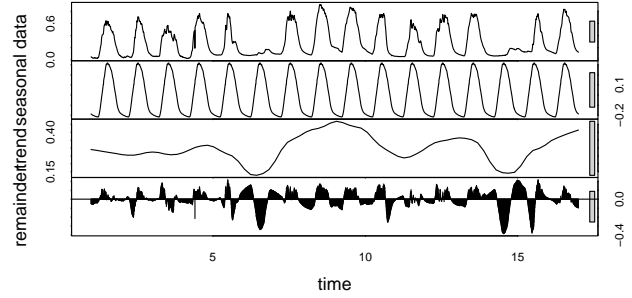


Figure 6: STL-decomposition according to Cleveland *et al.* (1990). Smoothing window for trend = 288 time lags (2 days). From top to bottom: original series, season, trend, remainder. The grey bars indicate a segments of equal length.

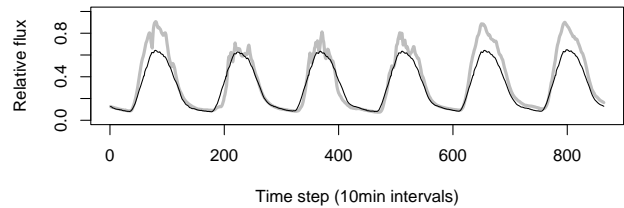


Figure 7: Predictions of the stl-model (model 4) fitted to the trend and remainder series. Leaving out the two rainy days with low sap flow for the training period does not improve the unsatisfactory fit. SSR = 8.43, bold grey line: real data, fine line: predictions.

$$\nabla^1 rem(y) = \beta_0 + \nabla^1 \phi rem(y-1) + \beta_1 wind + \beta_2 light + \beta_3 vpd + \beta_3 SMA, \quad (\text{model 4}).$$

This model seems to predict the nightly shape of the sap flow series very well (Figure 7), in contrast, the amplitudes of the individual days are predicted badly, there is no sensitivity to the reduced flux of day 2-4. Despite its relatively low value of sum of squared residuals, the plot clearly shows that the model is not appropriate (see the Conclusion section below). A possible cause of this insensitivity might be the two days with very low sap flow in the training set, thus I also tried to train the model without those two days. However, this does not improve the model fit.

Nevertheless, decomposing a sap flow series into season, trend and remainder may be of high descriptive value in a biological sense. It would be desirable however to get the remainder as close as possible to white noise, for which purpose no algorithm exists to date.

Table 2: Summary of the four models (simple linear model (1), ARIMA model (2), linear model with time lagged predictors (3) and model on stl decomposed series (4). 'SSR' = sum of squared residuals of real data to model prediction, 'SSR day' for daytime only (6am to 6pm).

model	properties	SSR	SSR (day)
simple linear	'light' and 'vpd' as predictors	12.5	9.4
simple linear with spline (1)	as above, but spline smoothed	9.5	6.4
ARIMA (2)	arima(5,2,7) , 'light' and 'vpd'	-	-
lagged linear (3)	linear model incl. 6 time lags	3.2	2.3
stl (4)	season, trend, rem. separately	8.43	7.45

Linear model using generalised least squares

I also tested the option of using generalised least squares for the linear model instead of ordinary least squares. In this case, the assumption of independent error terms can be relaxed and the autocorrelation structure of the error specified:

$$flux_{ij} = \beta_0 + \beta_1 X_1 + \beta_2 X_2 + \dots + \beta_j + \epsilon_{ij}$$

$$\epsilon_i = \begin{pmatrix} \epsilon_{i1} \\ \epsilon_{i2} \\ \vdots \\ \epsilon_{ij} \end{pmatrix} \sim \mathcal{N}(0, \Lambda_i),$$

where Λ_i is the variance-covariance matrix. For example, we can assign an autocorrelated structure of order 1 to the error term. Such a model with the same autocorrelation order as used in the ARIMA models with external predictors, however, yielded exactly the same result as the latter. It is noteworthy on the other hand, that in the statistical software 'R' (R Development Core Team, 2004), such a fit took several hours of computing time using `gls()` while only a few seconds using the `arima()` command.

Conclusion

In summary, the linear model with time lagged regressors (model 3) predicts tree sap flow by far the best (Table 2, Figure 5). followed by the smoothed simple linear model (model 1) with only two parameters (plus the intercept). The other two models are a lot less useful. The reason why model 4 (stl-decomposed model) predictions appear relatively good is the seasonal component. The seasonality that is extracted from the training period represents the invariant part of the daily shape of the curve well, but does not account for the changes caused by environmental parameters during the day. This variation that should be incorporated by the trend and remainder component however is the essence of such predictions. The ARIMA model (model 2) is faulty, possibly because the procedure used by the software 'R' is not appropriate for the present dataset where predictors show strong autocorrelation. Model 1, the simple linear

model is convincing, especially when its simplicity is taken into account. The smoothing of the prediction adds to the quality of the fit, as the overall level is usually good, but there is a lot of (regular) noise that can thus be removed. Clearly the best predictions emerge from model 3, the time lagged linear model. This emphasises the importance of the history of the environmental parameters.

The final application of this model needs two further steps: (1) a longer dataset which covers a very wide range of environmental conditions, in particular of the variable 'SMA', soil moisture. This parameter was not included as a predictor in model 1, because the range of conditions and especially the range of combinations with other predictors covered is too narrow. High soil moisture for example can occur during heavy rain, where there is no sap flow at all, but also after heavy rain, in full sun, when sap flow can be maximal. If the model is not trained for both conditions, it will never be able to predict accurately. (2) A manual calibration that defines maximal sap flow and relates it to environmental conditions. In fact, since *relative* sap flow is predicted only, level shifts are not of interest and an empirical intercept must be included in the model anyway. With model 3, I have a valid, simple and useful prediction tool at hand that proves that relative sap flow depends mainly on light, but also on the history of most environmental variables.

References

- Cleveland R, Cleveland W, JE M, I T (1990) STL: A Seasonal-Trend Decomposition Procedure Based on Loess. *Journal of Official Statistics*, **6**, 3–73.
- Granier A (1985) A new method of sap flow measurement in tree stems. *Annales des Sciences Forestieres*, **42**, 193–200.
- Pepin S, Körner C (2002) Web-FACE: a new canopy free-air CO₂ enrichment system for tall trees in mature forests. *Oecologia*, **133**, 1–9.
- R Development Core Team (2004) *R: A language and environment for statistical computing*. R Foundation for Statistical Computing, Vienna, Austria.

Chapter 8

The analysis of relative data - A novel approach with the example of sap flow data

The analysis of relative data - A novel approach with the example of sap flow data

Introduction

In many scientific disciplines (ecology, medicine, psychology), we often collect data of treated and control groups which we wish to compare in absolute terms. Often however, absolute values are masked by factors that are either impossible to account for (e.g. the weight of whales of which songs are recorded) or proper estimation is too expensive or time consuming (% bodyfat in patients). The same applies to the trees at the SCC site: when measuring sap flow, it is impossible (unless they are cut down), to take into account their sap wood width, exact canopy size, leaf area index, soil properties etc. Yet, in order to distill a CO₂-induced signal in sap flow, the absolute signal is of importance and needs to be compared.

To date, the interpretation of sap flow signals was restricted to scaling the data to absolute flux rates in order to compare total mass flow between trees (Granier 1985. If, however, the effect of CO₂ on tree sap flow results in a decrease of around 5 to 10% for example, then this signal is prone to be masked by the high variation between trees mentioned earlier. Here, I scale each tree's sap flow signal series to its own maximum during a trial period and discuss attempts to work around the problem of losing the absolute signals following standardisation of the data. The example is on trees, but can be applied to other time series data. The detection of the CO₂-effect consists in the first place of assessing the significance of the difference in sap flow between control and CO₂-treated trees. Later, a more ambitious (and speculative) way of reconstructing the absolute signals is shown.

Methods

The sap flow data used (for details see chapter 2) originate from two sunny periods in 2004: period one lasted from June 5 to June 10 2004 (6 days), period 2 from August 4 to August 8 2004 (5 days). To avoid confusion and clarify the terminology used, the process of standardisation of the absolute sap flow data is illustrated in Figure 1. The left panel shows the mean

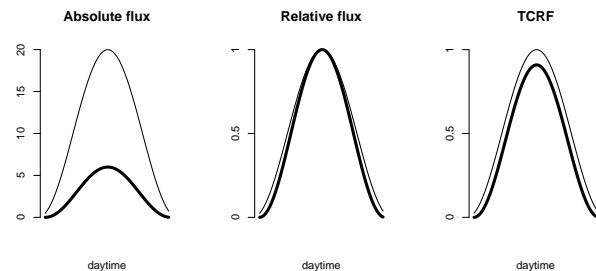


Figure 1: Theoretical illustration of absolute flux, (arbitrary y-axis), relative flux, and treatment corrected relative flux (TCRF), the variable of interest when trying to quantify reduced sap flow. The bold line simulates a treated tree, the fine line a control tree on the same day.

absolute flux of the treated (always bold line) and the control trees. After standardisation, we are left with the centre panel, and, if we manage to reconstruct the absolute signal uniquely due the treatment effect, we obtain what is shown on the right. In fact, the ratio of the integrals of the two curves in the right panel of Figure 1 is the percent decrease or increase in sap flow due to the treatment, the quantity of interest. These curves will be referred to as ‘TCRF’, meaning ‘treatment corrected relative flux’, because they originate from the relative curves, but with a post-hoc correction that reconstructs the treatment effect. Henceforth, I will speak of ‘relative flux’ or simply ‘flux’ when referring to relative flux as shown in the central panel of Figure 1, and of ‘absolute flux’ when referring to the left panel of Figure 1. (Note that this terminology differs from the one used in chapter 2!)

The CO₂-effect on sap flow - is it significant?

To start with, the variable of interest is relative flux, from which the treatment corrected relative flux shall be inferred later. It is of interest whether the CO₂-effect on sap flow, if present, occurs in all three species and whether it is significant. If there is a difference

in relative transpiration rates between treated and control series and among species, it should become apparent when looking at the difference between relative sap flow rates of treated versus untreated trees. Therefore, I created six new time series (henceforth called difference series), e.g. for *Fagus*:

$$DF_1 = F_{ambient,1} - F_{elevated,1},$$

where DF_1 is the difference between the mean ambient ($F_{ambient,1}$) and the mean elevated ($F_{elevated,1}$) flux-series of the first period of *Fagus*. The series DQ_1 (*Quercus*) and DC_1 (*Carpinus*) were obtained similarly. Figure 2 (upper panels) shows the difference series for both periods and all three species. I also looked at the ambient-elevated difference of all trees pooled (Figure 2, lowest two panels); these series are called D_1 and D_2 respectively. In some instances, there seems to be a pattern of midday depression, particularly in beech at the beginning of the two periods. Generally, the difference series seem to be above zero more often than below (less so for *Quercus*). The specific question that emerges is: are the difference series significantly different from the empirical distribution? If they are, what is a robust estimate of the observed pattern?

Before testing whether the daily differences are significantly different (e.g. by means of a sign test), I render the estimate of the difference in relative sap flow for an average sunny day as stable as possible. This is done by bootstrapping on two levels: the individual tree and the day (assuming that all days during period 1 and 2 yield similar sap flow patterns). More specifically, the difference of flux calculated and shown in Figure 2 is recalculated by subtracting a random sample (with replacement) of treated trees from a corresponding sample of control trees. This is done 99 times for all 1584 time steps (144 per day times 11 days), and the curve is smoothed with a spline function (command `smooth.spline()` using automatic determination of the smoothing parameter). This new series of 1584 time steps (10 min intervals for 11 days) is then resampled again: a random sample of size 11 (number of days) with replacement is taken 99 times for all 144 time steps per day. This condensed summary over all species and all days is shown in Figure 3. The same procedure was also carried out for each species individually, but as the resulting plots look similar, only the pooled species plot for both periods is shown. Note that Figure 3 differs from the one shown in chapter 2 which is computed with ratios rather than differences. Therefore, the interpretation is not the same, i.e. the units in Figure 3 are unspecified. The midday depression that was suspected from the raw plots and the spectral analysis of the ambient-elevated series (D_1 and D_2 joined) emerges clearly. Note here that this is the difference in *relative* flux from which no conclusion

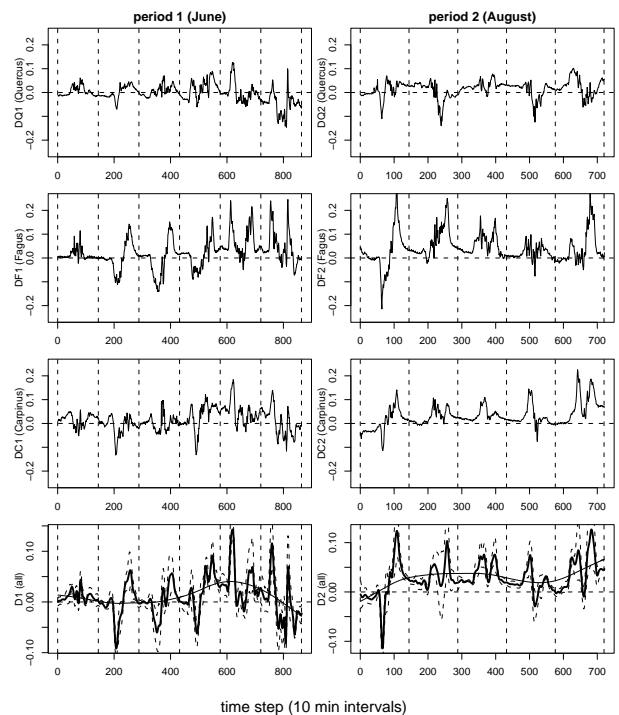


Figure 2: Raw plots of differences between ambient and elevated series. Graphs show *Quercus* (oak), *Fagus* (beech), and *Carpinus* (hornbeam). Bottom two panels: Smoothed raw plots of differences between ambient and elevated series (all species pooled) with smoothed standard error bands. Solid line shows an overall trend (smoothing spline with large span). Dashed vertical lines delimit days, left side: period 1, right side period 2.

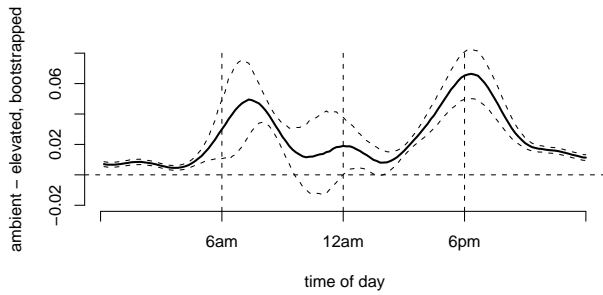


Figure 3: Smoothed and double bootstrapped (individual tree and day) difference series of relative flux (ambient - elevated). The units of the y-axis are % (1 = 100 %). The pattern looks similar for the individual species, hence the plot for all species pooled is shown only. Error bands show normal confidence intervals.

can be drawn on the actual difference in sap flow (see chapter 2).

Next, I need to know the probability that such a pattern of the same intensity appears by chance. Therefore, I take all original relative sap flow series for each tree (*Quercus*: 5 controls, 3 treated, *Fagus*: 4 controls, 3 treated and *Carpinus*: 3 controls and 4 treated) and reassign the treatment factor (0 or 1) randomly 99 times. I then compute the difference series as outlined above and compare them with the true difference series DQ_1 , DQ_2 , DF_1 , etc. The same procedure is also carried out with all trees pooled. The plots of the 99 random difference series (grey lines) together with the real difference series (bold black lines) are shown in Figure 4 (line plots only). At first sight, it looks like there are no clear patterns in *Quercus* (Figure 4, top panel). In *Fagus*, *Carpinus* and all species (3rd, 5th and 7th panel from top) however, the real difference series seems to be on top of the random series most of the time, in particular during the second period. To visualise this, the quantiles (which are nothing but the ranks from 1 to 100 of the real series among the 99 random difference series), are plotted below each panel (Figure 4, scatter plots). The grey bars indicate rank 1 to 10 and 90 to 100, where the probability of drawing such an extreme sample passes below 20%. This however is only valid for the individual time step, provided there is no timely dependence (but in fact there is). These ranks are linked to the p-values of a nonparametric rank test by the equation $p\text{-value} = \text{rank}/100 - 2((\text{rank}/100) - 0.5)$, where values below 0.05 are usually considered significant (on a 5% level).

At this stage, I am still unable to tell whether the patterns of the ranks as shown in the scatterplots of Figure 4 could occur by chance (which is the null hypothesis). There lies a difficulty in finding a sta-

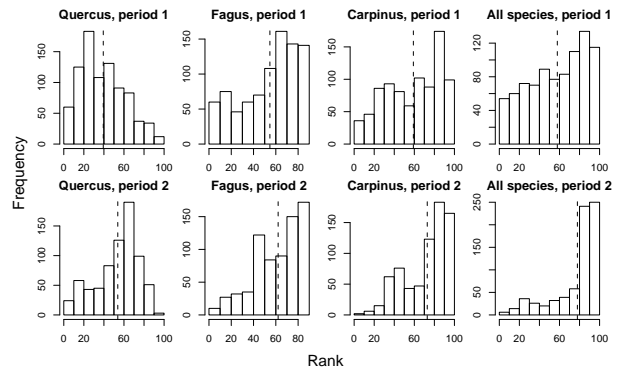


Figure 5: Frequency distributions of true ranks for all three species and both periods. The dashed line indicates the median.

tistical test for this issue: The ranks are timely dependent and cannot be tested individually, e.g. by means of the classic Wilcoxon Test. The envelope test presented in (Davison & Hinkley 1997, p. 153) is one option to test the above hypothesis, taking the number of bootstrap samples into account. Such confidence envelopes are shown for the ranks in Figure 4. According to this test, a series is significantly different when one single value lies outside the envelope, which is the case for all series in my case. I prefer a more intuitive test on the distribution of the true ranks over one period for a particular species. If we assume, based on the bootstrapped differences (Figure 3), that relative flux is consistently higher in control trees, the median of the ranks shown in Figure 4 will be an adequate measure. (Note that it would not be, were the true ranks expected to be *either* higher *or* lower. This is the drawback of looking at the distribution only: we lose the information of the time series. I will try to overcome this below by looking at certain times of the day only.) For example, the median of the true ranks of series DQ_1 of 40 seems clearly non-significant while the median of the true ranks of series D_2 (all species, second period, see Figure 5, bottom right panel) of 78 might be significant. Generally, *Quercus* looks insignificant, but in *Fagus* and *Carpinus* the ranks are strongly skewed to the right (Figure 5). Period 2 shows a consistently more distinct pattern than period 1.

To formally test the significance of the rank series (and hence of the difference series) using their distributions, I use the following algorithm:

- Compute 99 random rank series by comparing one random difference series (i.e. one of the grey lines in Figure 4) to the remaining 98 random difference series. Do this for all three species, all species pooled and both period 1 and 2 separately.
- Calculate the 99 medians of the ranks for each

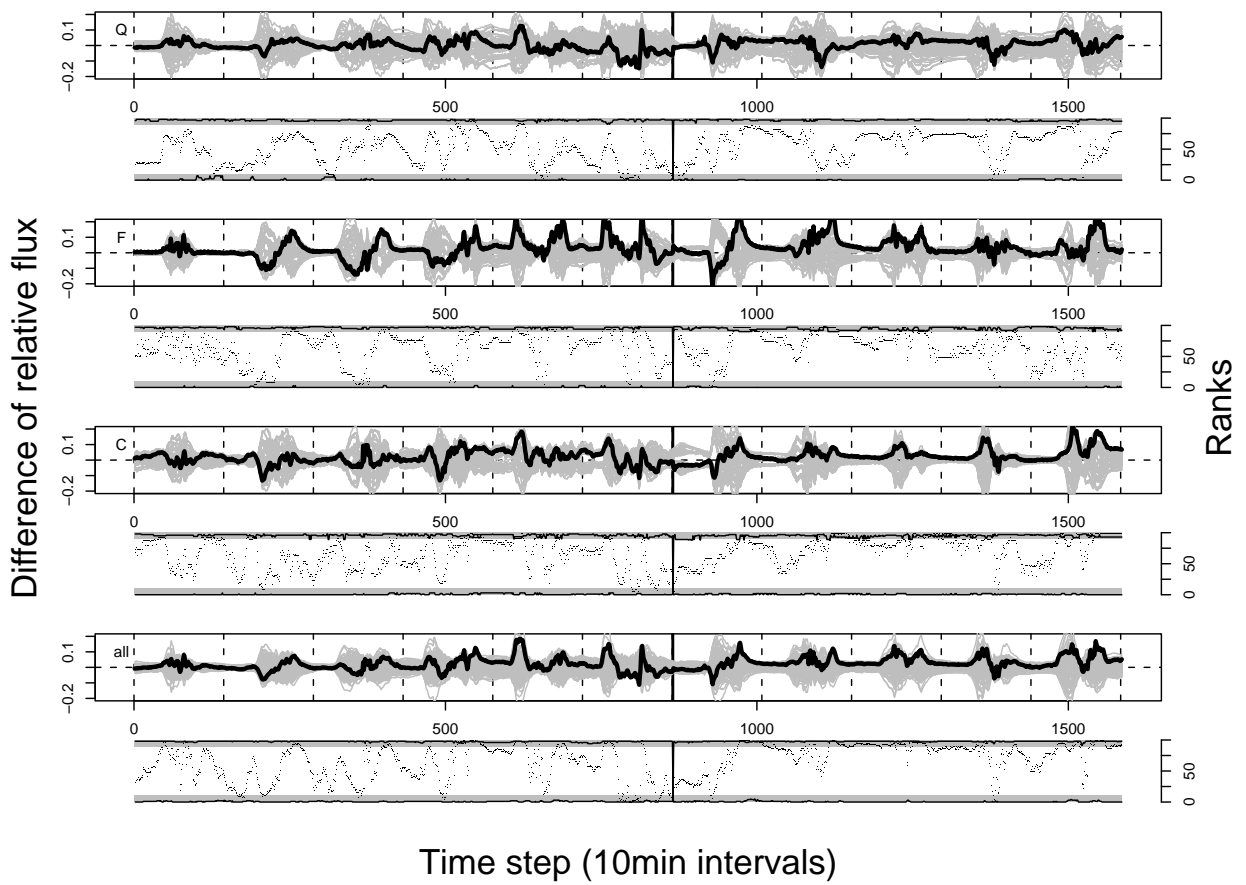


Figure 4: Differences between series with randomly assigned treatment ($R=99$, grey lines) and true difference series. Below are the respective ranks of the true difference among the random differences series for each time step. Grey bands show lowest 10 and top 10 ranks (corresponding to a pointwise error probability of 20 %, lines are overall confidence envelopes (see text)). From top to bottom: *Quercus*, *Fagus*, *Carpinus* and all species pooled.

case.

- Compare the median of the true rank series with the 99 series from the previous step. This yields a rank: If the true rank series has rank <5 or >95 , the true rank series is considered significantly different from the empirical distribution. Translate rank into a p-value.
- Carry out steps one to three 99 times in order to get a more stable p-value. (From the distribution of these p-values, I indicate normal confidence intervals to give an idea the range although the p-values are not normally distributed).

The results of the above algorithm are presented in Table 1. The negative values of the normal confidence intervals originate from the fact that p-values are not normally distributed (and hence normal CI's should not be used), but they are still kept to indicate a plausible range. It becomes clear that there is a species specific as well as a seasonal effect. *Quercus* is clearly not responding to elevated CO₂ by decreased sap flow, the other two species react marginally significantly (except *Carpinus* in period 2. However, when only the morning and afternoon values are considered (6.20 to 8.00 and 15.00 to 20.00 hours), *Carpinus* and *Fagus* as well as all species pooled show significantly higher true ranks (compared to the random rank series, 1). This is reasonable, because it is clear that the significance of this characteristic pattern is wrongly underestimated when all timesteps of the day are considered: the pit in the 'camel-shape' (Figure 3) as well as the nightly values blur the effect in the morning and in the afternoon. Only now, knowing that all rank series except the ones of *Quercus* are significant with an error probability of below 5%, does it make sense to try to quantify the reduced sap flow of CO₂-treated trees. This will be the topic of the next section.

Table 1: Summary of mean ranks of the true rank series among the 99 random rank series with normal confidence intervals (negative values: see text) as from the algorithm described in the text. When the algorithm is applied to morning and afternoon hours only, all species but *Quercus* fall below the 5% level.

species / period	mean rank (all)	CI	mean rank (morning and aftern.)	CI
Quercus 1	57.3	(47.7,66.8)	46.9	(36.0,57.9)
Quercus 2	28.2	(19.5,36.8)	35.8	(26.9,44.7)
Fagus 1	14.7	(7.5,21.9)	3.0	(0.1,6.0)
Fagus 2	15.9	(8.9,22.9)	1.7	(1.4,4.9)
Carpinus 1	15.4	(8.7,22.1)	0.8	(-0.7,2.3)
Carpinus 2	2.2	(-.07,5.0)	3.2	(-0.3,6.6)
all 1	28.7	(19.3,38.2)	2.1	(-0.7,4.9)
all 2	4.4	(0.6,8.2)	1.8	(-0.8,4.5)

Amplitude of the CO₂ Effect

Given that data of relative flux are available only, but, in fact, the treatment corrected relative flux (TCRF, see the Methods section) is of interest, I now develop a technique to infer TCRF from relative flux. I first looked at the plausibility of the difference in sap flow between treated and control trees being significantly from the random difference series. Now I develop a way of inferring the absolute amount of the CO₂-effect on sap flow.

Trying to infer TCRF, it lies close to look for a relationship linking relative flux to TCRF (inferring the right panel from the centre one in Figure 1, Methods section). This is possible if and only if the quality of the curve somehow relates to its amplitude. The problem is to distinguish between the effect of the properties of the tree (mainly tree size and sap wood width, see Methods section) and the effect of the treatment. This is possible if the other properties (I refer to them as 'size effects' for now) only affect the amplitude of its sap flow curve while the CO₂-effect affects both amplitude and quality of the curve. In what follows I will show that exactly this is the case in the present dataset. If the quality of any two curves of different amplitude is the same, their ratio of integrals after standardisation to their own maximum will be unity:

$$\begin{aligned} y(x) &= k \cos(x) \quad \text{curve 1} \\ z(x) &= l \cos(x) \quad \text{curve 2} \end{aligned}$$

and the ratio of their standardised integrals:

$$\frac{\frac{\int k \cos(x) dx}{\max(k \cos(x))}}{\frac{\int l \cos(x) dx}{\max(l \cos(x))}} = \frac{\cos(x)}{\cos(x)} = 1.$$

I assume that the standardisation process to eliminate the size effects (going from the left to the centre panel in Figure 1) is exactly such a process, i.e. the absolute sap flow curves of different (control) trees on the same day only differ in amplitude, but not in their quality or kurtosis. In fact, plotting the ratio of two daily integrals (of two randomly selected control trees of the same day) against the same ratio of integrals, but each curve standardised to its own maximum first, yields approximately a straight line with intercept ≈ 1 (Figure 6):

$$\frac{\int_{day x} \frac{\text{absolute flux of tree 1}}{\max(\text{absolute flux of tree 1})}}{\int_{day x} \frac{\text{absolute flux of tree 2}}{\max(\text{absolute flux of tree 2})}} \approx 1.$$

On the other hand, when looking at the difference of the relative series (Figure 3), we observe a distinct 'camel-shape', which already hints at the fact that the

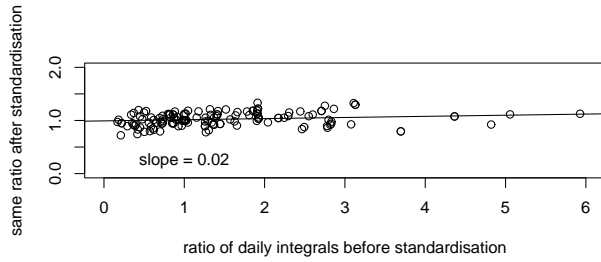


Figure 6: No relationship exists between the ratio of sap flow integrals before and after standardisation (200 randomly selected couples of control trees only). This means that the size of a tree only acts on the amplitude of a sap flow curve, not its quality.

treatment effect might not only act on the amplitude of the curve, but also on its quality. I simulated pairs of different sinus and cosines functions (differing both in amplitude *and* in quality, in order to reconstruct the origin of the ‘camel-shape’. I then standardised the two curves and subtracted one from the other. It seems that if the functions

$$y_t = \cos(0.9x) \times 1.1$$

(simulating the control tree) and

$$y_c = \cos(x)$$

(simulating the treated tree)

are standardised and subtracted from each other:

$$y_c - y_t = \cos(0.9x) - \cos(x),$$

this characteristic ‘camel-shape’ occurs. Figure 7 illustrates this example with the empirical trigonometric functions shown above. The important point is that both the amplitude and the qualitative shape of the curves change. The next step is now to find a proxy to predict TCRF from relative flux (or the corresponding ratios of the integrals). In other words: how can we get back from the centre panel to the left panel of Figure 7?

One option is to find an effect other than CO₂ which simulates the latter, and with which we can create a relationship that links TCRF to standardised flux. Or, better, one that links the ratio of two integrals before and after standardisation. (Note that I use the term ‘standardisation’ for both getting from the left *and* the right panel to the centre one in Figure 1, Methods section) There are sound biological reasons why a CO₂ effect can be simulated by a change in water relations. In reality, a sap flow series during fair weather with ample water supply will yield increasing curves due to daily rising water vapour pressure of the air. Two such days of the same tree provide a situation where we have two curves, one with a higher

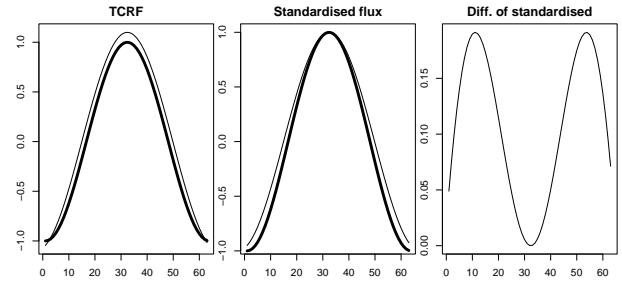


Figure 7: Theoretical illustration as to wherefrom the ‘camel back’ shape observed in Figure 3 may have originated. The bold line simulates the treated series. X-axis represents a diurnal course in unspecified units, y-axis are relative units between 0 and 1. Left: original series, centre: standardised series, right: difference of standardised series. This hints at a correlation between TCRF and standardised flux.

amplitude and maybe also with a different kurtosis or quality. Whether this is true is now tested. I do so by plotting against each other a series of integral ratios of pairs as described above before and after standardisation:

$$\text{integral ratio from day } a \text{ to day } b = \frac{\int_{\text{day } a} \text{flux } dt}{\int_{\text{day } b} \text{flux } dt}.$$

With the two biologically reasonable assumptions that

- (1) the CO₂ effect is proportional to the amount of sap flow, and
- (2) the way unstandardised curves change in relative shape as they gain in amplitude is constant and identical whether caused by changing weather conditions or by elevated CO₂,

we can now create a linear relationship with ca. 30 pairs (all species and both periods, less if species or periods are considered separately, see Figure 8). The plots clearly show that in this case, the amplitude correlates with the quality of the curve, otherwise we would find no relationship as was the case for the size effect (see Figure 6). Since different species and periods correlate similarly, the overall model (bottom right panel of Figure 8 is applied:

$$\frac{\int_{\text{period}} \text{TCRF}_{\text{treat}} dt}{\int_{\text{period}} \text{TCRF}_{\text{ctrl}} dt} = 1.11 \times \frac{\int_{\text{period}} \text{flux}_{\text{treat}} dt}{\int_{\text{period}} \text{flux}_{\text{ctrl}} dt},$$

with the intercept forced to zero. (Including an intercept increases the coefficient to 1.29). This model thus allows to reconstruct the effect of CO₂ on reduced absolute sap flow from the effect on the relative sap flow curves.

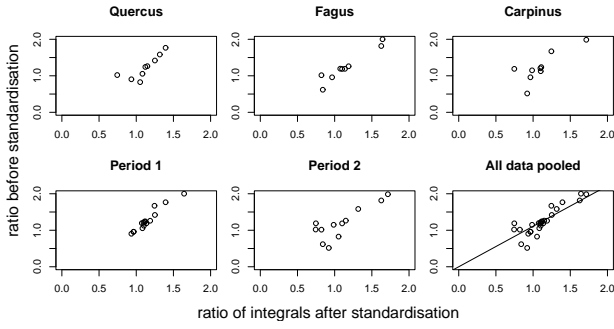


Figure 8: Regressions of absolute flux on relative flux. The correlations are convincing and the model for all species and both periods can be used for inferring the percentage of the area under a sap flow curve lost upon the standardisation. Overall model (bottom right panel): $abs = 1.11 \times rel$, $p < 0.001$, $R_{adj}^2 = 0.82$).

In summary, I have now been able to distinguish between the two consequences of standardising absolute flux: the wanted one of eliminating tree size and other confounding factors, and the unwanted side effect of masking the amplitude of the treatment effect. This was possible because I could show that the tree size effects only influence the amplitude of sap flow curves, while the treatment effect influences both the shape and the amplitude of sap flow curves.

Discussion

High variability or low signal to noise ratio not only dominates the present dataset, but is typical in ecological datasets with many sources of error (from the technicalities of the data collection to the often highly heterogeneous environment). For the present example of forest trees, I was able to extract a proof of (1) a significant effect of CO_2 on sap flow via the analysis of the relative (standardised) data, and (2) a means of inferring absolute sap flow from relative sap flow.

As the effect of elevated CO_2 is significant, it makes sense to finally combine the canopy sap flow model of chapter 7 with the CO_2 -effect in order to predict longterm changes in sap flow under climate change. The way the CO_2 -effect is added to model 3 is not trivial. It is most reasonable to assume that the decreased sap flow in treated trees spreads out evenly over the day, or, even more likely, follows the amplitude of sap flow in the course of a day (such as the difference of the TCRF curves in Figure 7 would look like). The CO_2 -effect could for example be added to model 3 of chapter 7 as follows:

$$\alpha \cos(\beta t) \times flux_t = \beta_0 + \beta_1 T_t + \beta_2 SMA_t + \beta_3 light_t + \beta_4 wind_t + \beta_5 per_t + \beta_6 RH_{t-1} +$$

$$\beta_7 light_{t-1} + \beta_8 light_{t-2} + \beta_9 light_{t-3} + \beta_{10} light_{t-4} + \beta_{11} light_{t-5} + \beta_{12} T_{t-6} + \beta_{13} light_{t-6} + \beta_{14} SMA_{t-6} + \epsilon$$

with the condition

$$\frac{\int_{period} \alpha \cos(\beta t) dt}{period} = p$$

Instead of the cosine function, the distribution of the CO_2 -effect could also follow the regressor 'light', as long as the integral of the effect over the whole period and divided by it does not exceed p , the factor of increase in sap flow due to elevated CO_2 which lies around 1.11.

References

- Davison A, Hinkley DV (1997) *Bootstrap Methods and their Application*. Cambridge Series in Statistical and Probabilistic Mathematics, Cambridge University Press, Cambridge, UK.
- Granier A (1985) A new method of sap flow measurement in tree stems. *Annales des Sciences Forestieres*, **42**, 193–200.

Chapter 9

Summary

Summary

Aims

This thesis investigates water use in tall forest trees subjected to elevated atmospheric CO₂ (540 ppm), a concentration expected to occur in ca. 50 to 70 years. The key questions are: (1) Do higher levels of CO₂ affect water use? (2) If so, how does this effect interact with drought conditions that are likely to occur more frequently over Central Europe as global change progresses? (3) How does leaf-to-air temperature difference vary among species, how strongly are forest trees coupled aerodynamically, and can leaf temperature be used to assess water relations of tall forest trees? (4) Among the several methods available to characterise water relations in plants, which are best applied to tall forest trees where statistical replication is often compromised by logistic feasibility? (5) Can sap flow be expressed as a function of environmental parameters, and thus possibly replace mechanistic parametrisations of tree transpiration in coupled land-surface climate models? These questions are not answered by the order the chapters appear in, nor does each chapter answer one specific of the above questions. I here synthesise all chapters, trying to arrive at a general conclusion.

(1) Water savings under elevated CO₂

Our detected water savings under elevated CO₂ of ca. 14 % (not including interception and run-off, chapter 2) are within the range of results from studies conducted with coniferous trees (ca. 0 to 25 % savings) but higher than expected when compared to the reduction in stomatal conductance (chapter 4). However, much of the data on stomatal conductance was collected in 2001, in the first year of CO₂-enrichment, during which up to 22 % water savings was found for *Carpinus*. This species also responded strongest to elevated CO₂ in terms of stomatal conductance. In theory, reduction in stomatal conductance under elevated CO₂ should always be higher than reduction in sap flow, because the leaf boundary layer adds a serial resistance to the pathway of water from the soil into the atmosphere. Comparisons of stomatal conductance and sap flow are always prone to con-

foundng factors like a decrease in LAI, which would not be detected by stomatal conductance measurements but which would appear as ‘water savings’ in sap flow. LAI of *Fagus* indeed decreased (C. Körner & S. Peláez-Riedl, unpublished data), partly explaining the discrepancy between water savings measured by sap flow instruments (chapter 2) and by porometry (chapter 4). It is important to note that neither of the methods discussed here measure tree water use *per se*. Sap flow signals, with the advantage of integrating over the whole canopy, are influenced by stem repletion and night-time transpiration. Stomatal conductance measurements do not account for boundary layer resistance and cannot immediately be transformed to a transpiration signal. Nevertheless, the relative differences are informative, but they vary between methods. Overall, taking into account interception and run-off which will probably remain constant under elevated CO₂, decreased net water use in temperate broad-leaved forests will be around 10 %.

(2) CO₂ and drought

The centennial drought and heat wave of the summer of 2003 gave us an unforeseen chance to look at the combined effect of drought and elevated CO₂ (chapter 3). The water potential data suggests an improved water status of CO₂-treated trees under prolonged drought. This is in line with the soil moisture data from chapter 2, showing a reverse effect of soil drying (soil under CO₂-treated plot starts to dry faster because there is more soil moisture left and hence more transpiration possible). Water potential (especially predawn water potential) and soil moisture measurements are generally useful, because they measure the net effect (soil matrix potential) of changes in transpiration rather than the plant physiological mechanisms causing them. These methods complement one another, because water potential measurements are only of interest for the CO₂-induced water saving effect under dry conditions, while soil moisture in the top soil layer only differs between treatments if the soil is above the permanent wilting point. Water potential measurements proved that rooting depth of forest trees might be underestimated. These deep roots also play a role in responses to elevated atmospheric CO₂, they may be the key water supply

of CO₂-enriched trees during drought. Soil moisture data showed lower rates of soil drying in the CO₂-treated plot, maybe the most reliable evidence of reduced overall water consumption: it is an average measure across the whole CO₂-enriched canopy and all species. Since precipitation and temperature (the two parameters apart from CO₂ most likely to be affected by global change) experiments are not feasible in tall tree experiments, one will have to investigate longer time-spans to observe responses under unusual weather conditions.

(3) Leaf temperatures and CO₂

Thanks to the high resolution of the state-of-the-art thermal camera used, we could characterise spatial and temporal temperature distribution of forest trees in an unprecedented way (chapter 5). Leaf temperature data in combination with stomatal conductance data of chapter 4 allowed to calculate leaf boundary resistances, which showed that broad-leaved forest trees are less aerodynamically coupled than assumed. This may explain in part why differences in transpiration were not consistently seen in comparisons of treated and control canopies (chapter 2), because it means that the leaf boundary resistance was relatively high (and influential) compared to the stomatal resistance. For example, leaf boundary resistance was only 3 times smaller than stomatal resistance in *Fagus*. However, since a CO₂-effect was seen in the sap flow data, there must be other reasons while water savings were not readily measurable by way of leaf temperature. It is possible that microclimatic turbulences (warm rising air parcels, cooler air drawn in from below) are simply blurring the CO₂ effect, even if present. Another concern is that the CO₂-jets from the irrigation tubes bring some cooling, interfering with the signal from latent heat loss. We conclude that thermography is not appropriate as a means of detecting reduced transpiration caused by elevated CO₂ in tall forest trees with very heterogeneous canopies.

(4) Methodologies and statistics at the SCC site

Despite at times only marginal significance, all three studies on water savings under CO₂ at the present site (chapter 2 and 4 of this thesis and previous studies at the same site) point in the same direction and agree predominantly on the species-specific responses. This substantiates the conclusion that water savings in this type of vegetation will be small (around 10 %), but present. The combined results from the other methods (soil moisture and leaf temperature) further support this finding. The fact that all three studies struggle to some extent with statistical significance

of their results however raises the question whether conventional statistics adequately test the hypothesis of reduced water consumption at this particular site, above all in chapter 4. The delicate point is the level of replication: if it is the tree, then a statistically significant result is extremely difficult to obtain, since $n_{treated} = 12$ overall and $n_{treated} = 3$ (4 for *Carpinus*) per species. Depending on the branch autonomy however, one could argue for the branch being the level of replication, in which case things would look largely different. (If coral reefs are studied for example, it is often uncertain whether different individuals taken as replicas are not in fact clones.) The trade-off lies in the degree to which a site represents natural conditions (e.g. mature trees) and the sacrifices made in terms of replication of individuals and homogeneity of the site. Methods integrating over the whole CO₂-treated area or tree (soil moisture, sap flow) have the benefit to avoid the variation between leaves and branches. For leaf-level measurements, viewing branches as replicates should be discussed in this context.

Another attempt to overcome the small signal/noise ratio largely brought about by the deliberately natural set-up of the experiment was to standardise sap flow data (chapter 8). While standardisation works well if the maximum of the series in question is known (e.g. soil moisture sensors), it is calamitous if it is not. The solution presented here is speculative, but convincing, because fully in line with the results from non-standardised data. The results show that, in the case of relative data in general, if treatment and confounding effects can be separated (for example by a proxy simulating the treatment effect, as has been done here), the original (absolute) signal can be inferred.

(5) Sap flow model and atmospheric feedback

Maybe more important than absolute water savings under elevated CO₂ are response functions that link environmental data to sap flow (or better transpiration). This is because, as mentioned in the general introduction, even if we *do* obtain an accurate response of water consumption to elevated CO₂, we might still be making erroneous predictions for the future, as neither soil nor atmospheric feedback are included in the experiment. If however we know the plant's specific reaction to a particular set of environmental parameters under elevated CO₂, the results can be incorporated in a land-surface climate model to predict net water savings. The vpd-response curves shown in chapter 2 are an example from which I conclude that such response curves will be highly species specific. The predictions from a land-surface climate model would be conspicuously

different if the vpd-response curve of *Quercus* was included instead of the one of *Carpinus*. This confirms the current trend to see biodiversity as a major player of global vegetation-atmosphere interactions. Ideally, the predictive model presented in chapter 7 should be extended to operate at a species level and with CO₂ as an additional predictor variable in order to predict species-specific vegetation responses to a future climate. This however would require a higher level of replication.

Curriculum Vitae

Name Sebastian Leuzinger
Date of birth 29.09.1976
Place of birth Basel
Nationality Switzerland (Basel)

Education

2003-2006 PhD position at the Institute of Botany, University of Basel. 'Water relations in deciduous forest trees under elevated CO₂', supervised by C Körner and P Niklaus

2003-2005 MSc in Statistics in parallel to PhD, University of Neuchâtel

2000-2001 Honours Thesis at the Marine Biology Department, James Cook University, Townsville, Australia. rated Class IA 'Energy allocation patterns in scleractinian corals', supervised by KRN Anthony and B Willis

1997-2000 Undergraduate studies in biology, University of Basel

1996-1997 Undergraduate studies in civil engineering, EPFL Lausanne

1995 High school leaving exam

Professional experience

2002-2003 Private science teacher on sailing yacht 'Alithia'

2001 Dive Instructor in Malta

1996-2003 Substitute grammar school teacher for all subjects, total of 300 lessons taught

Lecturers

University of Basel B Baur, T Boller, B Bruderer, P Duelli, D Ebert, WJ Gehring, U Gisi, HP Hauri, C Körner, E Lüdin, P Oehlhafen, D Senn, G Schatz, V Schmid, U Séquin, H Siegel, SC Stearns, J Stöcklin, M Tanner, N Weiss, A Wiemken

James Cook University K Anthony, D Bellwood, T Hughes, G Jones, M McCormick, G Russ, B Willis